Swarm Carrier: An Autonomous, Multi-vehicle System Capable of Deploying and Recovering Groups of sUAS

MEIE 4701/4702

Technical Design Report

Swarm Carrier: An Autonomous, Multi-vehicle System Capable of Deploying and Recovering Groups of sUAS

Summer II Report

Design Advisor: Professor Mehdi Abedi

Design Team
John Buczek, Joshua Field
Erik Little, Blake McHale
Noah Ossanna, Michael Tang

October 25, 2021

Department of Mechanical and Industrial Engineering

College of Engineering, Northeastern University

Boston, MA 02115

Swarm Carrier: An Autonomous, Multi-vehicle System Capable of Deploying and Recovering Groups of sUAS

Design Team

John Buczek, Joshua Field
Erik Little, Blake McHale
Noah Ossanna, Michael Tang

Design Advisor
Professor Mehdi Abedi

Abstract

The purpose of the Swarm Carrier capstone is to design, manufacture, and demonstrate a system to deploy and recover several small unmanned aerial systems (sUASs) from a carrier unmanned aerial system (UAS). Development for this capstone will focus on achieving system-level functionality defined by a full-circle test of deployment, recovery, and mission execution. Hardware developments concern Finite Element Analysis (FEA) analysis of UAS designs, system validation tests, and subsequent design iterations of the Carrier Drone, Swarm Drones, and Multidrop Bay. Software development will focus on behavior trees, autonomous landings, Drop Mode, and collaborative swarm control. The concept of the Swarm Carrier system and its sub-components originated from research conducted by AerospaceNU. Building upon this, Capstone-specific development will involve final prototypes and integration as well as system-level software development to achieve the full test.

Contents

List of Figures

List of Tables

1 Acronyms

ACP ANSYS Composite PrepPost 56
AMA Academy for Model Aeronautics 8, 95, 97
AUW All Up Weight 8, 15, 23

CNC Computerized Numerical Control 28, 29
CPP Coverage Path Planning 4, 31, 32

DFM Design for Manufacturing 16, 19

EMI Electromagnetic Interference 84
ESC electronic speed controller 55

FAA Federal Aviation Administration 8, 33
FC Flight Controller 24, 25, 92
FEA Finite Element Analysis 1, 2, 55, 56
FMU Flight Management Unit 74
FPV first person view 24
FSM Finite State Machine 4, 17, 18

GPIO General-Purpose Input/Output 77
GPS Global Positioning System 18, 30, 31, 58, 77, 81, 84
GUI Graphical User Interface 29, 81, 97

HITL Hardware in the Loop 31

I2C Inter-integrated Circuit 35
IMU Intertial Measurement Unit 24, 31, 77, 81

MassDOT Massachusetts Department of Transportation 33, 95, 97

OTS Off the Shelf 19

PCB Printed Circuit Board 4, 16, 19, 55
PDB Power Distribution Board 16
PID Proportional Integral Derivative 58
PX4 Pixhawk 4 4, 18, 24, 29–31, 58, 74, 78, 89, 97

RGBD Red Green Blue Depth 78
ROS2 Robot Operating System 2 4, 17, 30, 31, 56, 78, 81
RTPS Real Time Publisher Subscriber 29, 30

2 Acknowledgements

The Swarm Carrier team would like to thank its advisor, Professor Abedi for providing improved direction and critiques towards the quality of presentations of complex systems. Alongside faculty members, Alexander Wittich (Assistant Director of Northeastern's Risk Services) consistently expedited the team's requests for vehicle tests. His work allowed for the validation of the Swarm Carrier system within a realistic timeframe. Lastly, the team would like to express its gratitude towards Professor Gouldstone for his incredibly active role in the years leading up to and during the culmination of Swarm Carrier as a Capstone project.

Outside of Northeastern University members, the Swarm Carrier team would like to express its thanks towards Noel Zamot, Rob Knochenhauer, and other members of the MassDOT. From their review of the system, the team gained invaluable connections to high-level Federal Aviation Administration (FAA) and Academy for Model Aeronautics (AMA) representatives and insight into the most up to date drone regulations.

3 Introduction

3.1 UAS Definition

unmanned aerial vehicle (UAV) are defined as un-piloted flight systems that consist of a vehicles and their associated sensors, payloads, propulsion. The distinction between sUAS and UAS is driven by weight requirements dictated by the FAA. For vehicles below 55 lb All Up Weight (AUW) on takeoff, the distinction of sUAS is officially recognized. Correspondingly, vehicles over 55 lb are defined as UAS and require special flight approval. Fig. 1 below breaks down sUAS and UAS into broad categories of multirotors and fixed wing vehicles. Multirotors are defined by vehicles that use electronically-controlled brushless motors to adjust attitude in flight and provide lift. In comparison, fixed wing vehicles use an airfoil and control surfaces for thrust and attitude adjustments respectively. These differences define key strengths and weaknesses of each vehicle such as comparisons between flight time, maneuverability, and payload capability [1].

Of the comparisons listed above, capabilities relating to control precision, payload capability, and flight time are the most critical for multi-vehicle systems. For such applications, multirotors have the benefit of increased fidelity of control but suffer from shorter flight times. Fixed wing vehicles have greater range but are larger and far less maneuverable than the former vehicle type [1]. The purpose of the Swarm Carrier system is to combine the strengths of these vehicles to create a multirotor system capable of longer mission duration and high fidelity tasks such as deployment and recovery.

3.2 Problem Statement

The problem statement for this Capstone Project is to design, manufacture, and test a system capable of deploying and recovering a swarm of multirotor UAS.

Figure 1: Multirotor vs. Fixed Wing Capability [1]

3.3 Constraints

Prior to this project, some work had been done towards the development of a swarm of sUAS. While Section 4.3 outlines the previous work in greater detail, this section provides the physical constraints for this design of a system to deploy and recover a swarm of UAS. From previous work, it is known that the Swarm Drones each weigh approximately $2.3kg$ with a maximum flight time of 9 minutes. A total of 3 Swarm Drones will be deployed and recovered. Both the Carrier Drone and all the Swarm Drones will be fully autonomous and require synchronous communication both inter-drone and with the ground station for system monitoring. Finally, the Carrier Drone will be required to have a minimum flight time of 15 minutes with the full payload of all Swarm Drones. This final constraint is to ensure sufficient flight time for all the Swarm Drones to be deployed.

3.4 Goals

The goal of this capstone is a proof of concept for a swarm UAS deployment and recovery system. The metric of success for this goal can be broken down into the individual subsystem tasks of deploying and recovering UAS. Given this, the primary objectives will be successful subsystem tests for aerially deploying a singular Swarm Drone and recovering a single Swarm Drone in separate tests. Following the confirmation of these subsystems, a full deployment and recovery test of a single Swarm Drone will be performed. Finally, after successful single Swarm Drone testing, full Swarm Drone payload testing will be performed to fully confirm the functionality of the deployment and recovery system.

3.5 Concept Development

Alongside many applications of UAV are limitations in range, effectiveness, and payload capacity. Many tasks need to be performed quickly, precisely, and over unknown terrain which are demanding feats for any flight system. However, by combining multiple vehicles to accomplish

goals, mission capabilities can be increased by distributing the demands of tasks across multiple agents. This section outlines such use cases, limitations, and the solution of multi-vehicle systems to accomplish tasks more quickly.

3.5.1 Swarm UAS Applications

Applications of single and multi-vehicle drone systems largely involve time-sensitive or large area coverage missions. The motive for these is the increased efficiency associated with UAV over unmanned ground vehicle (UGV) or manned operations. Current applications include search and rescue in spatially denied or large environments, wildfire detection, Naloxone delivery, and geological surveying. [10] describes applications of UAV to autonomously recognize injured personnel and deliver medial supplies. Their investigation provides an excellent example of automation of search and rescue to remove survivability barriers. Such barriers include the limited response times of volunteer rescue teams and the legal ramifications of parks or property owners having to publicly declare lost individuals. Furthermore, [11] provides an outline of a drone-system to monitor wildfires faster than existing satellite methods with the goal of limiting human intervention. Specifically, they formulate a variety of collaborative drone behaviors, such as leaders and zones of occupation, to efficiently search an area with multiple vehicles. In addition to wilderness operations, [12] performed a case study on the use of drones to deliver Naloxone to overdose victims faster than manned methods. Naloxone is a nasal medication administered to victims of opioid overdose that if performed rapidly, can save the life on an individual. Results showed that the use of sUAS drastically decreased the time interval required between 9-1-1 calls and antidote administration. Lastly, a study performed by [13] found that UAV can be applied for precise coastal surveying missions with equivalent accuracy to existing methods and easier implementation.
From the analysis of the above sources, it should be understood that the mission of a UAV is directly a function of payload. For time-sensitive and area coverage use cases, rescue versus delivery versus data collection are all dictated by what the system carries. Studies also outlined the greater efficiency of task completion using one or multiple UAV. Based on the assumption of vehicle modularity and known benefits of multiple vehicles from research, it was affirmed that any of the above tasks could be optimized, in terms of efficiency, speed, and simplicity, using a rapidly deployable group of multiple sUAS.

3.5.2 Swarm UAS Limitations

While there are endless applications for swarms of multirotor UAS, the main reason that they are not prevalent today is because of flight time limitations. Flight time t_f can be calculated as:

$$t_f = \frac{E_T}{P_T}. \tag{1}$$

Where E_T is the total energy capacity (J) on board the UAS and P_T is the total power consummation (W) of the UAS. For multirotor UAS, typical flight times are below 45 minutes and decrease with additional payload weight [14]. For a swarm of UAS, total flight time becomes more of an issue when the swarm needs to traverse to a target region before performing their application.

3.5.3 Solutions to Limitations

There are numerous ways to increase the flight time of a UAS. The easiest is to increase the battery capacity with a larger battery. However, increasing the battery also increases the overall drone weight and causes the motors to draw more power [14]. Other solutions include increasing individual drone sizes as larger multirotor UAS can typically fly for longer at the same payload weight. This may not be possible if the Swarm Drone size is a constraint due to their application. Another possible solution is to incorporate onboard power generation. Current solar technologies unfortunately are insufficient for sustained multirotor flight and gasoline generation requires a significantly larger airframe. The solution that this work focuses on is the use of a single larger vehicle to carry the Swarm Drones to and from their operational area and increase their overall flight time.

4 Background

4.1 Existing Technologies

Existing patents and technology were researched in order to determine novelty and assist in the brainstorming process. Both fixed wing and multirotor patents were considered due to the greater number of fixed wing UAS deployment and recovery methods. The only method found for deploying and recovering multirotors specifically was in [2] which outlined the process of using a cargo plane to aerially drop a packaged multirotor. Once the package was dropped, a parafoil or parachute would deploy and guide the UAS safely from the ground. Then, the package would open and the UAS would deploy. The recovery system outlined in [2] involved a grappling cable that the cargo plane would snare to recover the UAS. Figure 2 displays the UAS package, parafoil deployment, and grapple recovery from [2]. This and several other patents use a grapple hook and line or similar methods to recover drones. This method was deemed insufficient for swarm applications as it would require at least one grapple line and hook per drone or would require a human operator to reset the apparatus between drone recoveries.

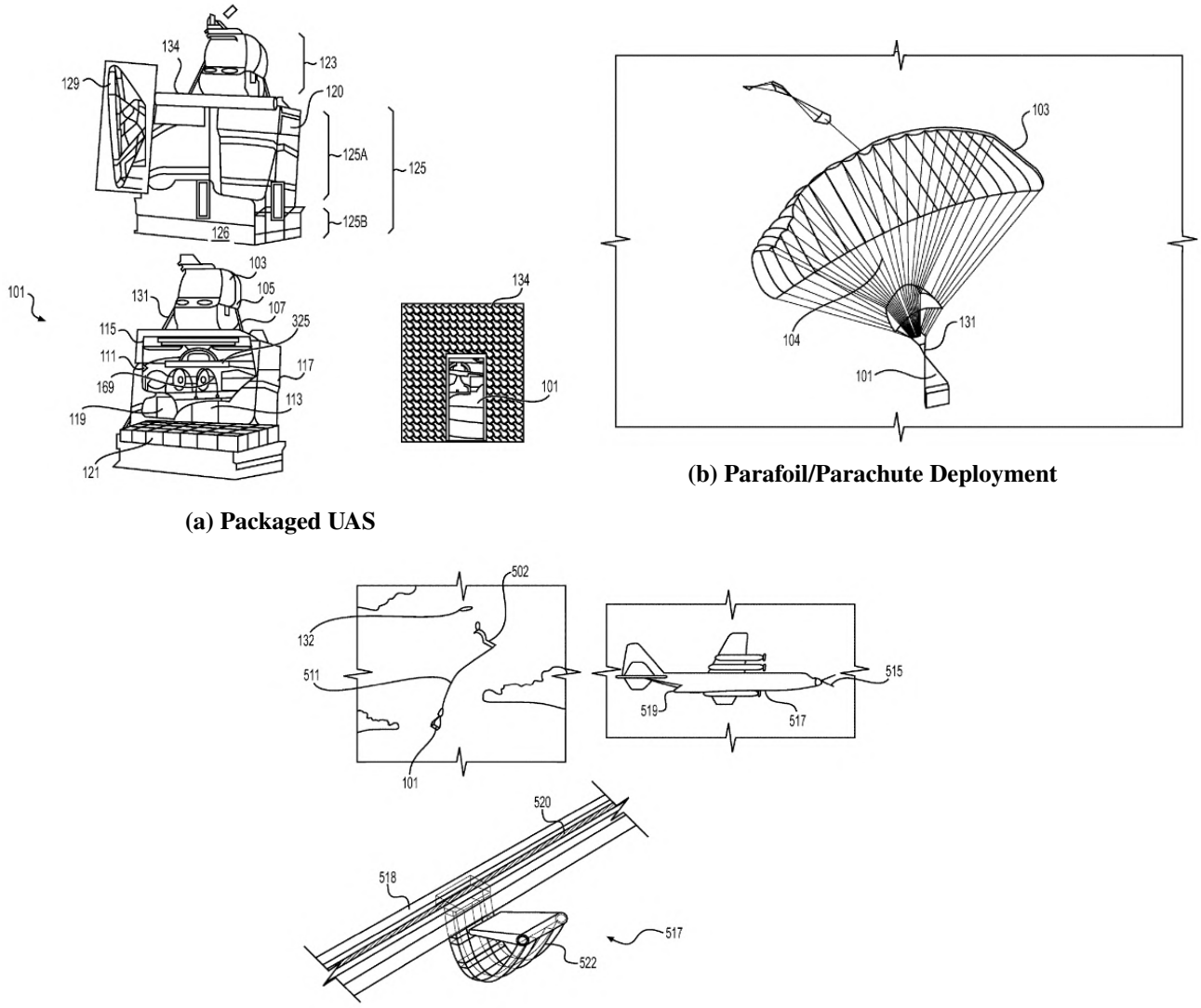

(a) Packaged UAS

(b) Parafoil/Parachute Deployment

(c) Cable grapple snare recovery

Figure 2: Multirotor deployment and recovery method [2]

Another patent similar to the solution proposed in this paper for UAS deployment and recovery was [3]. In [3], an airborne runway underneath the fuselage of a manned plane was used to both deploy and recover fixed wing UAS. The fuselage of the manned plane would act as a storage hanger with an elevator to the lower runway. Thus multiple UAS could be deployed and recovered. Figure 3 displays the deployment and recovery method from [3]. This runway method of recovery was deemed impossible for multirotors as they typically cannot achieve air speeds comparable to manned aircraft and the drones in this scheme would need to fly faster than the manned aircraft in order to land.

Table 2 compares the solution presented in this work to the existing patents regarding the deployment and recovery of UAS. The criteria compared includes the UAS type being recovered or deployed, the number of UAS affected, the carrier vehicle extending the UAS range, the deployment method, and the recovery method. The vast majority of discovered works were designed for

fixed wing UAS due to multirotors only being developed recently [15]. The only works found developing a deployment or recovery method specifically for multirotor UAS was [2]. The number of UAS deployed or recovered was recorded as the vast majority of systems are only capable of deploying or recovering a single UAS without the need for human resetting of their respective mechanisms. The only works found developing multi-UAS deployment or recovery systems were [16, 3]. The inclusion of both the deployment and recovery methods stems from many of the existing patents either only presenting a solution to deploy or only a system to recover their respective UAS. The method for deployment, storage, and recovery of UAS presented in this paper is unique and novel.

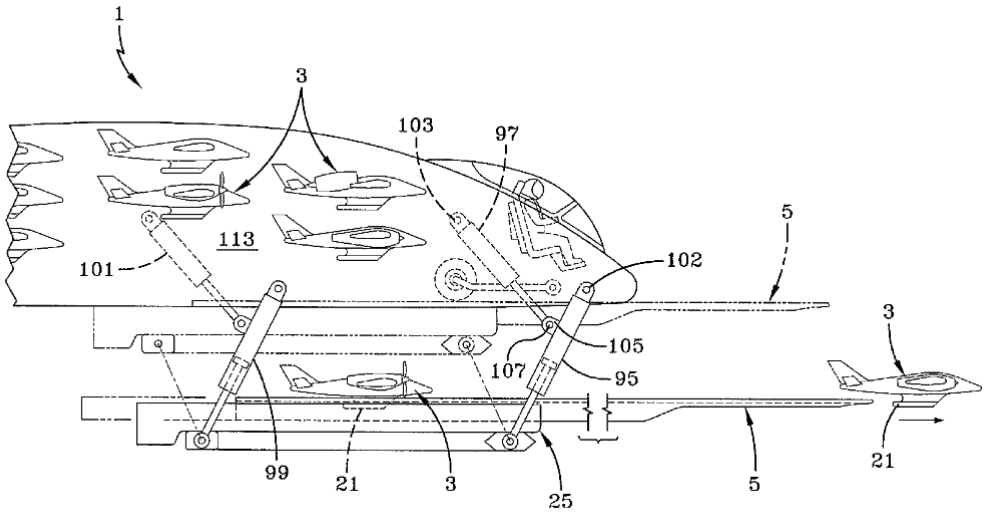

Figure 3: Fixed wing swarm deployment and recovery method [3]

Table 2: Related Patents

Patent	UAS Type	Num. UAS	Carrier Vehicle	Deployment Method	Recovery Method
[17]	Fixed Wing	1	Ship	-	Horizontal Net
[18]	Fixed Wing	1	Ship	-	Vert. Line Hook
[19]	Fixed Wing	1	-	-	Vertical Net
[20]	Fixed Wing	1	Aircraft	-	Aircraft External Arms
[21]	Fixed Wing	1	-	-	Horiz. Line Hook
[22]	Fixed Wing	1	Multirotor	Airdrop	Aerial Interception
[23]	Fixed Wing	1	Rover	Landing Pad	Landing Pad
[24]	Fixed Wing	1	Ship	Latching Cable	Latching Cable
[25]	Fixed Wing	1	Blimp	-	Engagement Cage
[26]	Fixed Wing	1	-	-	Pneumatic Net
[27]	Fixed Wing	1	Ship	-	Horizontal Net
[28]	Fixed Wing	1	Ship	-	Arm Hook Snag
[29]	Fixed Wing	1	-	-	Arresting Hook
[16]	Fixed Wing	> 1	Aircraft	Missile	-
[3]	Fixed Wing	> 1	Airplane	Airborne Runway	Airborne Runway
[2]	Multirotor	1	Airplane	Parachute Airdrop	Cable Snag Aircraft
this work	Multirotor	> 1	Multirotor	Tube Airdrop	Aerial Landing Pad

4.2 Key Theories

The design and development of a multi-vehicle UAS demands mastery of theories of propulsion, airframe design, computer vision, and autonomous decision making. In the pursuit of the Swarm Carrier system, extensive research and experimentation was performed to validate key methodologies such as those relating to motor configuration and flight algorithms. Subsequent sections show the results of these efforts and represent crucial methodologies that were leveraged to develop the project.

4.2.1 Co-Axial Motor Thrust Loss

One of the key issues in designing a multirotor UAS is the choice of propulsion system. The original quadcopter design from the 2000s has since been incorporated into various other solutions from tricopters to dodecacopters and beyond [15]. In addition to different numbers of motors, new mounting methods have been attempted. Other than single motor mounting, another popular motor mounting technique is the coaxial motor mounting. Fig. 4 displays the top, side, and isometric views for single, coaxial, and parallel motor mountings. For coaxial motors, two oppositely rotating rotors are mounted such that the central orthogonal axes of the rotors are colinear and the rotors are separated by a planar distance (D_P). Similarly, the parallel motor mounting configuration involves two oppositely rotating rotors positioned such that the orthogonal axes of the rotors are parallel and separated by an axial distance (D_A). For both coaxial and parallel mounting configurations it is common to rotate the rotors in opposite directions to equalize the momentum of the platform [4]. The benefits of coaxial and parallel mounting in multirotors is that they increase the overall thrust output of the multirotor with minimal increase if overall vehicle size. They allow for more compact vehicle designs and increased payload capacities. The drawback of coaxial and parallel mounting with overlapping rotors is that motor thrust to electrical power efficiency decreases. For coaxial mounting, the *upper* motor has a thrust to electrical power output consistent with that of a single motor, but the *lower* motor operates in the output airflow of the *upper* motor and has a significantly worse thrust to electrical power output than the single motor configuration. This is due to the *lower* motor spinning in turbulent air that already has a significant velocity. Since the air already has a velocity, the spinning *lower* propeller induced less velocity and thus less force onto the turbulent air thus producing lower upward thrust force for the same electrical power input. In experiments, this phenomenon has recorded an average motor thrust loss of up to 23% [4, 30, 31]. In studies, it has been found that increasing the planar distance does not significantly affect the coaxial motor thrust loss. Parallel mounting with overlapping propellers also causes thrust loss, but increasing the axial distance of the motors reduces thrust loss [30, 31].

4.2.2 Propulsion Systems

The method for choosing the motors, propellers, and batteries for a UAS can be determined from the desired application of the UAS. Design methodologies similar to those listed in [14] are used where the wireless systems, computational needs, payload, and desired flight time are first determined. From the needed electronics, the computational power P_C (W), Radio Power P_R (W), and

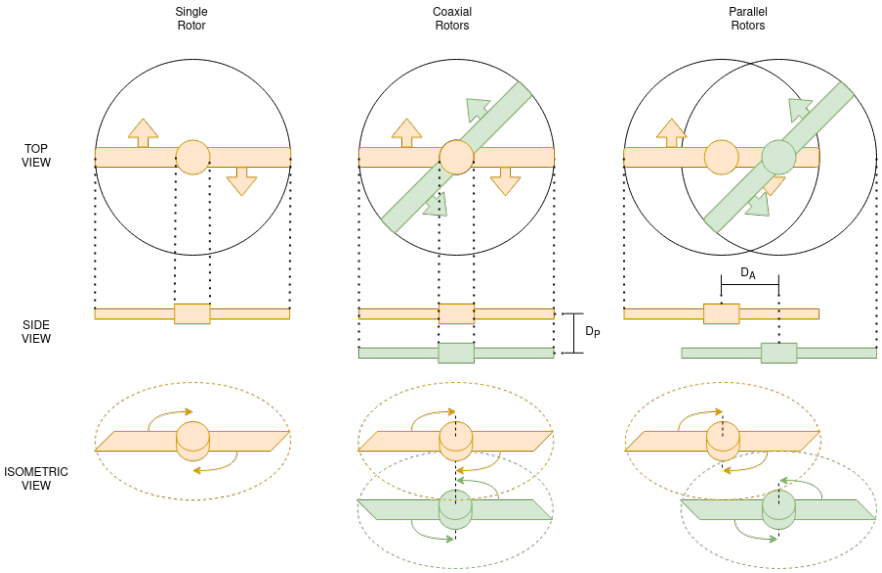

Figure 4: Single, coaxial, and parallel motor mounting configurations [4]

payload power P_P (W) can be determined. The flight time in Eqn. 1 can be expanded as:

$$t_f = \frac{E_T}{P_F + P_C + P_R + P_P + P_{loss}}. \tag{2}$$

Where P_F is the power required to keep the UAS airborne (W) and P_{loss} is the lost power (W). From [14], assuming that the lost power is significantly less than the other powers, UAS flight time can be approximated as:

$$t_f \approx \frac{0.8 Batt_{Wh}}{n * P_m(AUW/n) + P_C + P_R + P_P}. \tag{3}$$

Where $Batt_{Wh}$ is the carried battery energy capacity (J), n is the number of motors, $P_m(kgf)$ is the individual motor electrical power consumption (W) as a function of motor thrust (kgf), and AUW is the total AUW of the UAS and all attached items prior to takeoff (kg). Once the airframe is either chosen or designed, then the iterative method of choosing propellers, motors, and batteries outlined in [14] can be used to determine the overall flight time of the system.

4.2.3 Airframe Design

To implicate motor configurations of propulsion systems outlined in sections 4.2.1 and 4.2.2, UAS require airframes that are both lightweight and inflexible. These must withstand the reaction forces from motor impulses, steady state thrust output, and external forces such as wind to constrain deformation and be durable. To do so, the most common materials employed are woven carbon fiber sheets and tubes, injection molded plastic, 3D printed nylon alloys, and small aluminum parts in highly critical areas. Fig. 5 below shows an example of composite and molded airframe design by Freefly Systems for cinematography robotics. By leveraging carbon fiber laminate and machined components, the AltaX can achieve over 30 minutes of flight time with a payload of 10 lbs [5].

Figure 5: Industry airframe design example: Freefly Systems Alta X [5]

Due to the high ultimate strengths associated with these materials, static failure, in an ideal design, is far less likely during normal operation than damage resulting from vibration. As such, the engineer must mitigate elastic deformations in order to prevent high frequency oscillations from propagating through the frame and to critical inertial sensors. Methods to accomplish this include developing vibration-damped mounts for key components, utilizing thread-lock or nyloc hardware, and using a combination of airframe members in tension and compression to distribute load without flexing. Cable tensioning is also a common method for the development of larger UAS to prevent deformations without added weight from additional rigid members. Furthermore, simplicity of design is critical for optimizing cost and manufacturability. Carbon fiber is specifically costly and difficult to machine which necessitates airframes to be developed with a Design for Manufacturing (DFM) focus. Integration of electronics also becomes a challenge, especially for heavy-lift vehicles that require high steady-state current consumption. For this, custom designed Power Distribution Boards (PDBs) and Printed Circuit Boards (PCBs) can be developed to simplify and easily integrate peripherals.

4.2.4 ArUco Markers

ArUco markers are simple, matrix based fiducial markers that are easy for cameras to detect and compute a relative 3D pose. They are easy to view by using common computer vision techniques such as corner detection. This is why they are built from black and white squares. There are other

popular visual fiducial marker systems such as Apriltags and ARtags. However, the ArUco system was chosen as its detection library has been built into the OpenCV, an open source computer vision library, making it easy to use with Python and subsequently Robot Operating System 2 (ROS2). Additionally, the ArUco library makes use of error detection and correction techniques when decoding detected markers [6]. An example of marker detection and pose estimation is in Fig. 6

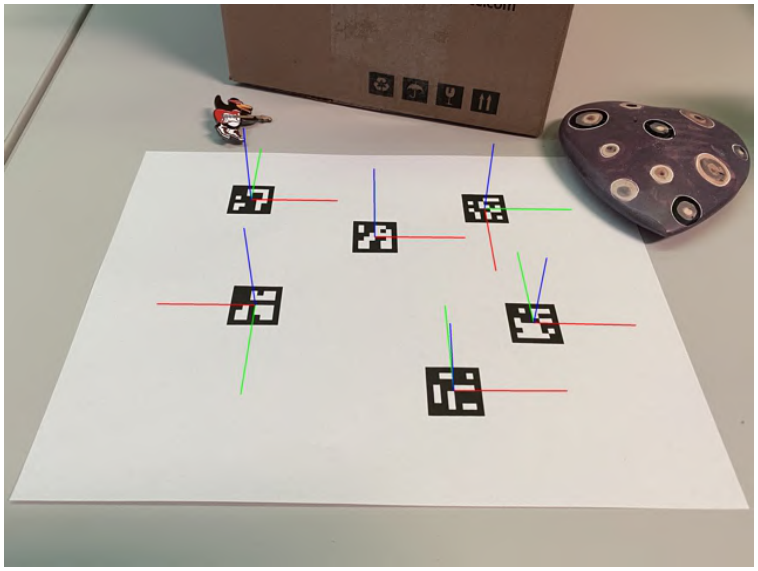

Figure 6: Example ArUco pose estimation [6]

4.2.5 Behavior Trees

Behavior trees will be used for high level mission architecture. Behavior trees are essentially hierarchical state machines. They have been used extensively in video game artificial intelligence as well as robotics and allow for reactive, modular missions to be executed. The most common comparison is to Finite State Machine (FSM). However, behavior trees are more expressive and easier to read or create due to the semantic meaning behind their structure. They are read left to right and top-down and contain modular logic blocks that enforce complex control flows. FSM can encapsulate the same logic of a behavior tree but it can get tedious quickly, as shown in Fig. 7. When constructing a behavior tree, the user does not have to define logic for success, running, or failure end conditions.

4.3 Previous Work

The Swarm Carrier system originated from a cluster of research projects called Northeastern UAV (NUAV). These were founded and lead by the authors of this paper as a project in 2018 within Northeastern University's aerospace club AerospaceNU (AeroNU) with the goal of exposing students to drone and robotics research. Swarm Carrier emerged in 2019 as the main initiative of the project with substantial following in both hardware and software domains. Since 2019, the authors investigated a variety of methods to achieve the project's goal such as compact drone design,

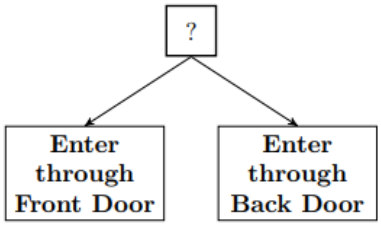

(a) Behavior Tree for entering a room

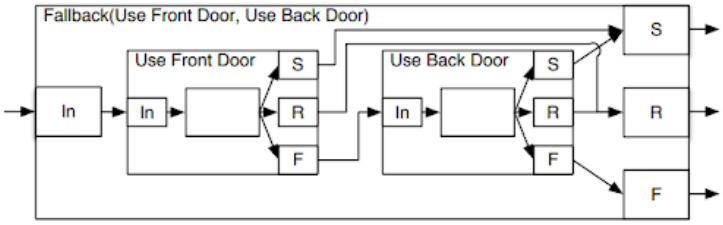

(b) FSM for entering a room

Figure 7: Example Behavior Tree vs. FSM design [7]

drop and landing payloads, sensor selection, autonomy development, and economic manufacturing routes. This section outlines the results of research which were early prototypes of Swarm Carrier's subsystems and flight algorithms. In section 5, these independent prototypes are extensively iterated and subject to integration within the larger Swarm Carrier system.

4.3.1 Swarm Drones

Independently, designing and developing drones is relatively easy with many solutions built off commercial platforms and widely accessible documentation. However, the integration of both of these functionalities in a custom system is far less trivial, especially when sizing constraints exist. Commercial solutions such as those by DJI and Skydio offer excellent flight performance, sensors and on-board computation but are prohibitive at $\$13,000 - \$20,000$ per vehicle [32], [33]. This solution drives many companies to develop their own vehicles capable of fitting a certain envelop while also allowing for custom software development [34]. Due to cost constraints and the niche operational requirements of Swarm Carrier, development of a custom vehicle, the Swarm Drone, was similarly pursued.

The previous development of the Swarm Drones was the most important foundational element of the Swarm Carrier system. As the agents meant to test flight algorithms and perform autonomous missions, early Swarm Drone prototypes were compact quadcopters. These combined Global Positioning System (GPS) based navigation with an on-board flight computer to facilitate advanced capabilities. To accomplish a variety of missions, they required a Pixhawk 4 (PX4) flight controller, Nvidia Jetson Nano computer, GPS, camera, and various other power distribution electronics. With these requirements, spatial constraints rapidly prevailed, so compact designs that retained required functionality were a critical point of research leading up to summer 2021.

In addition to their autonomous requirement, the Swarm Drones were developed with the notion

that one day, they would have to be compatible with a deployment and reintegration mechanism. In order to remain future proof in this regard, the Swarm Drones needed to be as compact in one axis as possible with little to no external sensors that might be subject to damage during interactions with this mechanism. Therefore, research shifted to custom airframes that were specifically designed to house the electronics that the goal autonomy required. The reintegration mechanism is discussed in depth in section 4.3.3.

The first iteration, titled Swarm Drone V1, was developed specifically around Off the Shelf (OTS) electronics to accomplish autonomous tasks. To meet future unknown methods of deployment, the overall vehicle's height was minimized in order to make them "stackable" in deployment mechanisms. Fig. 8 and Fig. 9 show early iterations of the Swarm Drone V1 that utilized waterjet carbon fiber as a rapid manufacturing process. The design also utilized 3D printed polycarbonate arms (shown in green) and a custom PCB (shown in blue) to organize electronics and sensors.

The prototype represented a substantial progression toward better DFM methods but was ultimately a failure due to poor handling and durability, short flight time, and being too large in the direction of its planar axes. Subsequent iterations, embodied as the Swarm Drone V2, sought to further decrease form factor and weight to increase flight time with an equivalent feature set. Shown in Fig. 10a, the Swarm Drone V2's notable improvements were a symmetric design and more compact PCB that increased vehicle performance and flight time respectively. The images below show the elimination of all unnecessary space in the design as well as a flight test that proved more stable than the V1 design.

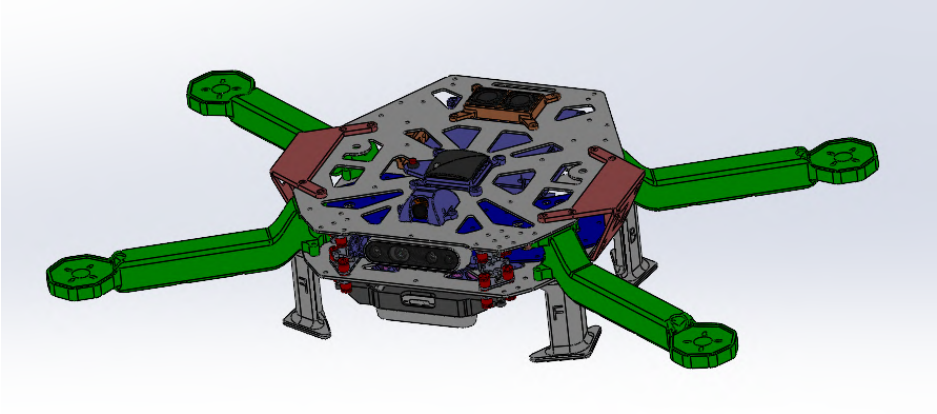

(a) V1 CAD model

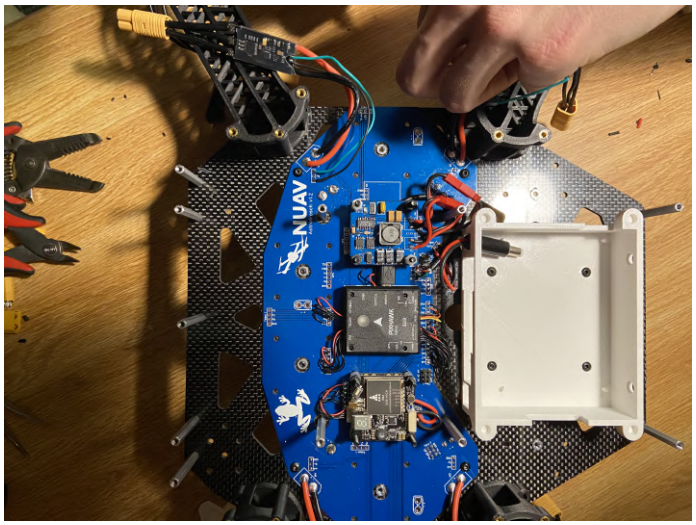

(b) V1 flight electronics

(c) V1 initial prototype

Figure 8: Swarm Drone V1

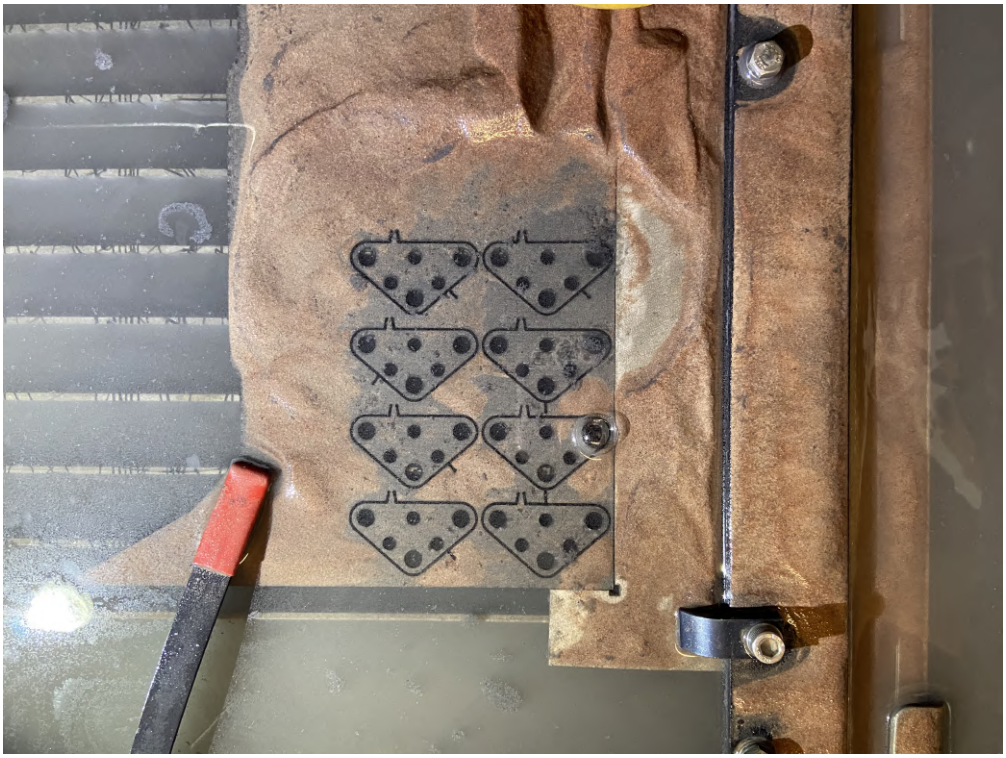

Figure 9: Waterjet-cut carbon fiber components

(a) V2 CAD model

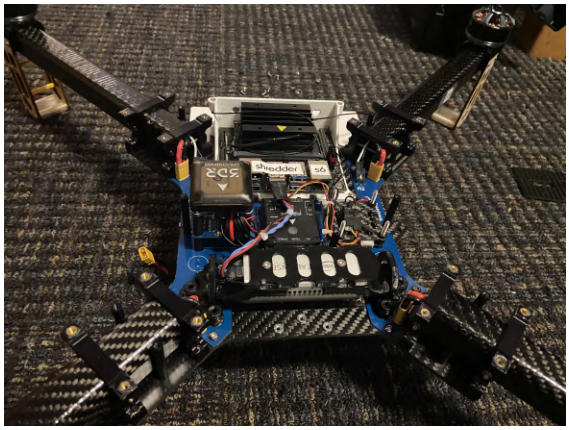

(b) V2 flight electronics

(c) V2 prototype flight test

Figure 10: Swarm Drone V2

Similar to the V1, the Swarm Drone V2 utilized mostly carbon fiber construction to be as light weight and inflexible as possible. It successfully increased flight times to approximately nine minutes and decreased AUW to under 2.5 kg. The V2 design was deemed functional enough to scale production to an additional five vehicles to make up the rest of the swarm. Fig. 11 below shows an image of all 6 of the early Swarm Drone V2 prototypes.

Figure 11: Swarm Drone V2.0 fleet of six vehicles

While successful, the V2 design was still not sufficient to properly interface with the emerging deployment and recovery concepts. Furthermore, requirements for electronics changed due to software developments towards newer flight controller firmware. As a result of these emerging requirements, a final V3 version of the Swarm Drone was established as a subsequent goal in order to meet new software and sensing requirements. Development of the V3 Swarm Drone is elaborated upon in section 5.8.

4.3.2 Drop Mode

Drop Mode is a flight mode that can detect when an sUAS is experiencing a vertical free fall, arm the motors mid-air to stabilize the vehicle, and then hover in position. The original autonomy solution for the V1 was to have the Swarm Drones in ”stabilized” flight mode, which automatically tried to level the drone with the horizon when the vehicle is armed. Of the numerous concerns about the validity of this procedure, one was the ability of the Swarm Drones to operate under

the downwash of the Carrier Drone. Another concern was the height necessary to allow for the Swarm Drones to catch themselves. In order to answer these concerns, a Tarot Ironman 1000 sUAS octocopter airframe was modified with an under slung payload rack to deploy first person view (FPV) quadcopters to test Drop Mode. The Tarot Ironman 1000 frame with three FPV quadcopters is shown mounted on initial payload rack system in Fig. 12 below.

Figure 12: Octocopter with three FPV quadcopters for the initial test of Drop Mode

This initial test concluded successfully with each of the FPV quadcopters stabilizing mid air before landing on the ground via pilot control. The test proved that the concept of Drop Mode was mechanically feasible and did not require any major hardware modifications to the Swarm Drones. Although from a software perspective, Drop Mode still had to overcome some significant barriers. The original Swarm Drones used in this initial test were manually piloted where humans visually determined when their Swarm Drone had been dropped. Many of these advanced features used in the Pixhawk 4 Flight Controller (FC) PX4 software also come with their own sets of preflight checks, safety parameters, and pre-requisites. One of the most important preflight checks was on the vehicle's Intertial Measurement Unit (IMU), which detects if the sUAS is stationary when an arm command is sent. If the vehicle is experiencing any movement outside of a certain threshold, the FC will reject the arm command, which could prove catastrophic for the Swarm Drone being deployed. Although these preflight checks could be disabled, it would introduce unnecessary risk to change low level parameters in stock firmware. This resulted in the need for a more integrated solution for the Drop Mode configuration.

Following the successful manual control drop test, the preliminary autonomous drop testing began. Using a DJI F450 drone enabled with a PX4 flight controller, a confirmation test was performed to confirm that the "Drop Mode" aerial deployment provided by the ArduCopter flight firmware could aerially arm and stabilize a UAS after being dropped. The test performed is outlined in Fig. 13. First, the F450 was powered on at the top of a tall stadium wall and placed into the Drop

Mode flight mode (Fig. 13a). Next, while the propellers were not spinning, the F450 was pushed laterally such that it fell off of the wall (Fig. 13b). During the free-fall, the F450 tumbled and even completely inverted. Approximately 4 meters into free-fall the Drop Mode was initialized, the propellers began spinning and the onboard FC began stabilizing the UAS (Fig. 13b). The FC finally stabilized the UAS at an altitude approximately 30 meters below the drop point (Fig. 13d). Following stabilization in the UAS autonomously landed itself, which showed that the vehicle was ready to perform any subsequent autonomous behaviors after its aerial deployment.

(a) Enable Drop Mode at top of wall **(b) Push drone off of wall** **(c) Drop Mode initializes, motors spin** **(d) Drone stabilizes**

Figure 13: Drop Mode testing

4.3.3 Multidrop Bay

In parallel to the developments of the Swarm Drone V1 (section 4.3.1), concept research for deployment and reintegration mechanisms began in 2019. Initially, work focused solely on the deployment aspect with constraints requiring a payload that could drop multiple drones while taking up minimal space. Progress was catalyzed by the V1 mechanism shown in Fig. 14 below and mounted to a vehicle above in Fig. 12. The orange 3D printed geometries shown in these images passively locked into the frames of sUAS which are released by servos.

In 2020, reintegration was prioritized as a design constraint. With this, the initial concept of the Multidrop Bay was created. Functionally, it was a payload with a large central void that would allow for drones to land on top of, pass through, and be dropped out of the bottom of a carrier vehicle. It was prototyped as a wooden lattice structure with levels of actuators that acted as an active, gravity-fed deployment mechanism for the mentioned Swarm Drones. Design iterations also involved research into light weight, pulley-based linear actuators as well as geometries on the top of the lattice for passively aligning Swarm Drone propellers during landings. These concepts all resulted in the Multidrop Bay V2 assembly and CAD shown in Fig. 15a. The blue 3D printed parts illustrate the mentioned linear actuators that control the passage and selective deployment of Swarm Drones through the payload.

Figure 14: Early Drone Drop Mechanism Prototype

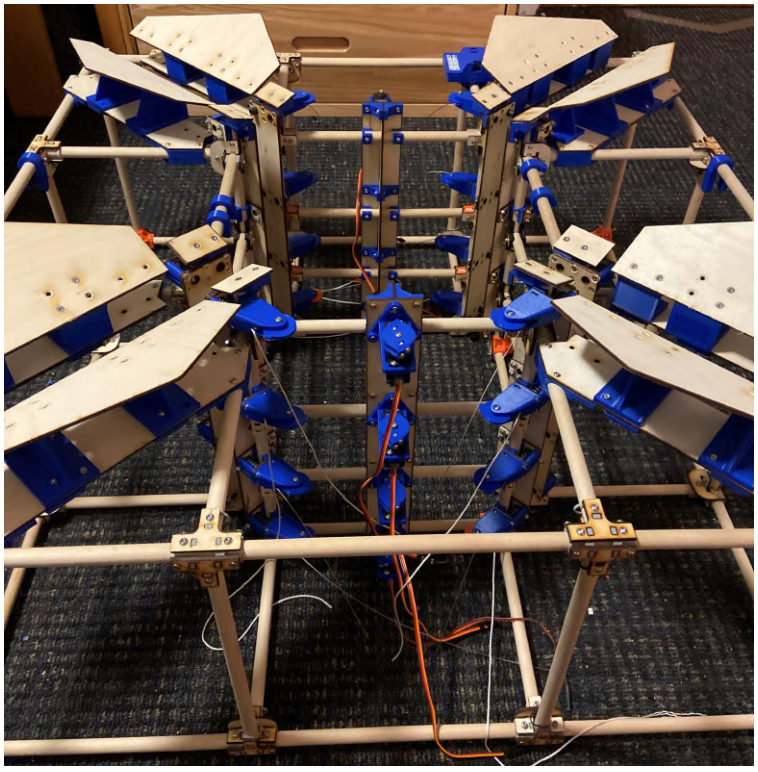

(a) Physical prototype

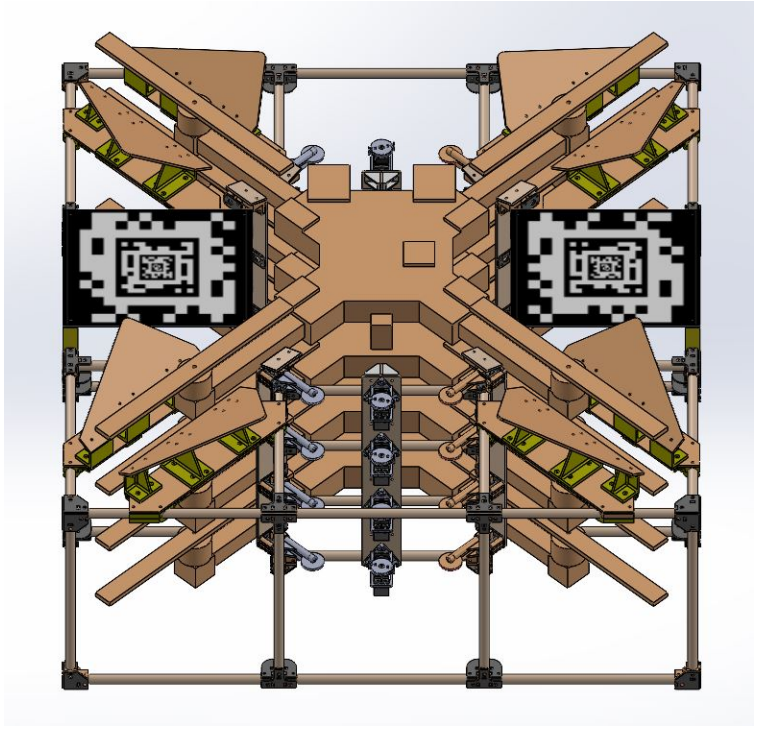

(b) CAD render

Figure 15: Multidrop Bay V2

The Multidrop Bay V2 used tension cables and pulleys to actuate the levels within the lattice of the design. These worked for actuation, though the assembly of the Multidrop Bay was difficult as each member required custom tuning and wire tensioning to work consistently. There were also issues with the manufacturing process of the frame. Due to having many connectors, the frame required hundreds of precision-drilled holes for assembly. Despite careful jigging during drilling, tolerance stack up errors accumulated, resulting in inconsistency in key dimensions, causing jamming when the Swarm Drones dropped between levels. Lastly, the corner connectors between the circular frame members did not have a common design, leading to a high amount of unique parts. All of these issues were noted for the future design and assembly of the Multidrop V3. To help with the assembly of the future Multidrop V3 with assembly in carbon fiber, a custom 3-axis Computerized Numerical Control (CNC) was developed to reliably and accurately drill holes in the frame to attach connectors to. Subsequent improvements are discussed in detail within section 5.7.

4.3.4 Carrier Drone

The proof of concept for the Carrier Drone used an off the shelf Tarot Iron Man 1000 sUAS octocopter frame, shown in Fig. 16. This frame was left mostly stock, with modifications made to outfit the on board Pixhawk flight controller, as well as the initial Multidrop Bay proof of concept. This was the same frame used in the Drop Mode test outlined in section 4.3.2.

(a) Physical prototype in the field

(b) CAD render

Figure 16: Carrier Drone proof of concept

After tests with the proof of concept Carrier Drone were completed, work began on designing a new frame that was both compatible with the ongoing development of the Multidrop Bay, as well as perform functionally as a UAS. To test and validate the new Carrier Drone, a 1:2 scale model was created shown in Fig. 17. Instead of using carbon fiber, the frame members were made out of wood and the connectors were largely 3D printed. This allowed for cheap and quick manufacturing, as it was purely for validation of flight characteristics of the frame.

(a) Completed model in field

(b) In flight

Figure 17: Carrier Drone scale model

From this data, the full scale version of the Carrier Drone was designed using square carbon fiber tubes and carbon fiber plates for the connectors. The custom 3-axis CNC used in the assembly of the Multidrop V3 was also used to drill out the members of the frame of the Carrier Drone. Due to the geometry of the frame, many different types of connectors are required to hold the carbon fiber tubes together. These connectors went through many stages of development, gradually moving away from laser-cut wood and 3D prints to only carbon fiber plates to optimize weight and structural strength. One of these progressions is shown in Fig. 18.

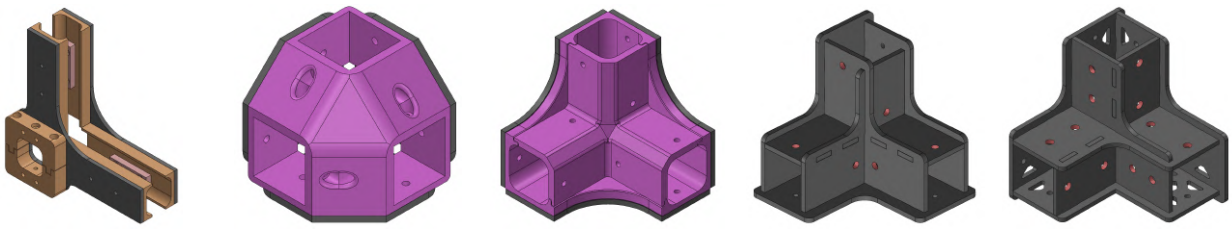

(a) Version 1 (b) Version 2 (c) Version 3 (d) Version 4 (e) Version 5

Figure 18: Corner connector design progression

4.3.5 Companion Computing

Companion computing is a general solution to vehicle control. It provides an interface to the PX4 flight controller running the PX4 software stack and generalizes a lot of the interactions to allow for a fully autonomous system with custom implementations. The way PX4 is implemented, it can be interfaced through a few systems: QGroundControl, MAVLink, and Real Time Publisher Subscriber (RTPS). QGroundControl is a high level Graphical User Interface (GUI) and it allows for users to create custom paths and see real time debugging (Fig. 19). MAVLink is a lower level interface where pre-defined messages can be sent over the network and then processed. This is actually what QGroundControl uses in the back-end. RTPS is the lowest level interface to PX4. It is similar to MAVLink in that it is sent over the network, however, it by-passes the pre-processing that occurs with MAVLink and directly communicates to PX4.

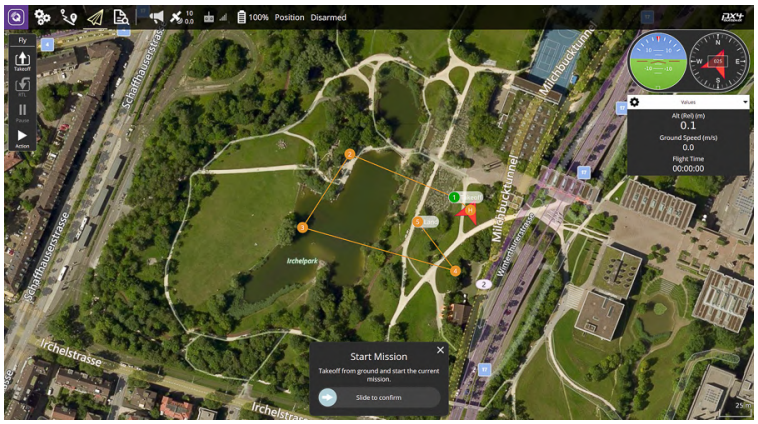

Figure 19: Example of QGroundControl GUI [8]

This project is using RTPS since it natively communicates with ROS2, allowing for easily building custom commands, and has significantly higher rates of communication (up to 500 Hz). ROS2 is an open source project commonly used in industry for controlling robotics. This project utilizes ROS2 for all of its communication and debugging. A diagram showing how PX4 and ROS2 communicate with each other can be seen in Fig. 20.

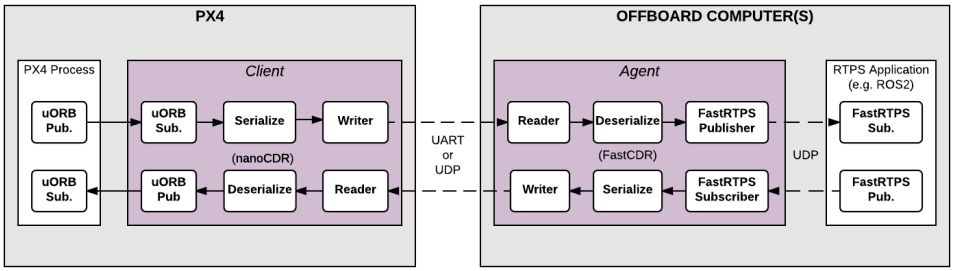

Figure 20: Communication framework between PX4 and ROS2 [9]

Using the tools mentioned previously, companion computing was built with an abstract interface for commanding positions and velocities to the vehicle. It also outputs relevant information of the vehicle state, such as GPS status, position, and orientation. This prior work established a strong foundation for capstone. As part of capstone, the goals changed to establishing a more consistent communication framework, making it easily accessible and testable via a a custom shell interface, extending support to control multi-vehicles, and improving upon the fail-safes for control commands.

The flight controller used is running PX4, as stated before, but there was initially another option for control called ArduPilot. There was initial testing using ArduPilot, but it was decided that PX4 supported a better interface for ROS2 and also had a more active community of developers. All problems that were run into when using PX4 were directly solved by talking with the people who wrote the software. Discussions were done through various resources, such as Slack and the PX4 discussion website. Even in cases where this project needed to implement custom solutions, such as Drop Mode, advice was received from those resources.

4.3.6 Simulation

To ensure that every autonomous action was working as intended the team used both Software in the Loop (SITL) and Hardware in the Loop (HITL). These two approaches were previously explored by the team and allowed for the rapid testing and validation of the flight software without waiting for possible hardware or manufacturing delays. Additionally this gave the team confidence in the validity of the software before all physical flight tests.

The SITL approach encompasses using the Gazebo open source robotics simulator with a custom built environment. Within Gazebo each sensor on the drone is simulated in software (i.e PX4 controller, GPS, Realsense camera, IMU, etc.) such that there is a 1:1 match with the real world. In testing, the team has found that in the field the main difference between Gazebo and the real world is additional sensor noise. Gazebo is designed to work with ROS2 so it makes the development process as smooth as possible. With ROS2, it is possible to spawn as many drones as desired, and the launch process for the simulation has been setup in a way to support multi-vehicle simulation testing.

HITL is a simulation mode where the software is running on a physical PX4 flight controller. However, the drone is still simulated in Gazebo. This allows for the verification of the PX4 firmware without having to physically fly the drone, and is usually the last step before actual field testing.

4.3.7 Path Planning

As noted in the Swarm Application section (3.5.1), collaborative UAV swarms have been used for efficient search of an area. A stretch goal of the this project would be do demonstrate various collaborative search algorithms using the entire system.

To accomplish the task of a Search and Rescue (SAR) mission (step 5 in Fig. 22) with a deployed swarm of UAVs the team is researching Coverage Path Planning (CPP) techniques for UAVs [35]. As the focus of this project is the deployment and recovery system, the actual SAR mission scope will be limited. The planned scope would be to utilize approximate cellular decomposition within a known search area, divide it into n polygons for n drones (Fig. 21a) and to test various CPP algorithms (Fig. 21b i.e. lawnmower, spiral etc.) These were early examples implemented in Python using the Shapely math library as a proof of concept for the algorithms.

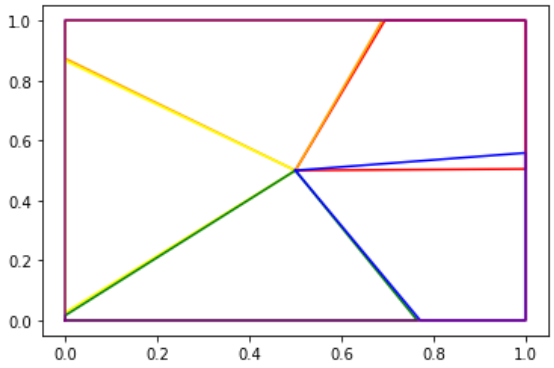

(a) Polygon division example

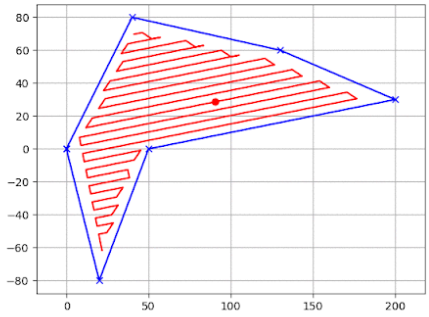

(b) Lawnmower coverage path planning example

Figure 21: Coverage Path Planning

4.4 Regulations

In the United States the FAA distinguishes UAV primarily based on their intended usage and weight class. The two categories of UAV operations are 14 CFR Part 107 and 49 U.S.C. 44809. 14 CFR Part 107, or more typically abbreviated as Part 107, are the regulations that dictate commercial operations of sUAS systems. This includes, but is not limited to, speed, altitude, pilot to vehicle ratio, and mission objective. 49 U.S.C. 44809 or the exception for limited recreational operations of unmanned aircraft, establishes regulations for purely recreational sUAS and UAS system operations. These regulations are much less restrictive than Part 107, allowing hobbyists and novices to continue their past time without significant overhead rules.

Although recreational regulations apply to both sUAS and UAS operations, Part 107 regulations are bound to sUAS operations only. Commercial UAS operations have much stricter system of evaluation before any flight operations can be conducted. There are currently two pathways, as of the time of writing, type certification and 49 U.S.C. 44807, Special Authority for Certain Unmanned Systems, also known as Section 44807 [36]. Type certification is an intense FAA design review process that seeks to verify and validate a UAS design to the same set of standards that conventional manned aircraft are held to [37]. The Section 44807 is on case by case basis waiver given to organizations that can demonstrate safe operations in national airspace and are in the best interests of the public. This is a very broad definition that allows the FAA to control who exactly has the ability to conduct commercial UAS operations. The result of this is a very difficult to enter procedure process that requires insider connections to initiate communication with the appropriate FAA officials.

The initial approach of Swarm Carrier capstone to legally operate was to register the Carrier Drone and the Swarm Drones as Part 107 sUAS. This would elevate the legitimacy of the system and increase the testing location operations as a commercial system. The problem though was as an overall system, the Carrier Drone and the Swarm Drones would be over the 55 lb limit and be classified as an UAS. This meant that the group had to go through one of the two routes to obtain UAS operation permissions, as explained previously. This proved to be a significant bottle neck within the time constraints of the capstone project. As even with connections and regular meetings with the Massachusetts Department of Transportation (MassDOT), the project was unable to guarantee test site to operate legally. This led the capstone to take a different path to operate the system legally.

5 Designs

5.1 Flowchart Overview

The original system functional flowchart is shown in Fig. 22. A Carrier UAS will contain one Multidrop payload bay of three Swarm Drones. The developed deployment and recovery system will function as such:

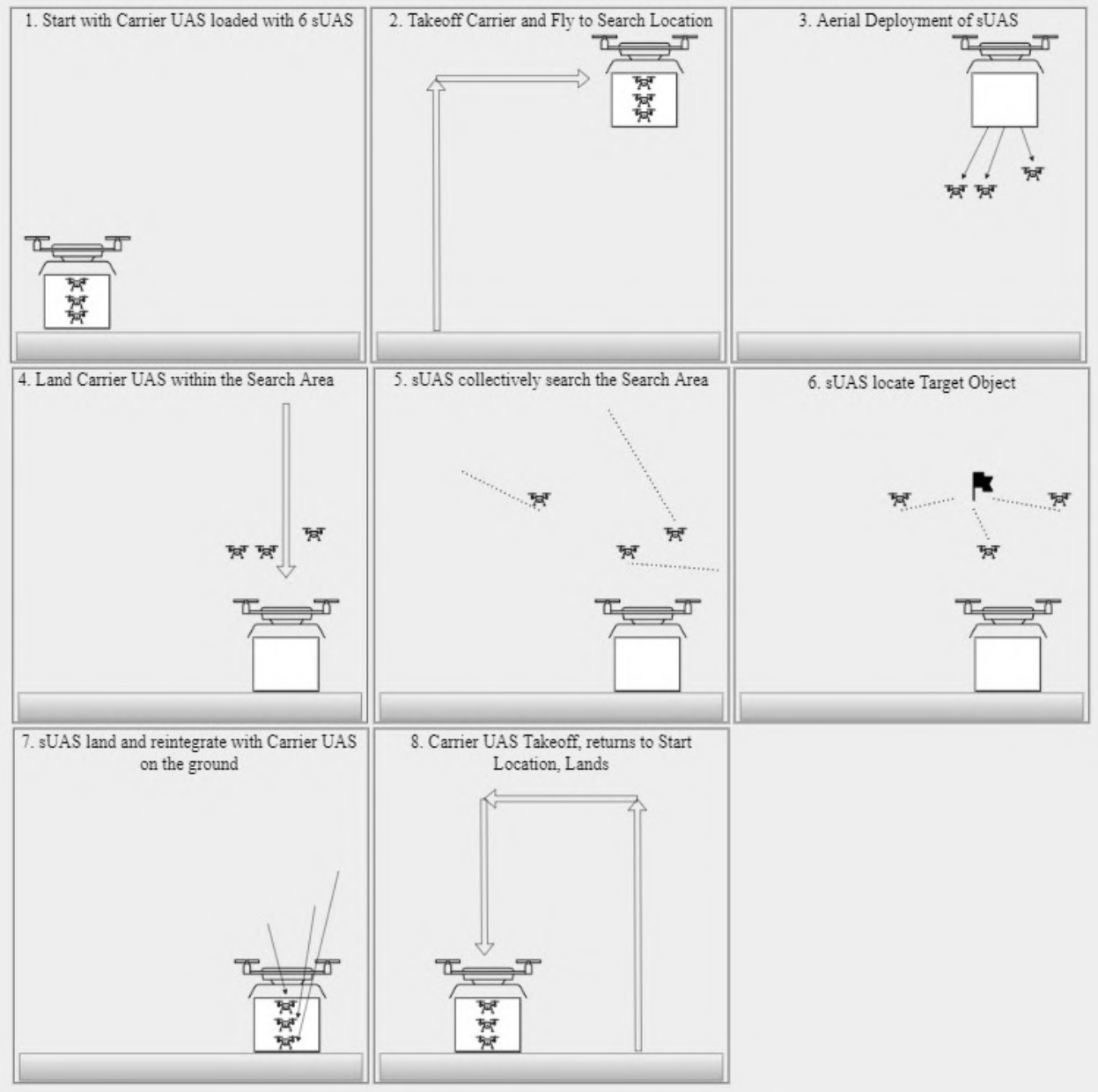

Figure 22: High level task flowchart

1. The Carrier UAS loaded with three Swarm Drones will start at its designated starting location.
2. The Carrier UAS will take off vertically to its designated drop altitude of 30 meters. The Carrier UAS will then traverse horizontally to the designated Search Location.
3. The Carrier UAS will deploy each Swarm Drone individually; dropping each out of the bottom of its multidrop bay.
4. Once all the Swarm Drones have been deployed, the Carrier UAS will land.
5. The Swarm Drones will then begin their mission. For this project, the designated mission is an area search.
6. The Swarm Drone mission will reach its end conditions. For this project, either the target will be located or the Swarm Drones exhaust their flight time.
7. Each Swarm Drone will sequentially land and reintegrate with the Carrier UAS.
8. Once all the Swarm Drones have been recovered, the Carrier UAS will takeoff vertically to its return altitude of 10 meters then traverse horizontally to its starting location. Once at the starting location, the Carrier UAS will land.

Due to the high complexity of deployment and recovery as well as the distributed nature of the control scheme, subsystem communication is required. Fig. 23 displays the subsystems and their communications. The Swarm Drones and Carrier UAS communicate with one another over a WiFi connection. For this Capstone Project, a single ground mounted TP-Link router is used to connect all the drones and the ground control system via an offline connection with static IP addresses. The Carrier UAS communicates via the Multidrop Bay via an Inter-integrated Circuit (I2C) connection to control the servo actuation. The feedback that the Swarm Drones receive from the Multidrop Bay comes from a contact sensing pad that acts as a hard stop, telling the Swarm Drones to stop motor spinning once triggered.

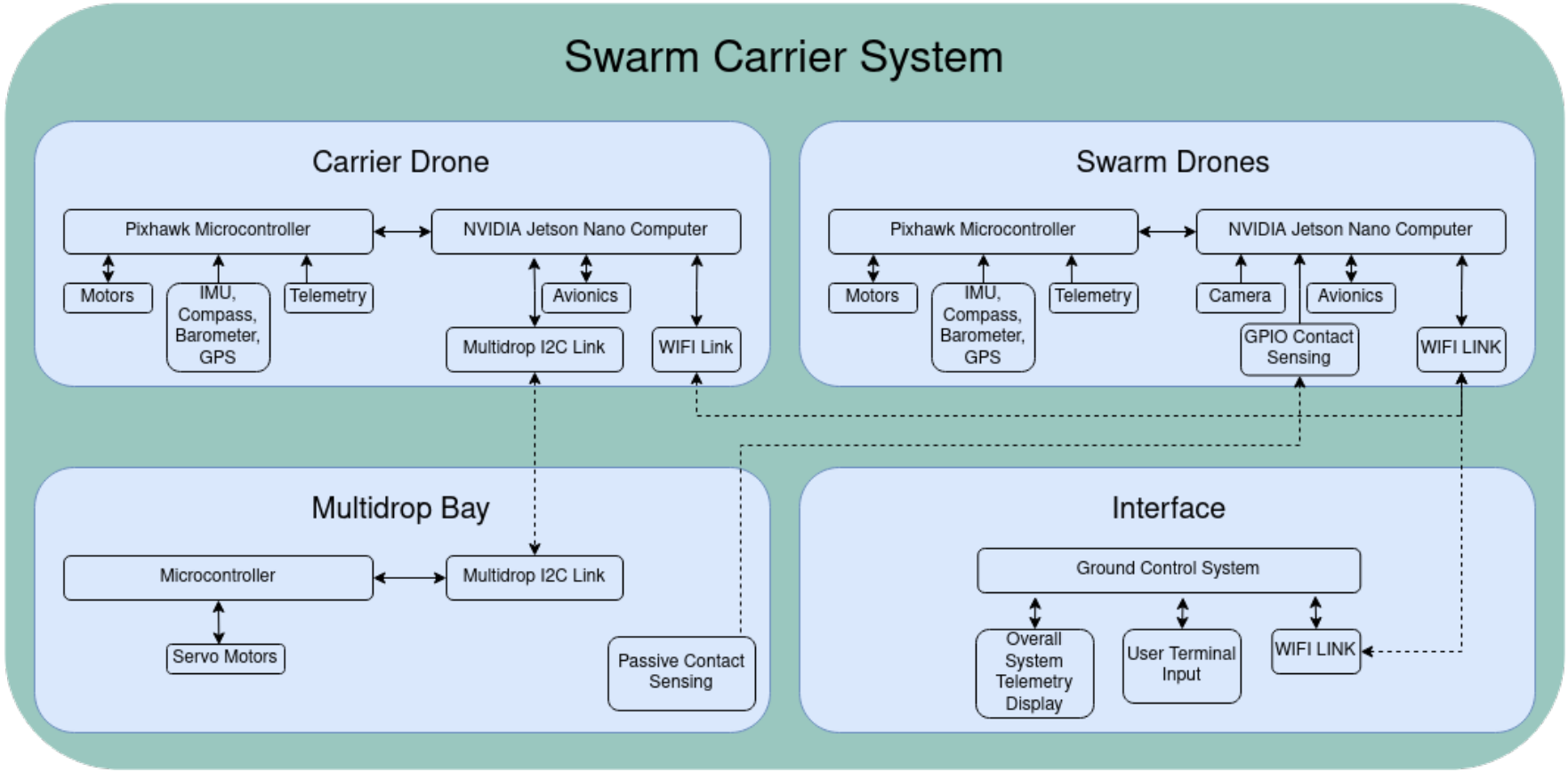

Figure 23: System flowchart

5.2 Swarm Carrier System Level Objective Re-evaluations

Before the beginning of Capstone II in the fall, the group met to evaluate the capability of the project to meet the original high level task flowchart objectives. This evaluation arose from the idea that certain subsystems and tasks could be removed while accomplishing the problem statement. A weighted decision matrix was created to decide the direction the project would take in the fall. Different configuration of the Carrier Drone, Multidrop Bay, and the Swarm Drones were considered in this decision matrix with four final combinations evaluated. Based on the criteria laid out for the decision matrix, the conclusion drawn was that the Carrier Drone would have a decacopter layout with a single Multidrop Bay, and three Swarm Drones would be used in the final system level test. This analysis drove the Carrier Drone V2 design, shown in the Carrier Drone 5.3 section. The Multidrop Bay V3 would remain the same, while three Swarm Drones be converted to their final V3 design. A figure of the weighted decision matrix used to guide the project's direction is shown in Fig. 24. Sections 5.3, 5.7, and 5.8 below discuss the progression of the Carrier Drone, Swarm Drones, and Multidrop Bay respectively. It should also be noted that the Carrier Drone V2 did not become the final design, which is detailed further in section 5.3.

Final System Options			Weights (1:poor-10:best)								
			5.5	8	2.5	6	7.25	1.5	6.75	4.75	
Carrier Configuration	**Number of Swarms**	**Number of Multidrop bays**	**Frog Outfitting**	**Capstone Fullfillment**	**Redesign Risk**	**Assembly Time**	**Drill Time**	**Cost**	**Flight Safety**	**Swarm Capability**	**Totals**
Decacopter	6	2	3	8.75	5	3.25	3.25	2.25	9.25	10	255.375
Decacopter	3	1	6.5	8	5.5	6	6	4.75	7.75	5	276.1875
Dodecacopter	6	2	3	4.5	7.75	5.5	5.5	6.5	5.5	8.25	230.8125
Dodecacopter	3	1	6.5	3.75	8.5	8.75	9.25	9	5	3.5	270.4375

Figure 24: System level objective re-evaluation weighted decision matrix

5.3 Carrier Drone

Within the Swarm Carrier system, the original Carrier Drone design was an ultra-heavy lift airframe responsible for carrying a group of up to six sUAS (Swarm Drones) within the mentioned Multidrop Bay payloads. It had a 2500 mm x 2500 mm (motor to motor diagonal distance) dodecacopter constructed from a carbon fiber laminate matrix. The frame itself weights just 9.5 kg despite its large size. The scope of the Carrier Drone's development encompasses continued frame design, payload interface, electronics routing, power electronics testing, and flight trials. Fig. 25 below shows an early render of the Carrier Drone and the assembly of the frame.

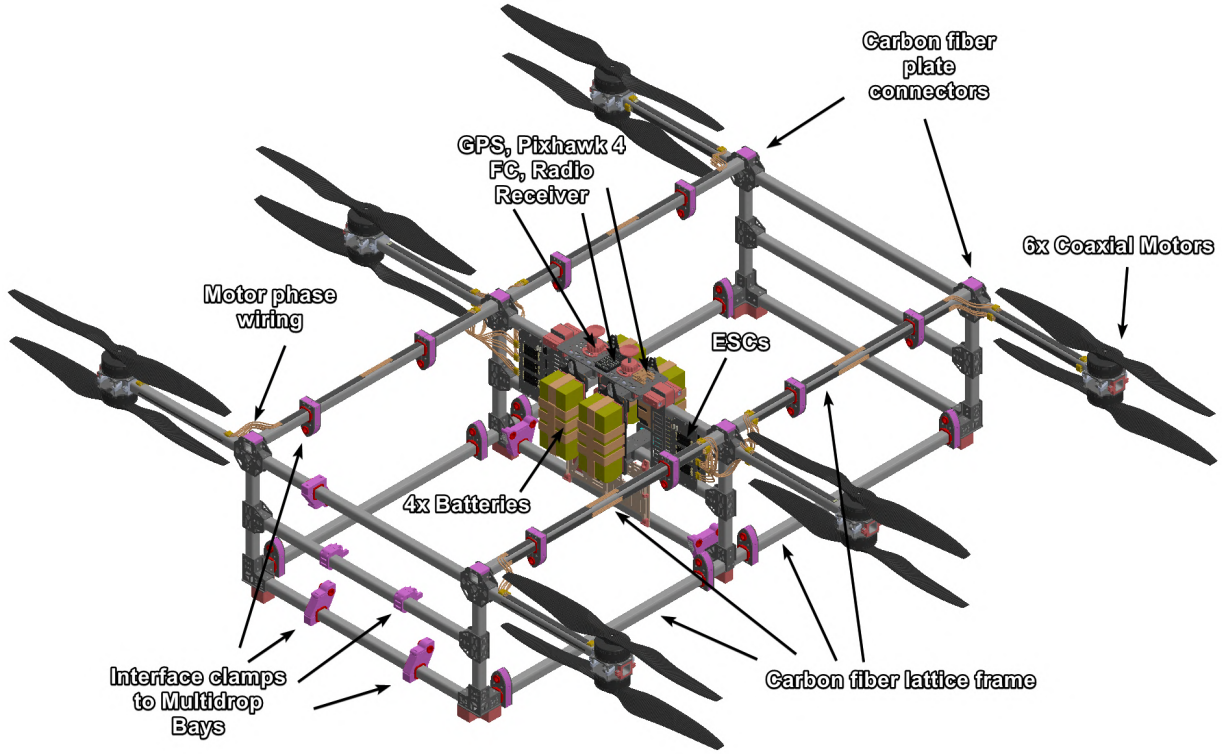

(a) Carrier Drone V1 CAD

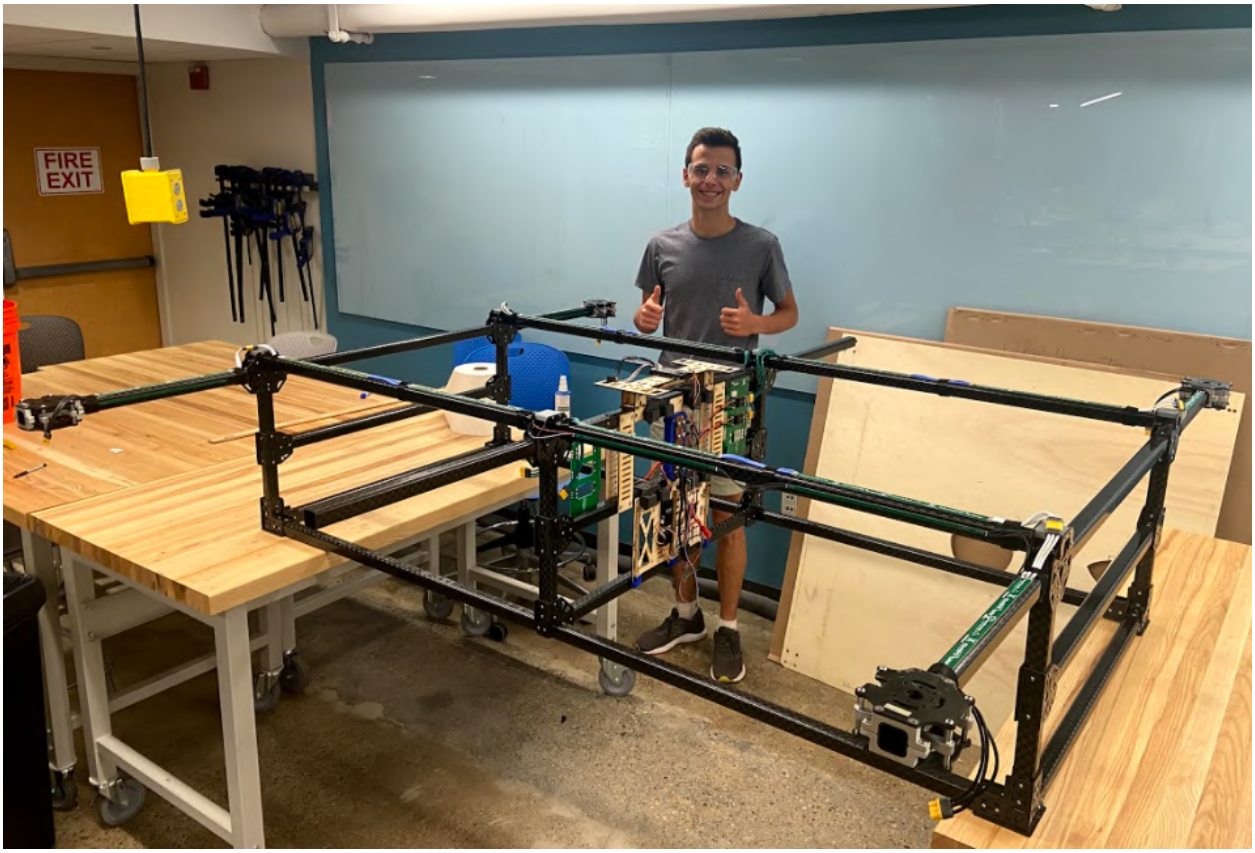

(b) Carrier Drone V1 Airframe Prototype

Figure 25: Carrier Drone V1

The design of the Carrier Drone has underwent two version iterations since its original design at the end of Capstone I. The V2 design of the airframe sought to create a planar configuration of a decacopter vehicle in order to have a more efficient design by avoiding propeller overlap. This airframe boasted a much larger size, having a 3400 mm x 3400 mm (motor to motor diagonal distance), which dwarfed the previous airframe's size. Problems arose after the initial quadcopter test of the Carrier Drone V1, which revealed that the frame dynamically deflected during operation. The frame not only deflected upwards with the thrust, but twisted torsionally, which was especially apparent on unsupported members such as the cantilever beams that supported the motors of the Carrier Drone V1. A visualization of this deformation can be seen below in Fig. 60. This cantilever design of the airframe proved to be a much larger concern than originally thought, which made the group rethink how it would move forward with its new designs. Due to its longer cantilever design, the planar Carrier Drone V2 design was deemed too much of a risk with its extremely long cantilever members. An image of the V2 design in CAD is shown in Fig. 26.

Figure 26: Carrier Drone V2 CAD

The Carrier Drone V3 design arose after the scope of the project was scaled back and it became apparent that a more conventional design was necessary to make the Carrier Drone feasible within the timeline of Capstone II. The design went with a more conventional octocopter design that the group had experience with operating previously. In addition, since only a single Multidrop Bay was necessary for the final design, the footprint of the frame was significantly reduced from the V2 design. The Carrier Drone V3 Cad is shown below in Fig. 27.

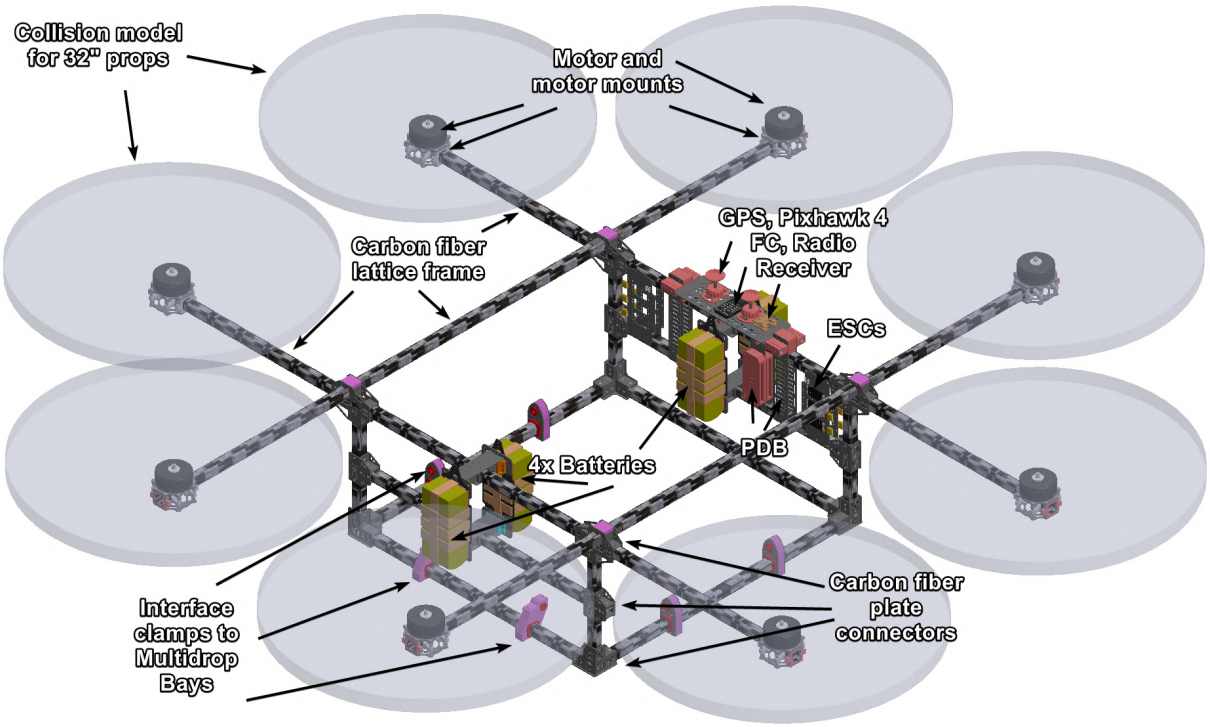

Figure 27: Carrier Drone V3 CAD

The V3 design addressed tolerance problems of straightness of the material by using cable tensioning to purposely pretension the frame members to maintain rigidity. The tensioning of the frame is a work in progress, some of the proposed tensioning schemes are shown in Fig. 28. The progression of the V1 through V3 design of the Carrier Drone's design are also shown in Fig. 29.

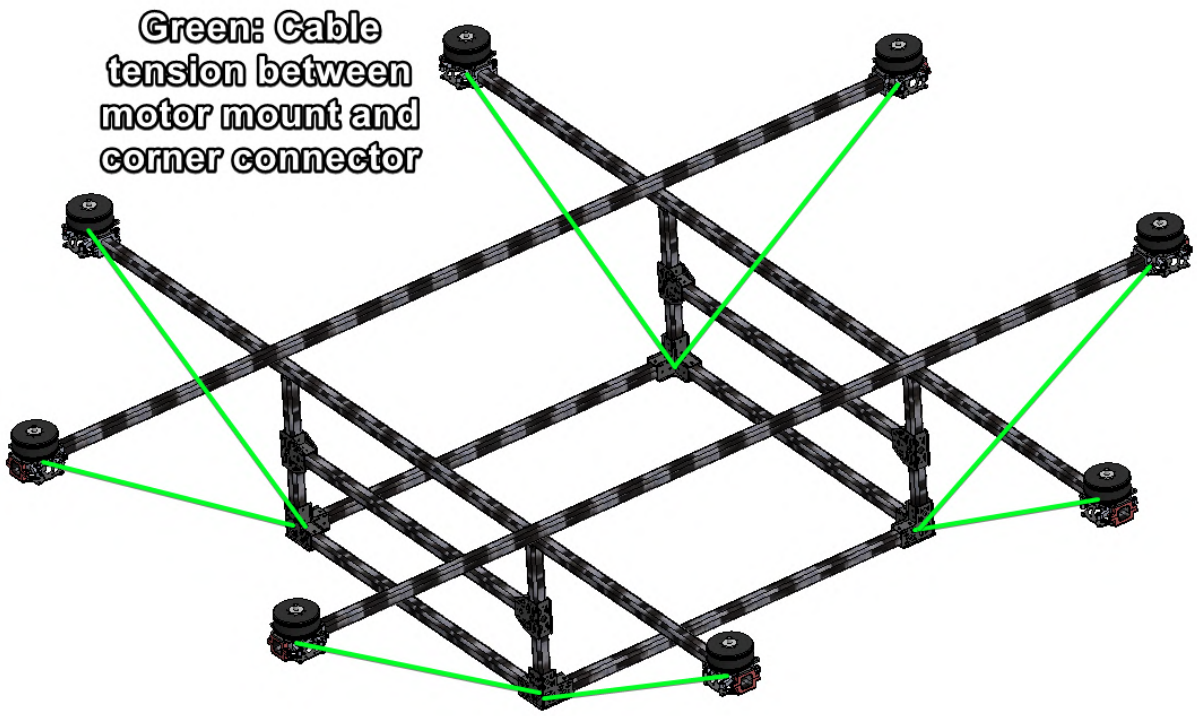

(a) Carrier Drone V3 tensioning scheme for motors to corner connectors

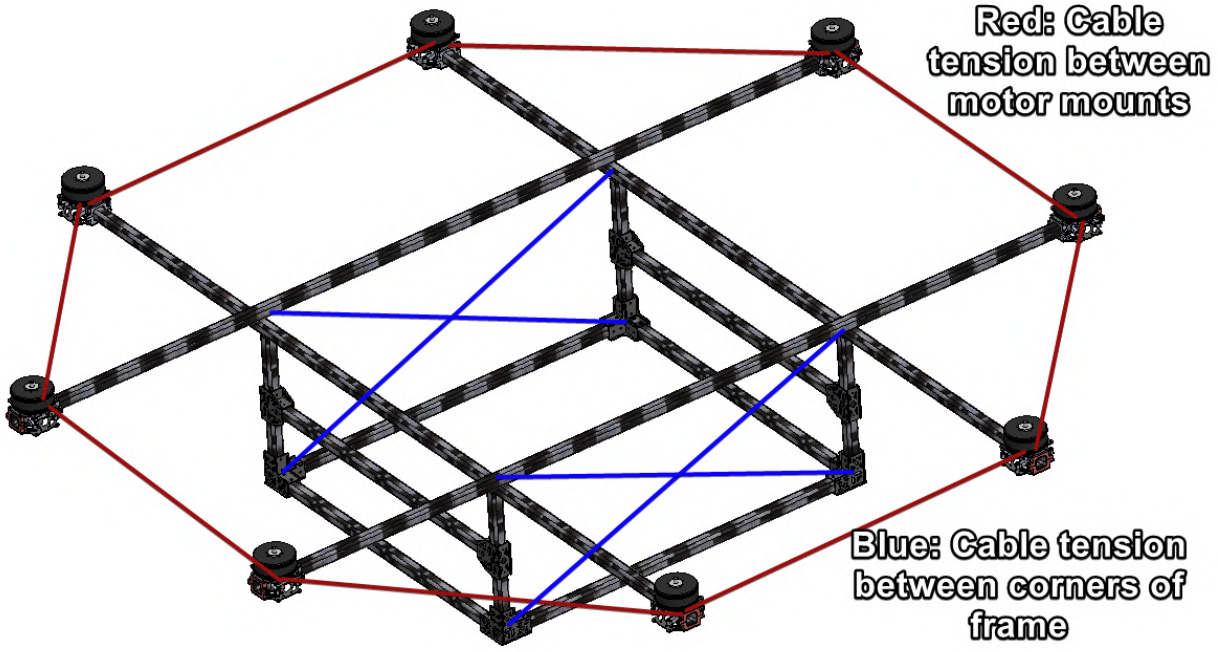

(b) Carrier Drone V3 tensioning scheme for individual motors and frame corner connectors

Figure 28: Carrier Drone V3 tensioning schemes

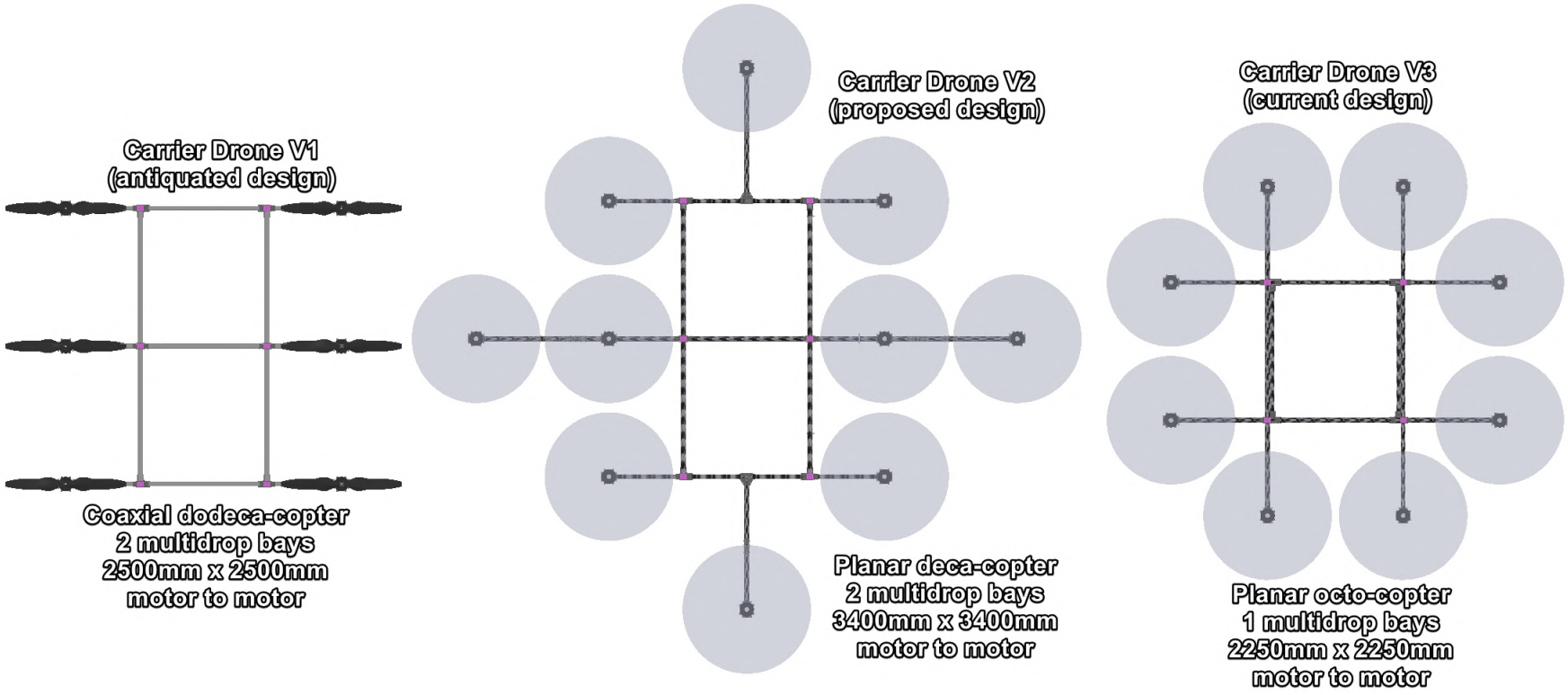

Figure 29: Carrier Drone Design Progression

5.3.1 Carbon Fiber Material Evaluation

In order to mitigate deflection and torsional twisting of the Carrier Drone's carbon fiber members, considerations were made to change the material to a higher stiffness material. The company Rock West Composites offers three modulus of carbon fiber square tubing in the dimensions currently used in the design. The current modulus being used is intermediate modulus, which utilizes Pyrofil MR60H 24K carbon fiber, has a modulus of elasticity of 42 msi [38]. The high modulus carbon fiber tube that was considered uses Pyrofil HR50 carbon fiber, which has a modulus of elasticity of 57 msi [39]. Although it is typically not possible to do a direct comparison between composite materials due to their orthotropic nature, due to the direct comparison of materials that use the same layup scheme, a direct comparison between laminate materials was possible. The high modulus carbon fiber had 35.7% increase in stiffness over the intermediate modulus. This came with a 52.4 % increase in cost though. The group realized that irregardless of the material stiffness, that wire tensioning would have to be used to correct previously mentioned tolerancing problems with the stock material. It was therefore determined that the price to benefit of using a higher modulus carbon fiber was unfavorable for the design, as the deformation problems of the airframe could be solved easier and cheaper using wiring tensioning schemes shown previously in Fig. 28.

5.3.2 Motor Mount Design

Within the overall development of the Carrier Drone, the choice and subsequent design of a motor mounting scheme is the most critical for the overall vehicle functionality. From July to August of 2021, extensive investigations and design iterations were performed to determine the propulsion scheme required to lift the desired payload of six Swarm Drones. Early designs leveraged composite waterjet-cut carbon fiber and machined aluminum to create a fixture capable of supporting co-axial motor configurations and tensile forces of up to 30 kgf.

Fig. 30 below shows the modularity of existing designs that are compatible with single and co-axial motor mounting configurations. In the future, only the single mount will be used due to results regarding efficiency and all up thrust in section 5.3.4.

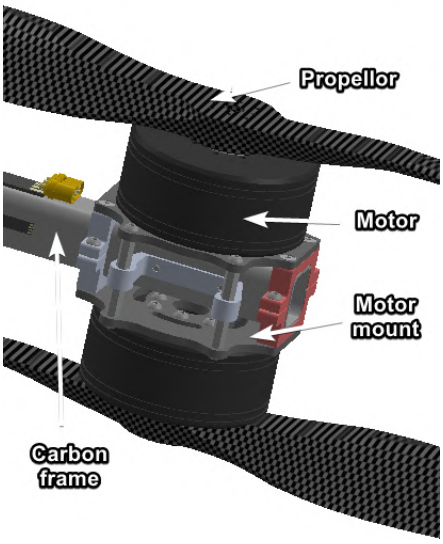

(a) Co-axial Motor Mount Configuration (CAD)

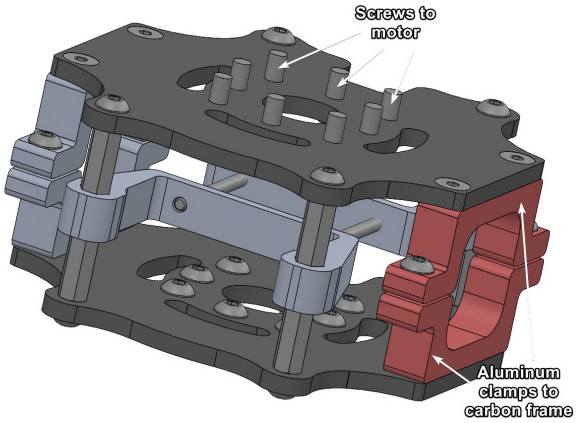

(b) Motor Mount Assembly (CAD)

Figure 30: Carrier Drone Motor Mount

5.3.3 Carrier Drone Battery Mechanism

To power the Carrier Drone, four Tattu 6s 22000mAh batteries were required. These weigh 2.65 kg each, and resemble a dictionary in size. The mounting location of the batteries also must be in the center of the Carrier Drone in order to limit inertial effects and to consolidate electronics and wiring. The last constraint is that the battery mechanism must extend far enough around the Multidrop Bay to avoid interference. For efficient operation of the Carrier Drone in the field, these batteries must be quickly and securely attached to the Carrier Drone. With these constraints and criteria in mind, during July and August, solutions were brainstormed and prototyped.

The initial battery mechanism is shown below in Fig. 31. The main body of the battery mechanism is fixed to the frame, and is composed of interlocking 2.5mm carbon fiber plates. The battery is attached to a sled, shown in Fig. 31b. When assembling the mechanism in the field, the sled attaches to the main body by aligning with four shoulder screws, which also hold the weight of the sled. The entire assembly is then held together by the latching mechanism shown in Fig. 31b, which makes the entire assembly a rigid body.

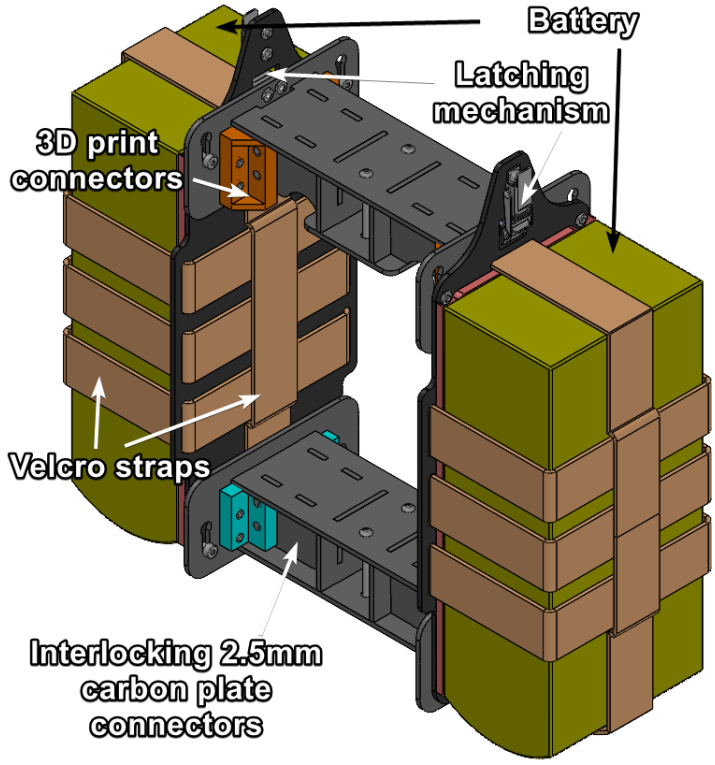

(a) Assembly of the battery mechanism

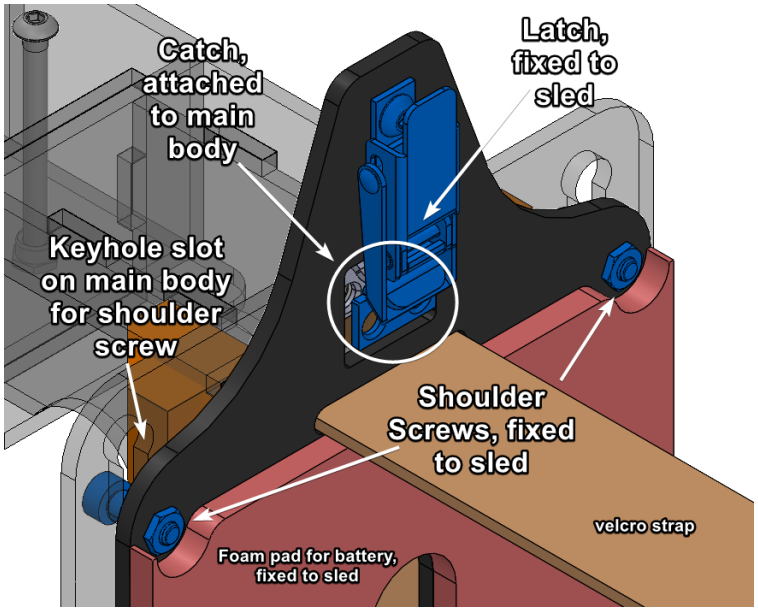

(b) Close up highlighting shoulder screws and latch

Figure 31: Battery mechanism

The location of the battery mechanism in the V3 Carrier Drone is shown below in Fig. 32. Each battery weighs 2.65 kg, bringing the total weight of the battery mechanism to around 6 kg. These provide a large amount of inertia to the frame, so it is important to keep the load balanced and as close to the axis of rotation as possible. In the V3 Carrier Drone shown, the battery mechanisms are symmetric across the frame, while still leaving room for the Multidrop Bay in the center.

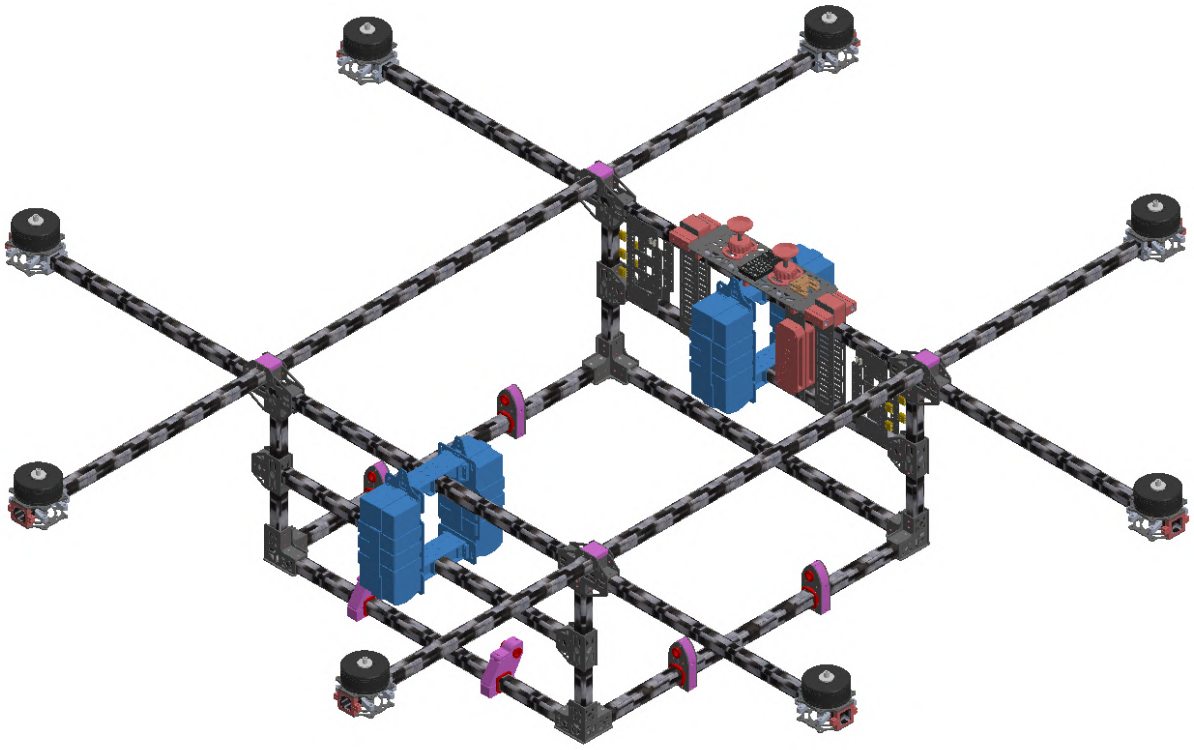

Figure 32: Location of the battery mechanism (highlighted blue) on the Carrier Drone V3

5.3.4 Motor Configuration

From the known Swarm Drone weight and number as well as approximations for the Multidrop Bay and carrier frame weights, the AUW was approximated to be $50kg$. Using the motor and propeller calculations outlined in [14] and Eqn. 3 it was determined that the most viable Carrier Drone configurations were a dodecacopter or a decacopter configuration with approximately 30 inch diameter propellers. With so many large motors and the difficulty of manufacturing carbon fiber tube frames, coaxial motor configurations for the dodecacopter and the decacopter were considered. The coaxial configurations would reduce the overall size of the carrier UAS and be easier to manufacture.

Prior to making definitive decisions on the carrier UAS airframe designs, the percent thrust loss from coaxial configurations needed to be determined. Researched sources appear to show that the percent thrust loss is not constant between different propeller sizes, thus the need for testing arose [4, 31]. Prior to this work, four TMotor P80III 100kv motors and Foxtech 3010 Carbon Fiber Propellers had been purchased. Subsequent thrust tests utilized an RCbenchmark S1780 motor thrust test stand, the motor thrust, voltage, current, torque, and rpm were recorded (Fig. 55). Once all the data was collected from the thrust tests, the group was able to conduct a detailed analysis for the system. The average of the upper and lower performances were averaged to display the average coaxial motor performance. The thrust vs rpm performances are displayed in Fig. 33a. It can be seen that all the motors are able to achieve the same rotational speeds. The upper coaxial motor had consistent performance with the single motor while the performance of the lower motor was significantly lower. The percentage of the single "control" motor's thrust as a function of RPM is shown in Fig. 33b. It can be seen that consistently across all RPM the lower coaxial motor had approximately 65% of the control motor's thrust output with the average coaxial motor thrust output being approximately 80% of the control. The recorded average thrust loss of 20% is consistent with [4]. From the test data, the motor electrical power vs thrust relationship $P_m(kgf)$ was determined (Fig. 33c).

With the approximated AUW, 12 cell 46Ah lithium polymer batteries, and Eqn. 3, the predicted flight time for dodecacopter, coaxial dodecacopter, and decacopter configurations were calculated for different numbers of Swarm Drones (Fig. 34a). In Fig. 34a it can be seen that the predicted flight time for the coaxial dodecacopter falls below the defined constraint flight time of 15 minute for all 6 Swarm Drones (Section 3.3). From the thrust data, a two dimensional polynomial regression for the PWM vs thrust was determined. From the different carrier airframe configurations, the individual motor hover PWM vs number of Swarm Drones is plotted in Fig. 34b. The PWM constraint of $1600\mu s$ (approx 60% throttle) is common in the UAS industry as a hover PWM value lower than 1600 guarantees a thrust to weight ratio of 2:1 which is required for good flight performance [14]. Both the coaxial dodecacopter and decacopter configurations show hover PWM values greater than $1600\mu s$. While the standard dodecacopter passed the quantitative analysis for the requirements, the complexity of manufacturing for a planar dodecacopter invalidated it. With all three of the considered Carrier Drone design configurations invalidated, different motor and propeller configurations were then considered.

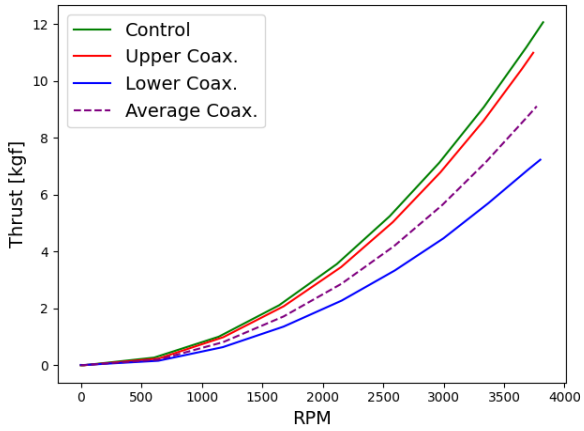

(a) Thrust vs. RPM

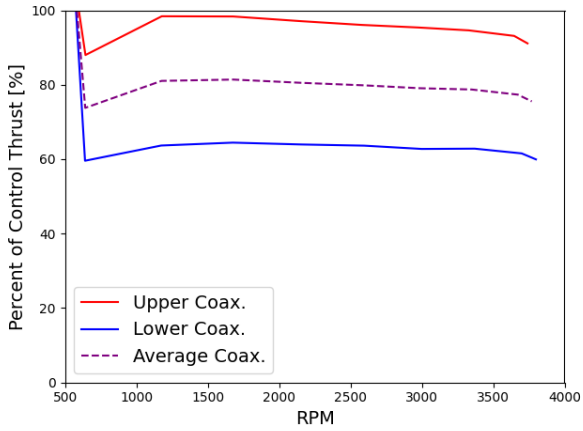

(b) Motor Power vs Thrust

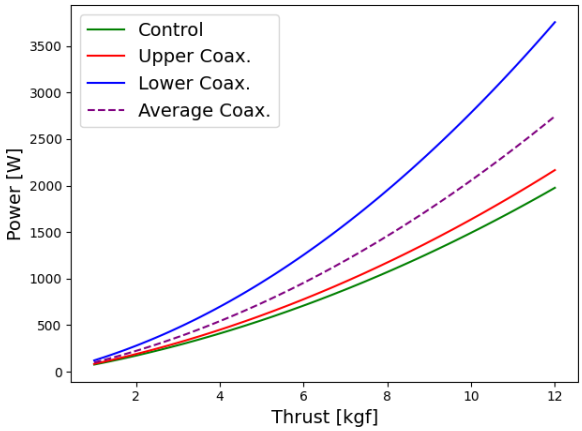

(c) Current vs. Thrust

Figure 33: Coaxial thrust test results

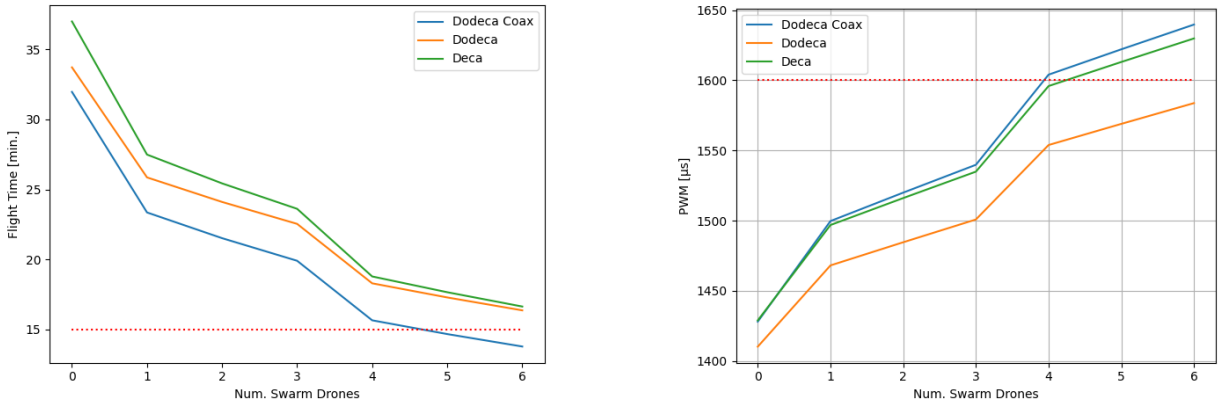

(a) Flight time vs. Num. Swarms **(b) PWM vs. Num. Swarms**

Figure 34: Experimental results design decisions

From the manufacturers' provided specifications and the known coaxial motor thrust loss of 20%, four different motor and propeller combinations were analyzed in coaxial dodecacopter and decacopter configurations for a total of 8 different configurations. Fig. 35c contains a legend of all the different configurations considered. The prefixes tell what motor configuration, different p80iii motor speeds were denoted by their kv value, 30 and 32 inch diameter propellers were denoted, and coaxial configurations were labelled as 'coax.' With similar analysis as above, the flight time as a function of number of Swarm Drones and the PWM as a function of Swarm Drones plots are displayed in Figures 35a and 35b respectively. The majority of the configurations were within the constraints as expected as they all used higher quality propellers than the experimental tests. As a result, the highest performing flight time configuration was chosen with the same TMotor P80III 100kv motors but using TMotor G32x11 propellers in a decacopter configuration with a predicted flight time of 21 minutes for all 6 Swarm Drones.

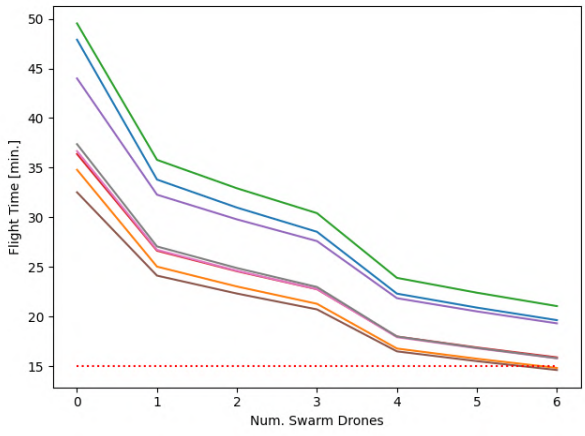

(a) Flight time vs. Num. Swarms

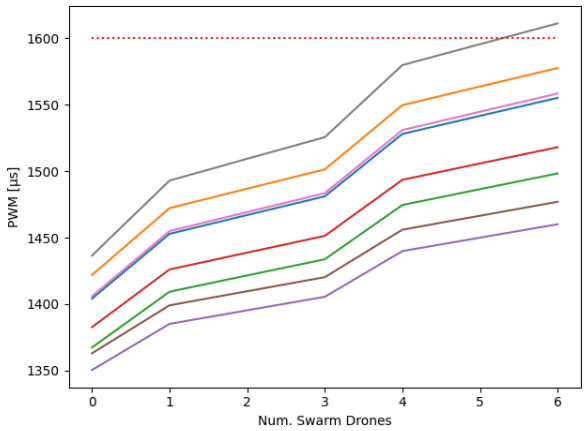

(b) PWM vs. Num. Swarms

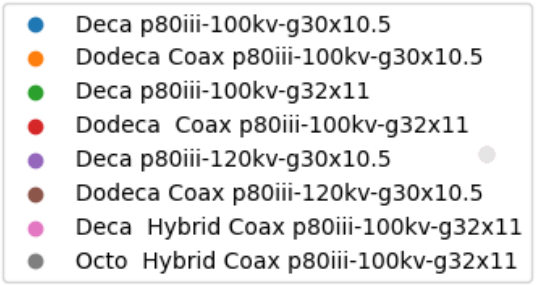

(c) Legend of motor and propeller configurations

Figure 35: Prediction design decisions

5.3.5 Power Distribution

Due to the nature of the carrier UAS carbon fiber frame design, internal wire routing is not possible. It was decided that the electronic speed controllers (ESCs) for all of the carrier UASs motors would be centrally mounted. This reduces the overall moment of inertia of the carrier UAS as more weight is located at the center of rotation. Additionally, centrally mounting the ESCs maintains the signal integrity of the PWM signals increasing the overall safety of the carrier. Thus the three brushless motor phases need to be routed from the center of the Carrier Drone out to each motor. PCB solutions were designed for wire management and easier mounting to square carbon tube than traditional wire. While the actual circuit design for these elements is trivial, the increased organization and robustness will make assembly and maintenance easier. Fig. 36a displays the ESC mounting board which allows an APD 120 F3 12S 50V 120A ESC and corresponding MR60 connector to be soldered onto the board. Fig. 36b displays the phase wire routing PCB which was designed to be mounted on the outside of the Carrier Drone carbon frame assembly. The most difficult part of the design process for these components was the trace width calculations to ensure that the PCBs could operate at the power demands of the motors using [40] for a two layer $2oz.$ copper PCB. On the Carrier drone (Fig. 25a), these boards can be seen passing power to the motors while also providing a rigid mounting point to the Multidrop Bay. Additionally they provided advertisement space to display the project's sponsors' logos as stipulated in their sponsorship agreements.

The power distribution of the LiPo batteries to the ESC exceeded the capabilities of standard PCB, thus it was more cost effective to use copper bus bars instead using [41] to meet the combine maximum continuous current draw of 12 ESC at 45A with an additional factor of safety.

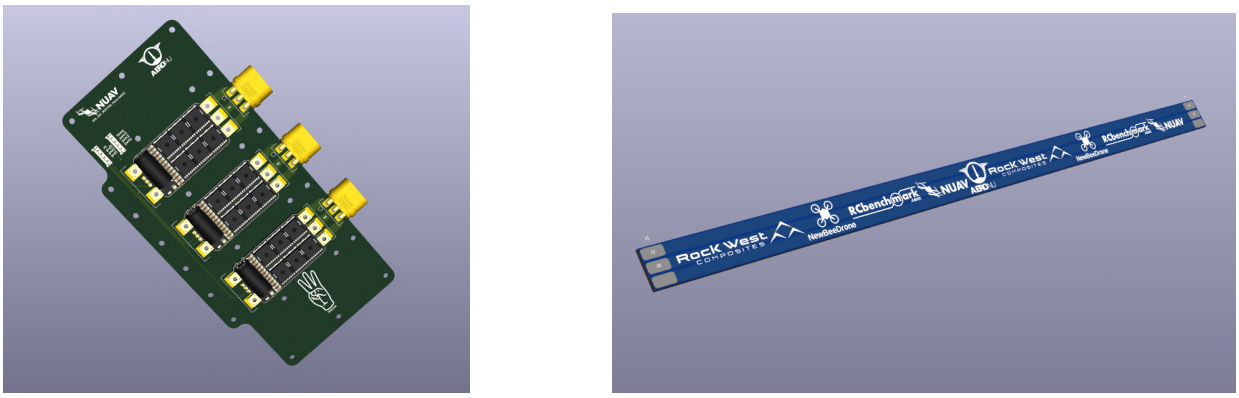

(a) ESC routing PCB **(b) Phase routing PCB**

Figure 36: Power distribution PCB

5.3.6 FEA of Carrier Drone

An important factor in the Carrier Drone's design is how it handles vibrations and its natural modes of vibration. This is critical to ensuring that the motor and propeller's frequency does not match with the resonant frequency of the airframe, which could prove worrisome to any flight operations. A difficult aspect of this analysis is the use of composite materials for the cross-sections of the airframe. Composite materials exhibit orthotropic elasticity that is very hard to mechanically measure

and simulate without specialized equipment. In addition, the mechanical properties of carbon fiber laminates are dependent on their fiber orientations and layer arrangement, which means samples to test on have to be provided by the manufacturer to gain any reliable data. The group has been in close contact with the carbon fiber tube manufacturer, professors who specialize in composite material analysis, and other composite laminate manufacturing company specialists on simulating composites in ANSYS Workbench. These contacts have provided individual lamina layer properties and resources to properly conduct FEA simulations in ANSYS Workbench using ANSYS Composite PrepPost (ACP). This powerful ANSYS package will allow the group to recreate the carbon fiber laminate on the Carrier Drone frame to determine the modes of the system. ACP is being heavily used during Capstone II to finalize the Carrier Drone V2 design and prove the structural integrity of design. Current research is focused on the necessity of FEA ACP over empirical tests due to the fast timeline of the project. Although FEA will still be used, its emphasis for the capstone project has been scaled back.

5.4 Behavior Trees

Behavior trees is implemented in software by using an open source project called "BehaviorTree.CPP" [42]. This project is used in various other ROS2 projects such as "navigation2", which is a general implementation for navigation algorithms in robotics using sensors. Behavior trees are necessary to handle the control logic and recovery behavior of failed missions. For more information related to how behavior trees work see Section 4.2.5.

Custom action nodes were created for each ROS2 action, like precision land and go to coordinate actions. There are specific behavior trees being created for many purposes. The higher level precision land tree in Fig. 37 shows one of these instances.

There are plans to account for various end conditions using nodes that check sensor information, such as battery and distance from home. In cases where the voltage drops to low, behaviors that initiate a return to home for forced landing may activate. These decision nodes are vital to the safety and effectiveness of the system.

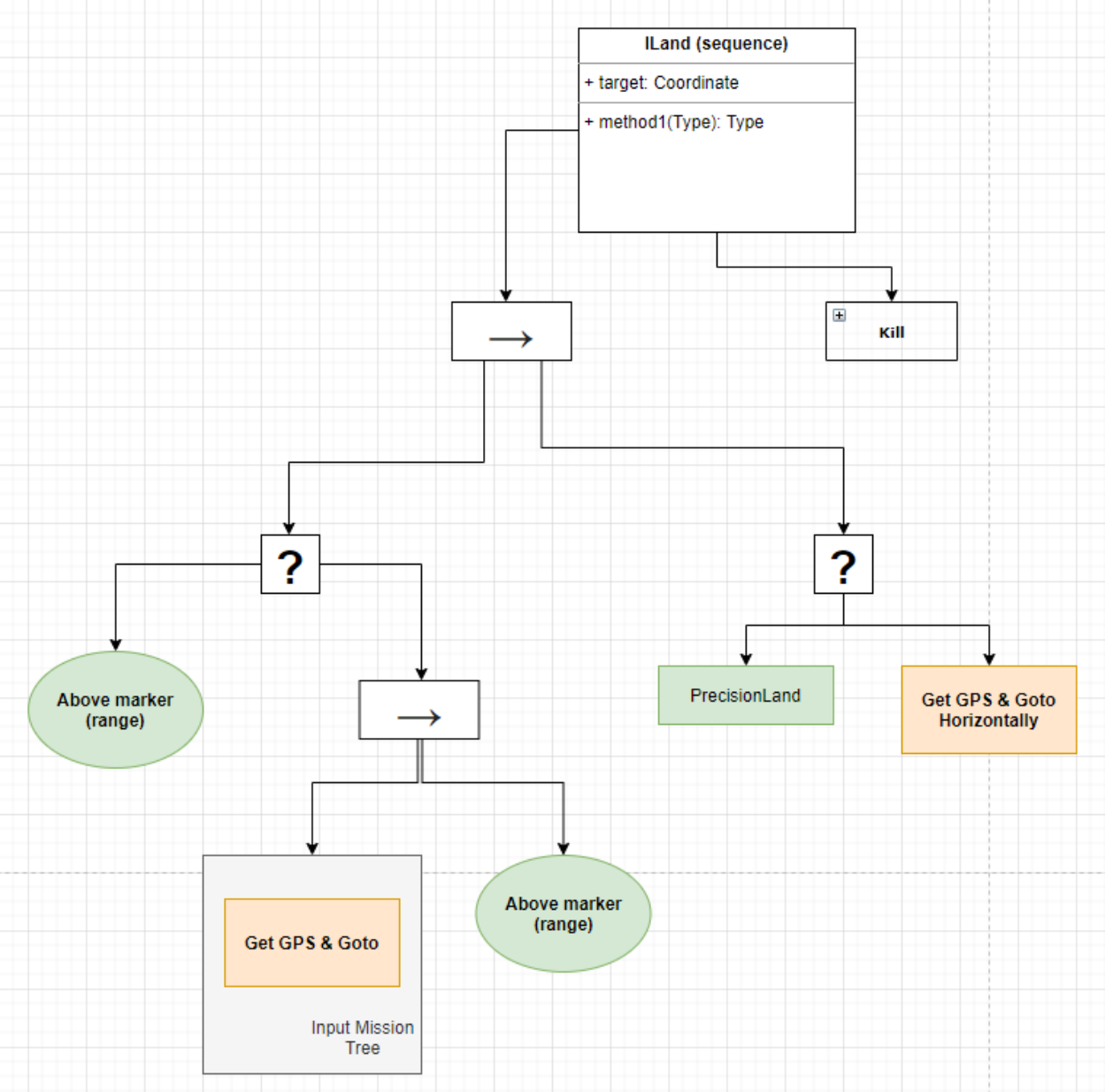

Figure 37: High-level precision land behavior tree

5.5 Drop Mode

Drop Mode is one of the fundamental actions being implemented for the software aspect of Swarm Carrier. Its purpose is to be an implemented mode within PX4 that catches the drone while it is falling. To implement this action, first the motors on the drone need to be blocked. This needs to be done since PX4 must spool up its internal logic assuming the motors have been activated, but for this project the motors cannot actually spin. The motors cannot spin since the Swarm Drones will be inside the Carrier Drone and would damage it. Once the motors have been blocked the vehicle must be told to move to a point higher than its current position. At this point it will try to takeoff but cannot since the motors are blocked. The Carrier Drone will then proceed to release the Swarm Drone. While the Swarm Drone is in free fall it will constantly have a loop checking if the drone reached a certain velocity and then unblock the motors. At this point in time the Swarm Drone should catch itself while it switches to a hover mode.

The current implementation of Drop Mode in the PX4 firmware is in the form of two acknowledgment (ack) message publishers. One for sending an ack message that the motors have been blocked, and one for acknowledging that they have been re-activated. The purpose of these is be able to constantly publish vehicle commands until the ack messages are seen so that no messages are lost, giving the drone the best opportunity to catch itself.

5.6 Precision Landing

The task of precision landing is to enable fully autonomous recovery of the Swarm Drones with the Carrier Drone. To achieve this a behavior tree was designed to execute the actions required. This is shown in Fig. 37. The basic control flow begins with giving the drone an initial GPS starting point, in this case representing the location of the Carrier Drone. The main tool utilized for this task is the computer vision required to detect ArUco markers and estimate their 3D pose relative to the Swarm Drone (see Section 4.2.4 for more information). For the task of precision landing multiple ArUco poses are used to determine the landing pose at any given height. Each marker is a different size in order to guarantee consistent detections. An offset is applied to each marker to return the actual landing pose, which is then smoothed using a moving average. Once the landing pose is calculated, Proportional Integral Derivative (PID) controllers are used to correct for errors and adjust velocity commands appropriately. This control phase is separated into two stages: horizontal alignment and vertical descent. First, the Swarm Drone will adjust its positioning so that it centers itself above the landing pose. Once within a certain tolerance, it will initiate a descent phase to land directly on the marker. If it ever falls outside the horizontal tolerance it will revert to the horizontal alignment stage and follow the same procedure again. The behavior tree is also structured so that if the ArUco marker is lost, a recovery action will be performed to regain visual detection of the markers. Fig. 38a demonstrates the simulated precision land process. Instead of the ground, the markers would actually be placed on the Multidrop Bay, shown in Fig. 38b.

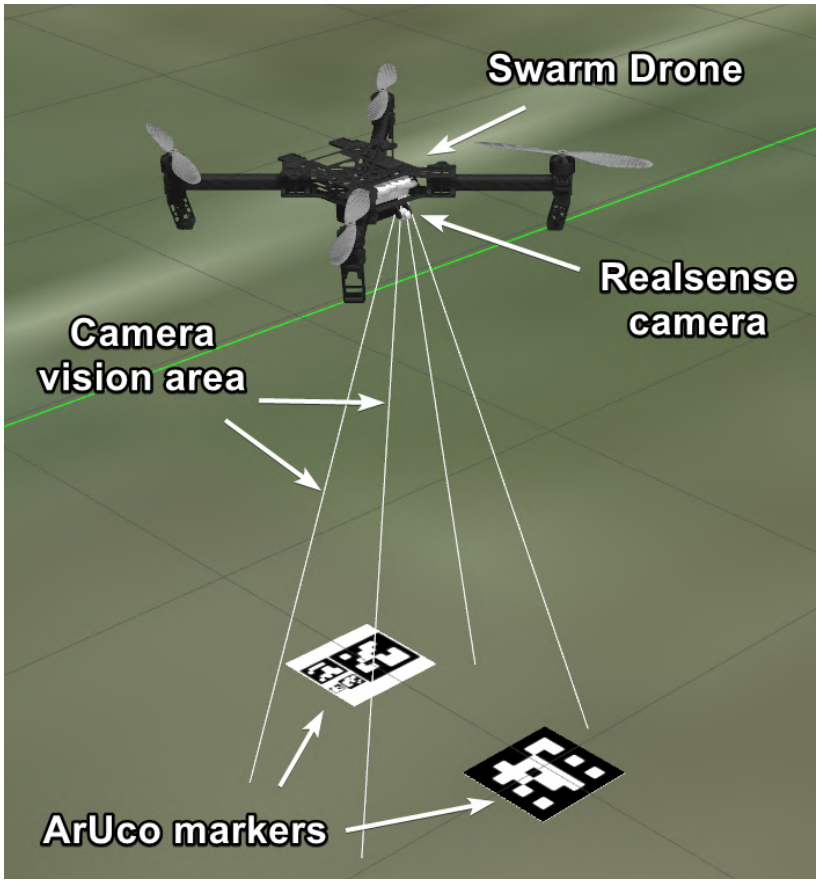

(a) Gazebo view of precision land

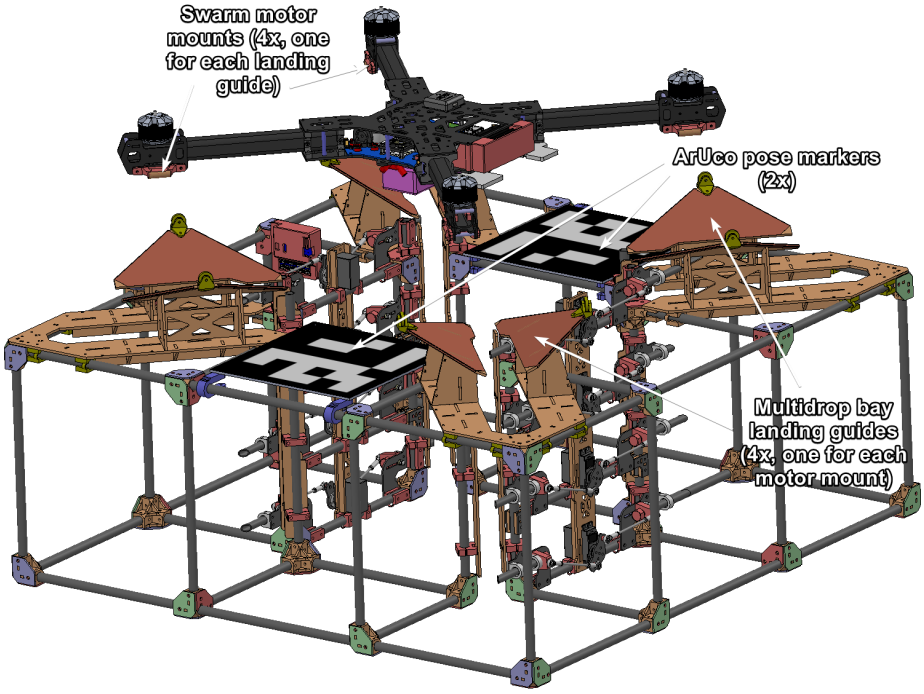

(b) Swarm Drone example landing position in the Multidrop Bay

Figure 38: Precision landing in simulation

5.7 Multidrop Bay

Development of the Multidrop Bay V3 began in July 2021 based on lessons learned from the previous iterations mentioned in section 4.3.3. Notably, the unreliability of pulley-based linear actuators prompted research into rigid linkages. These applied uniform force in tension and compression. Furthermore, given the high unique part count and assembly difficulty of the V2 design, the V3 required optimized frame dimensions and connectors to reduce the probability of tolerance stackup. Lastly, landing geometries and their associated fixtures were optimized to reduce weight and improve ease of assembly.

Functionally, the V3 iteration had the same constraints as the V2. It utilized gravity to reintegrate landed drones and then servo linkages to pass them through the carrier drone frame. Fig. 39 below shows the V3 CAD assembly and prototype of the lattice structure and mechanisms completed in summer 2021.

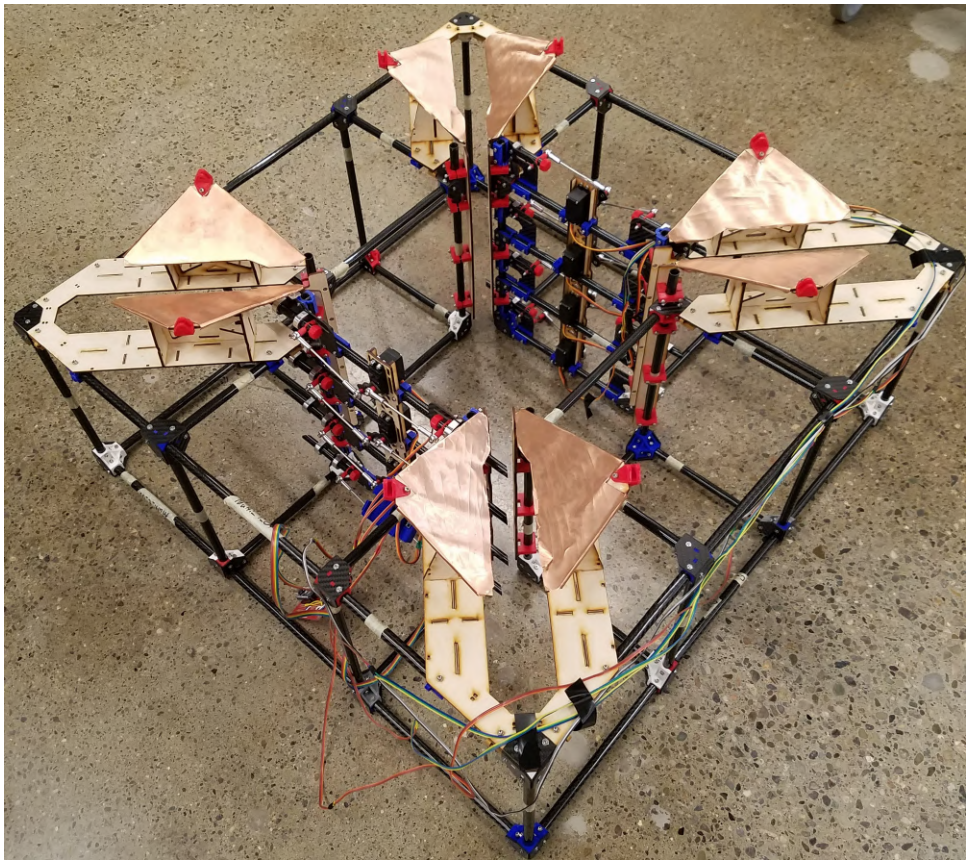

(a) Initial prototype

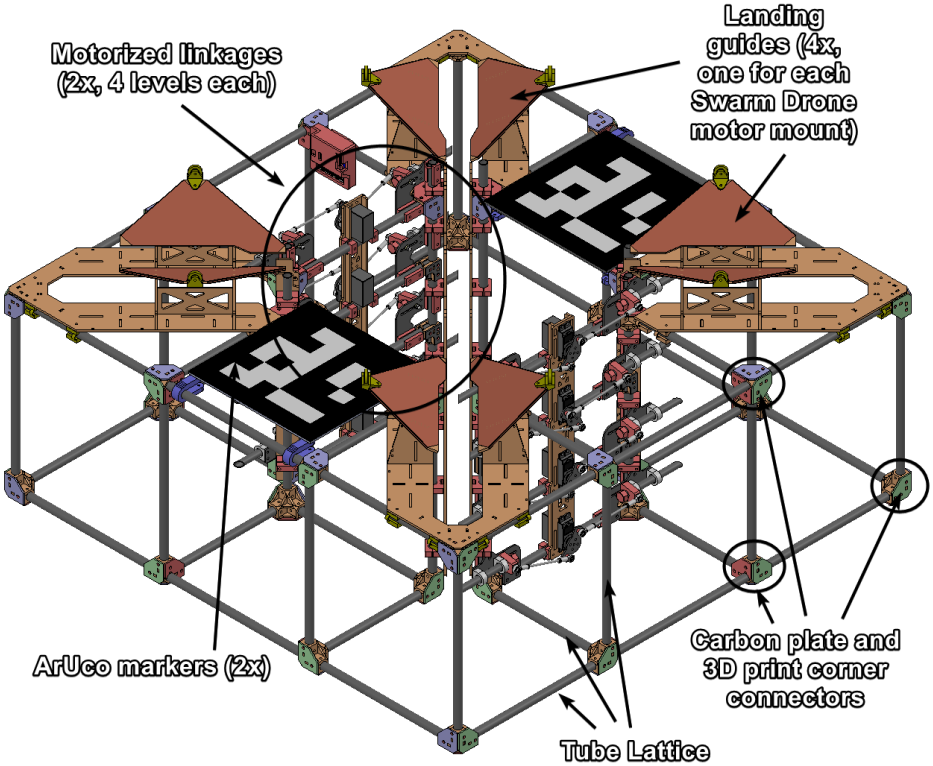

(b) CAD model

Figure 39: Multidrop Bay V3

The Multidrop Bay V3 was designed to sit inside square openings of any of the Carrier Drone designs, with empty space both above and below allowing for recovery and deployment of the Swarm Drones. Due to heavy usage of lightweight components like wood and carbon fiber, the overall weight of the Multidrop V3 frame was only 2kg. Most of the remaining weight came from the motorized linkages and hardware, which brought the overall weight to 5.5kg. Specific developments relating to landing guide geometries and linkage mechanisms are discussed in detail in the following sections (5.7.1, 5.7.2, and 5.7.3).

5.7.1 Multidrop Bay Lattice and Connector Optimization

The development of simple, light weight joinery for the Multidrop Bay designs was a critical constraint in order to produce a rigid design. Payload rigidity was prioritized to reduce internal sources of vibrational noise within the carrier drone as well as to prevent jamming of vehicles during passage through the mechanism. Adhesives were invalidated due to concerns with jigging, lack of control of tolerance stack up, and overall difficulty of assembly for round, hollow tubes. In order to produce a modular, rigid, and easily assembled design, bolted connectors were developed to join members of the lattice frame.

Initial connector designs for the Multidrop Bay V2 involved multiple configurations depending on the number of members at a given joint. Composite design was also leveraged with 3D printed clamps to comply to round tubes that were surrounded by carbon fiber plates to absorb the majority of loads on the frame. Prototypes for the V2 and V3 bay design can be seen below for fixturing joints with up to 4 members.

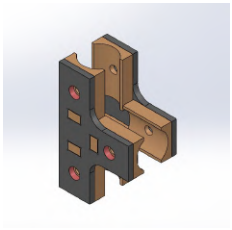

(a) Multidrop V2 t-Connector

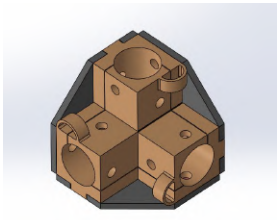

(b) Multidrop V2 corner connector

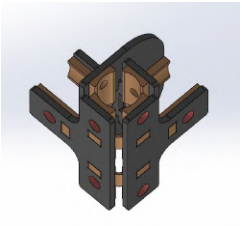

(c) Multidrop V2 tetrahedral connector

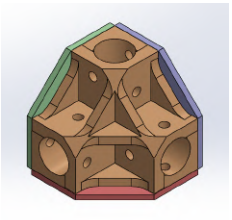

(d) Multidrop V3 Corner Connector

Figure 40: Multidrop Bay V2-V3 connector iterations

The t-connector, tetrahedral connector, and corner connector iterations all leveraged the clamping force of 3D printed elements to comply to round frame members. External carbon plates also provided constant compression of 3D printed components to prevent tensile failure modes. While capable, the t- and tetrahedral connectors resulted in large part counts and reduced manufacturability of the V2 bay design. The V3 corner connector shown above was designed to act as a corner or tetrahedral joint to reduce unique part count. Fig. 41 below shows the V2 and V3 bays with their respective connector configurations. It can be seen that the more versatile corner connectors of the V3 iteration can accomplish the same fixturing as the V2 tetrahedral joints with fewer unique parts.

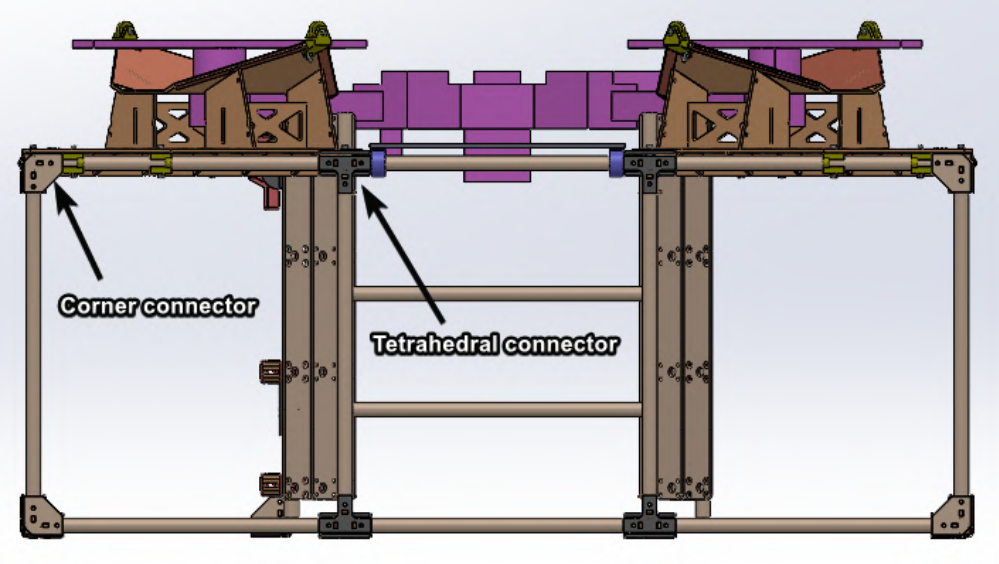

(a) Multidrop Bay V2 connector configuration

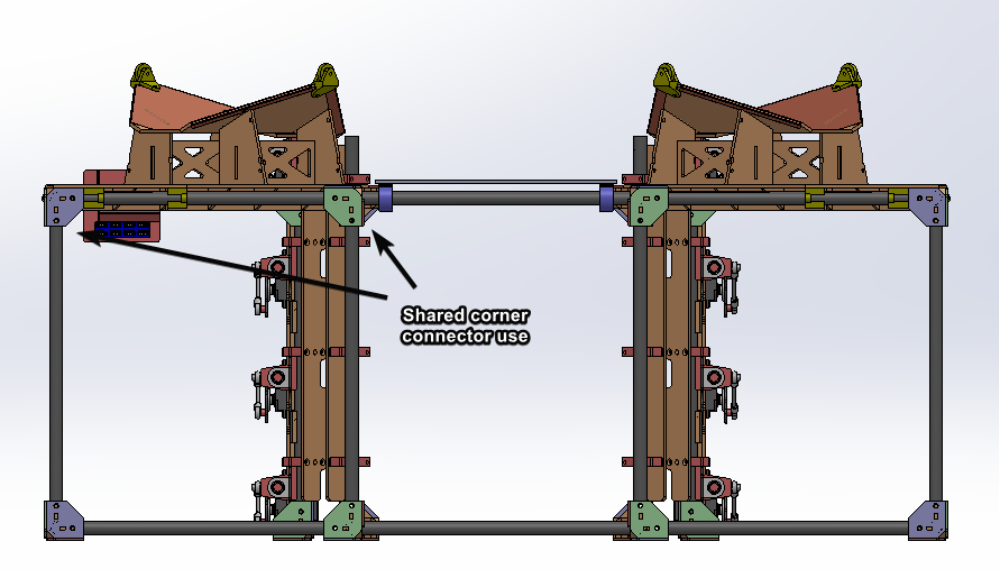

(b) CAD model

Figure 41: Multidrop Bay V3 connector configuration

The final area of development in the Multidrop Bay's frame is its attachment into the Carrier Drone. Fixture points and designs will have to be iterated in order to maintain guide rigidity. An example for the interface clamp between the Multidrop Bay and the Carrier Drone is shown below in Fig. 42. The purpose of these fixtures is to rigidly support the Multidrop Bay within the Carrier Drone. Due to the fact that the Carrier Drone is pre-assembled, fixture points cannot be slid onto its square frame members. Furthermore, given the flexibility of the Multidrop's lattice frame in multiple areas, fixture points had to be adaptable in order to determine the best mounting positions during tests. Therefore, the goal of the subsequent designs is to constrain the motion and flexure of the Multidrop while being adaptable to different placements based on need.

To accomplish this goal while maintaining strength, the developed fixtures used a 3D print-in-place hinge with TPU grommets to comply to varied frame cross sections. Similar to the Multidrop's frame connectors shown in 40, the clamp used external carbon fiber plates to absorb the build of tensile and compressive loads. With the design shown in 42b below, the clamp was easily opened, inserted around the frames of the Multidrop and Carrier drone, and subsequently tightened using two bolts.

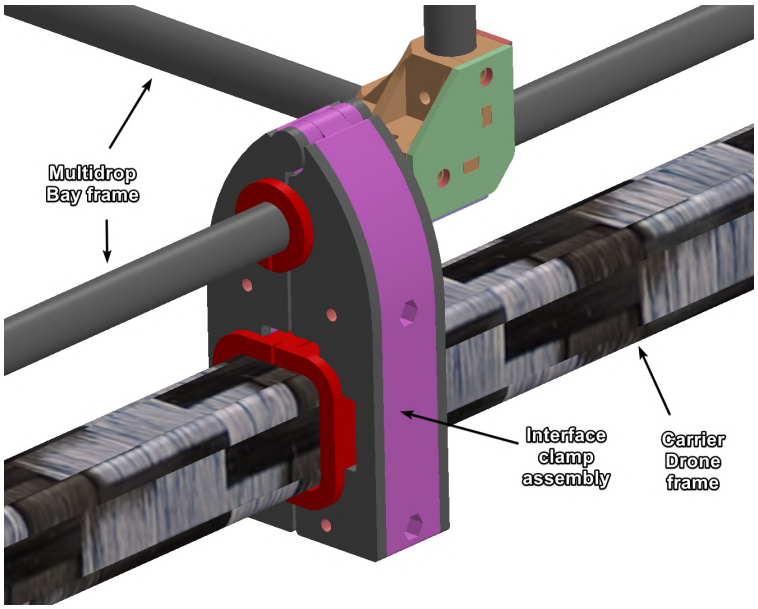

(a) Location of interface clamp

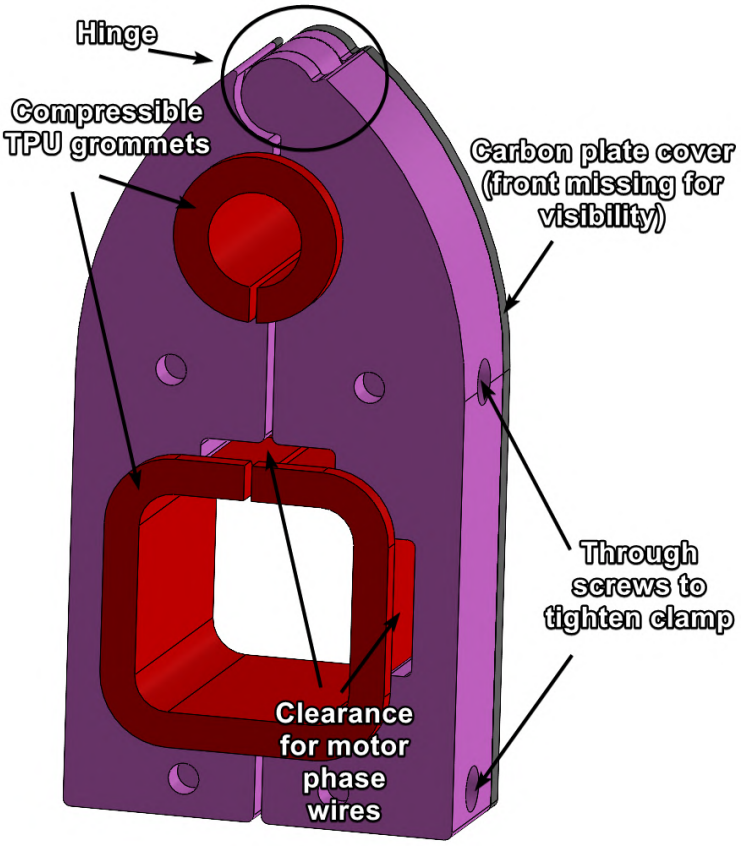

(b) Detail of clamp assembly

Figure 42: Interface clamp between Carrier Drone and Multidrop Bay

Crucially, Fig. 43 below shows the anatomy of the print-in-place hinge which has a hyperbolic cross section. This was specifically designed to mitigate shear stresses and maximize compressive strength.

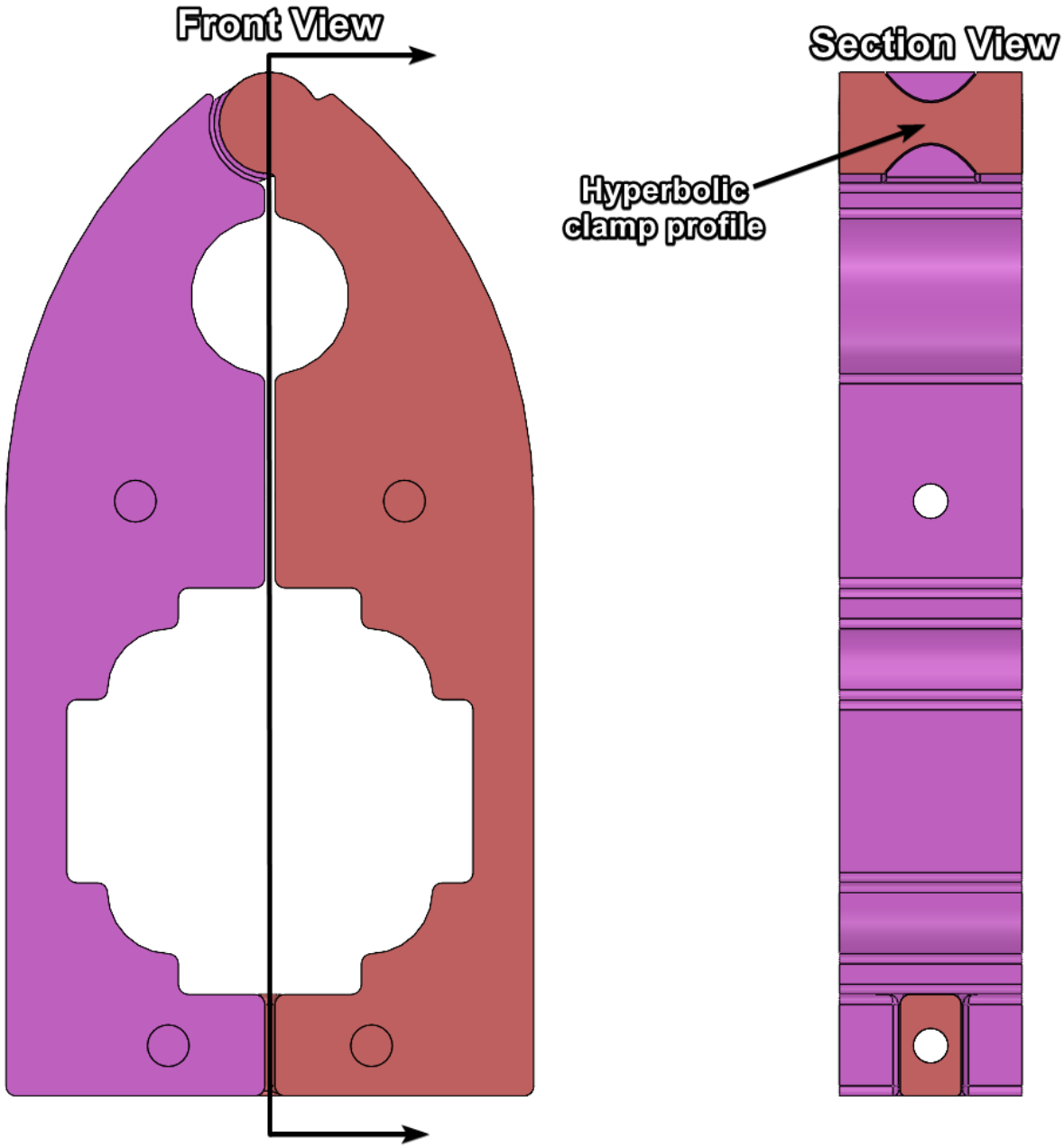

Figure 43: Hyperbolic profile of clamp

Subsequent iterations of the Multidrop Bay to Carrier drone fixtures are required in order to totally constrain the flexure of each frame respectively. These designs will also have to exist around the Carrier Drone's cable tensioning solutions, mentioned in 28, in order to satisfy the requirements for the payload to operate safely.

5.7.2 Landing Guides

In addition to actuating the Swarm Drones, a constraint of the Multidrop bay V3 was passive alignment of propellers during reintegration. To accomplish these, designs employed triangular geometries to maximize the area in which the Swarm Drone land and be successfully rebounded into the mechanism. Preventing propeller damage was also a key consideration of the guides which influenced their shape. Figure 44 below shows the differences between the guides of the V2 and V3 Multidrop Bay. The V3 improved upon the 3D printed supports of the V2 guide (shown in yellow) and reduced weight using a glued wood structure instead of bolted subcomponents.

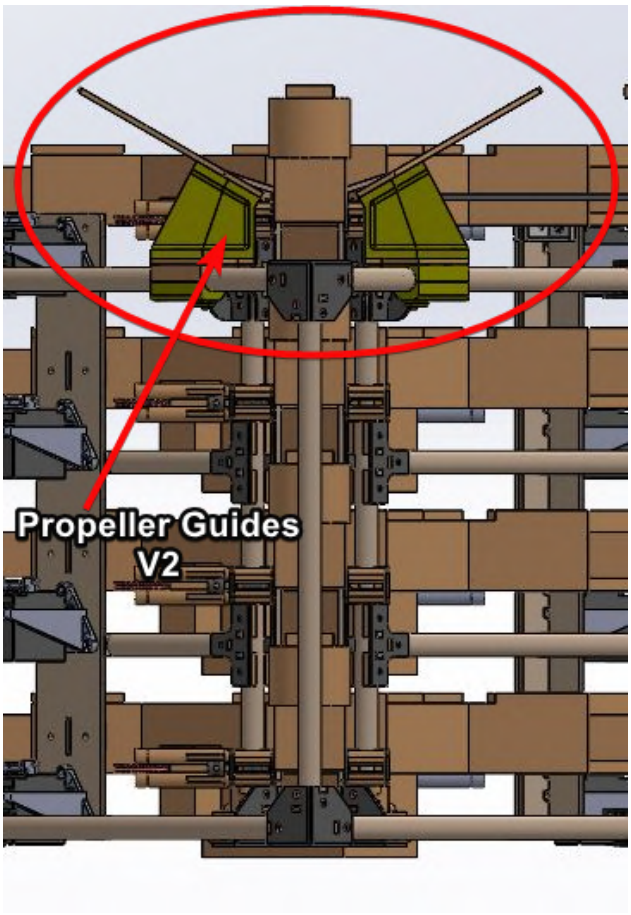

(a) Multidrop V1 propeller guides prototype

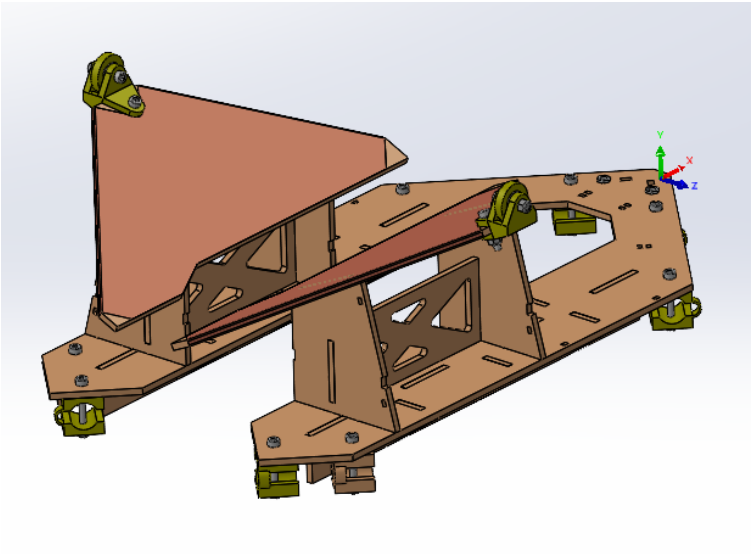

(b) Multidrop V3 propeller guides prototype

Figure 44: Landing guide designs for Swarm Drone reintegration

During summer 2021, the additional functionality of contact sensing was added to the Swarm Drones and Multidrop Bay V3. For the latter, this involved the addition of copper sheets to the V3 landing guides in order to interact with the contact sensors on the Swarm Drones described in section 5.8. The functional scenario for the use of the copper contacts is as follows: during a precision land, the Swarm Drone guides itself over the Multidrop Bay using the ArUco markers and descends to the landing guides. To have a physical motor kill, there are copper contacts on both the bottom of the Swarm Drone and the top of the Landing Guides. When at least two of these connections are detected, a motor kill is initiated on the Swarm Drone, and it drops into the top level of the Multidrop Bay. Fig. 45a below shows the copper contacts on the final Multidrop V3 prototype as well as their overall position in the CAD model in Fig. 45b. Fig. 45a below also shows TPU rollers on the tips of the triangles which are intended to induct the Swarm Drones during worst case alignments where their propellers are perpendicular to the slot between the guides.

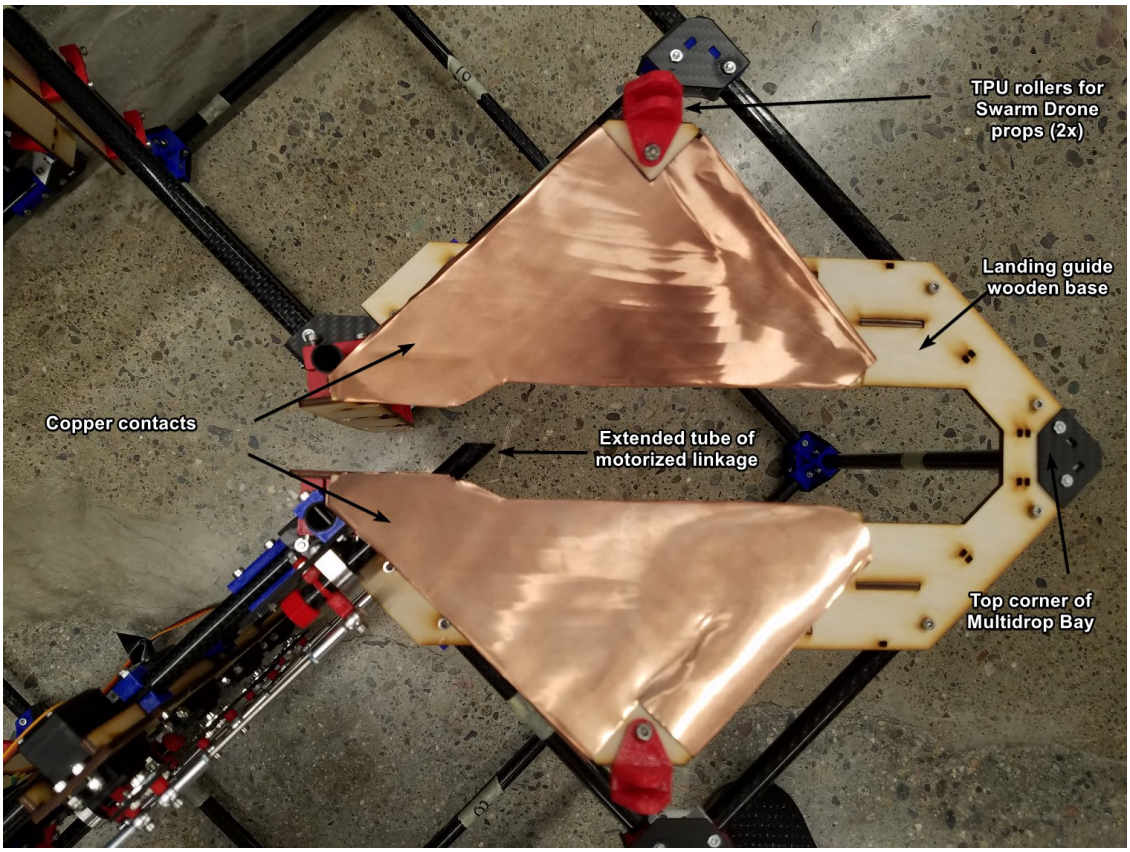

(a) Top down view of landing guide for one Swarm Drone arm (copper contacts shown)

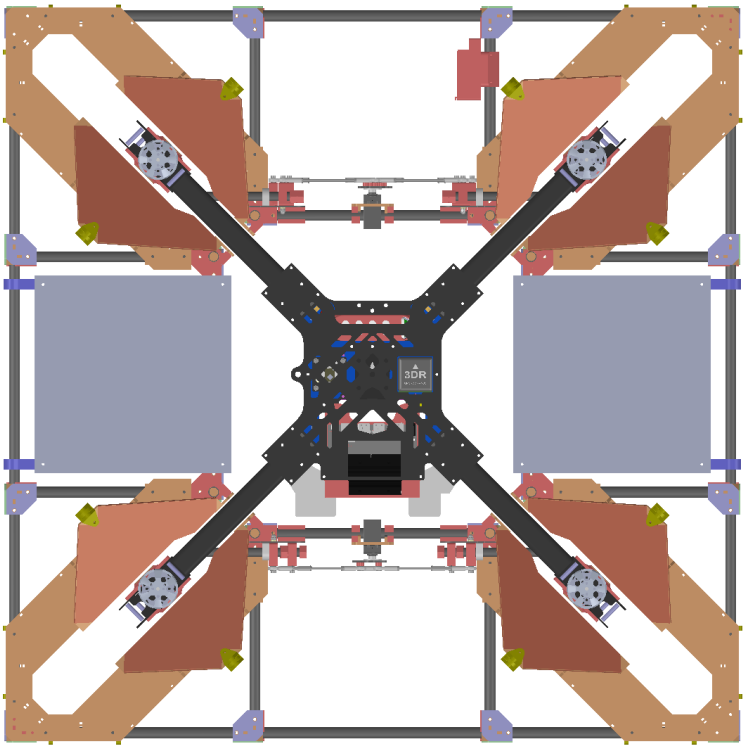

(b) Top down view of Swarm Drone aligned in four Landing Guides

Figure 45: Landing Guides

Extensive validation tests will also be conducted in order to confirm that the guide geometries can absorb any variance in the Swarm Drone's position during precision landings. These tests will validate the TPU roller geometries and drive further phase-in designs to ensure reliable reintegration and deployment of the Swarm Drones.

5.7.3 Actuators

To progress away from the unreliable, pulley-based actuators mentioned in section 4.3.3, subsequent iterations focused on simplifying the mechanisms. These were developed to allow Swarm Drones to selectively pass through the 4 levels of the Multidrop Bay. The top level is used as an initial location to first catch the Swarm Drone after it reintegrates. The first level of linear actuators was designed to prevent reintegrated drones from damaging their propellers by preemptively falling to lower levels of the mechanism. The remaining levels were intended to store up to three Swarm Drones during flights of the Carrier Drone. When a drop of a Swarm Drone is desired, the bottom level of the linkages can actuate, dropping only the bottom drone. The bottom linkage then closes, and the remaining Swarm Drones inside the Multidrop Bay can shift down.

The next iteration after pulley-based linear actuators used rigid linkages actuated by a servo to translate a linear pins. These pins extended extended into the path of Swarm Drones within the bay, therefore preventing their movement to lower levels. The linear pins consisted of carbon fiber tubes that were free to slide inside of tightly toleranced guide brackets, making for a reliable and compact method of actuation. Figs. 46 below shows the design of the linkage mechanisms and linear pin actuators, their assembly in the Multidrop frame, and an example placement of a Swarm Drone among the mechanisms.

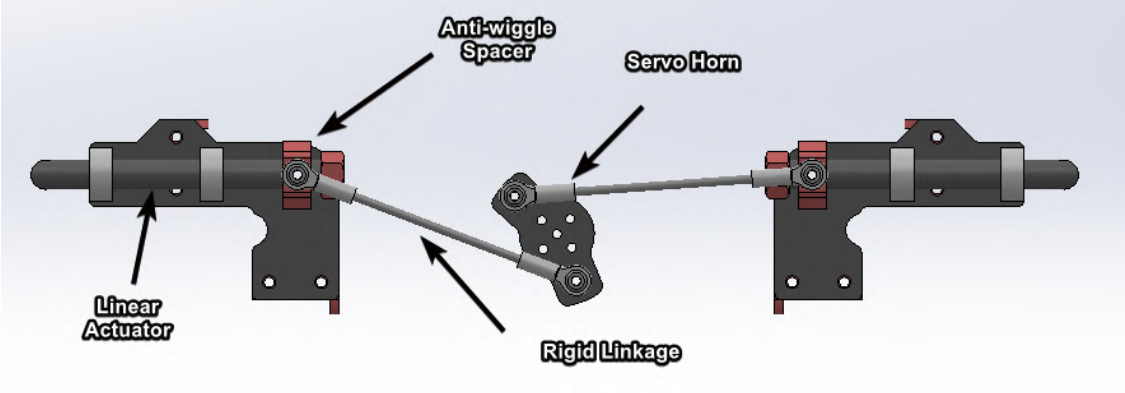

(a) Linkage mechanism CAD

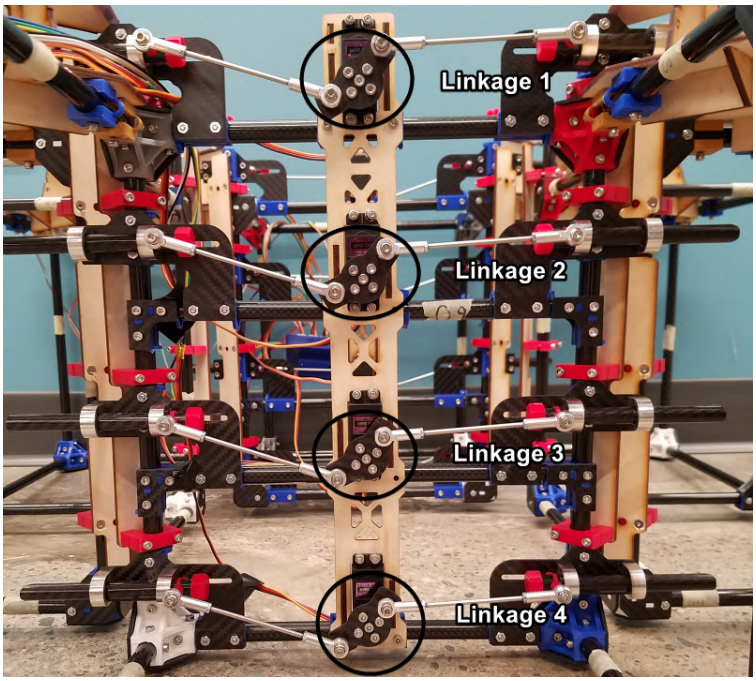

(b) Assembled view of linkage mechanisms

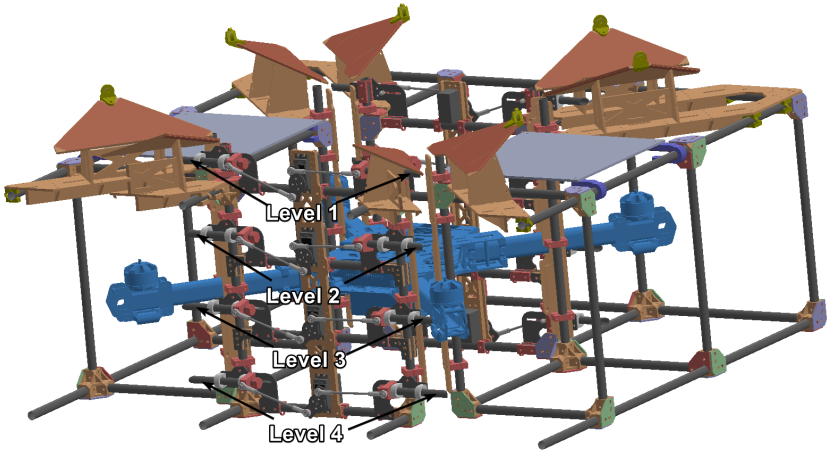

(c) Example Swarm Drone position within the Multidrop Bay

Figure 46: Motorized Linkages

While more reliable than the early, pulley-based actuators, the rigid linkages still suffered from jams due to loose tolerances in machined parts and wear during multiple cycles. These variances resulted in wiggle of the mechanisms and linear actuators, resulting in jams once the weight of Swarm Drones was applied to them. Misalignments were removed by adding 3D printed spacers within the mechanisms that prevented wiggle during actuation. These parts, shown in Fig. 47 below, were a simple phase-in solution that resulted in the completion of the Multidrop Bay V3's mechanisms to the required reliability for Swarm Carrier.

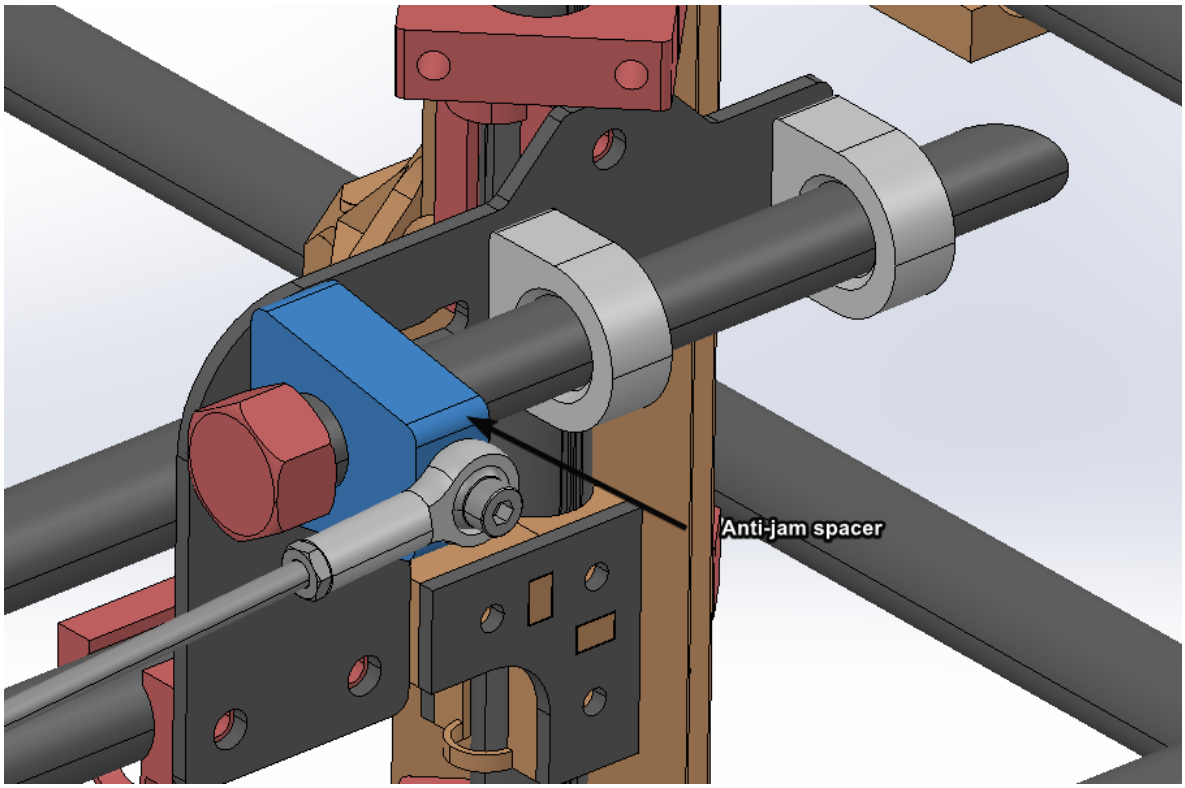

Figure 47: Anti-jam spacer on the Multidrop bay's actuators

5.8 Swarm Drone V3 Design

Building off of section 4.3.1, the next design under iteration was the V3 Swarm Drone. The V3 design was a series of phase-in improvements with the goal of modifying older components of the vehicles with current payloads and software in development. Required features included the replacement of older ArduCopter-preferred FMU-V3 flight controllers with PX4 FMU-V5 boards, vibration damped stereo camera mounts, new fixtures for mounting the flight computer, and new carbon fiber motor mounts with built-in collision sensing abilities.

Figures 48, 49b, and 49a below display these features as well as designs collision sensors. Designated as contact sensors, these were passive (un-powered) conductive contacts that delivered a logic input to the drone's flight computer. This feedback allowed the autonomy to sense the contact point between the Swarm Drone and Multidrop Bay during landing, power off the vehicles motors, and integrate into the bay without absorbing damage to propellers.

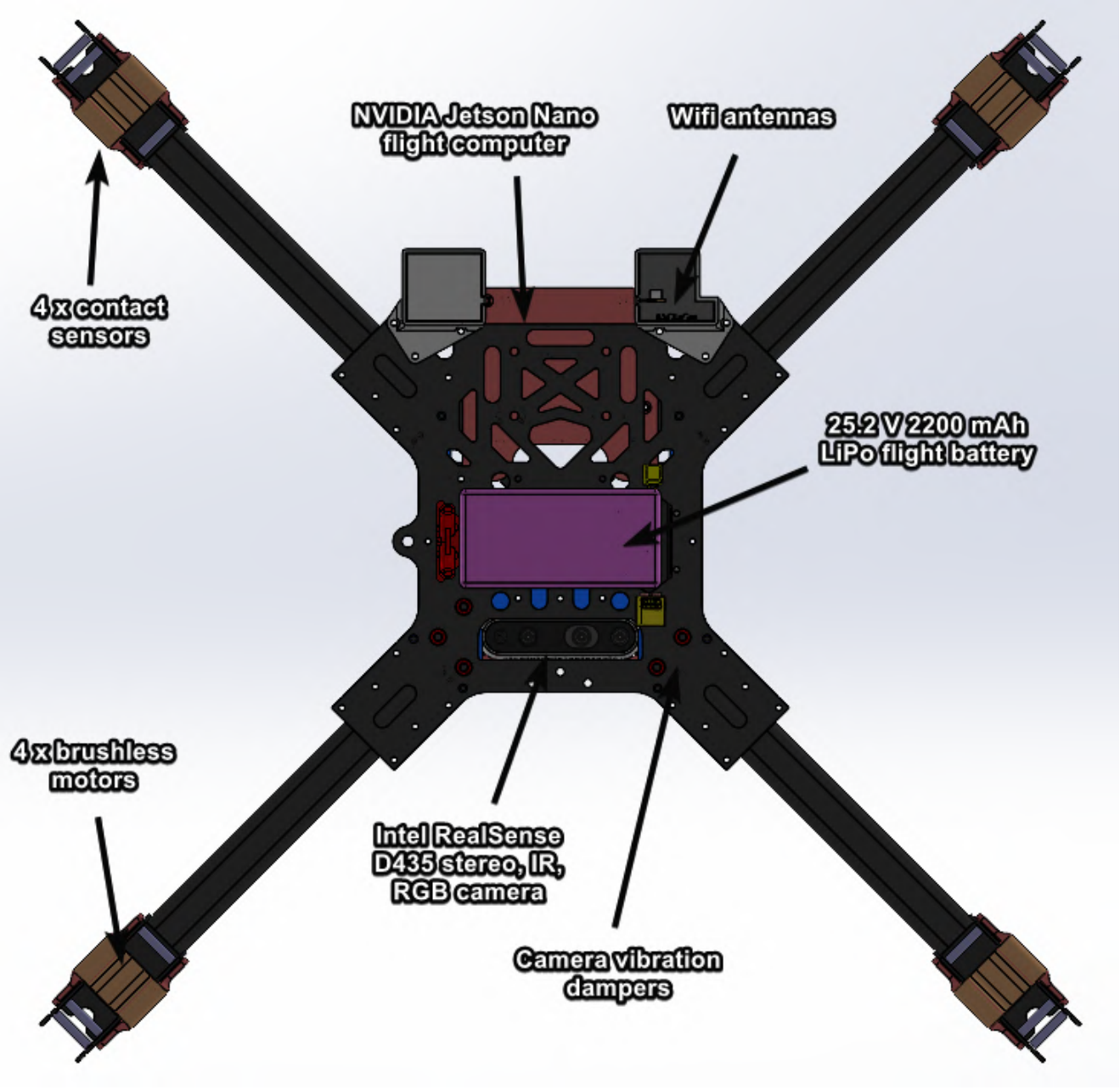

Figure 48: Swarm Drone V3 CAD

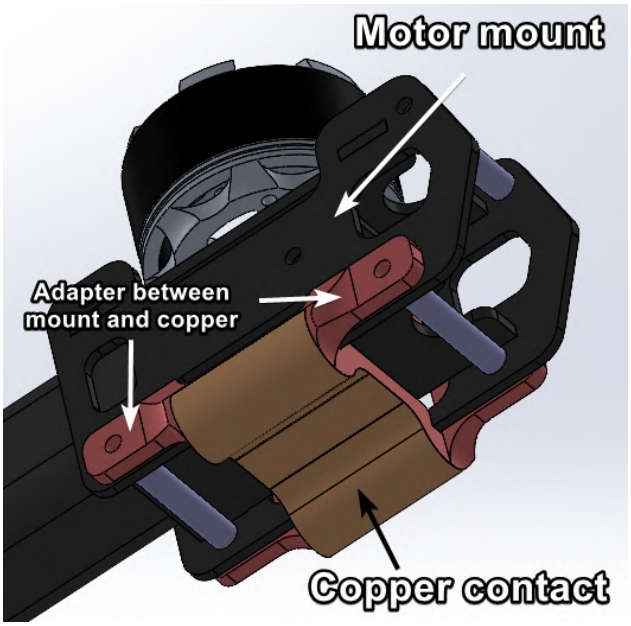

(a) Swarm Drone V3 motor mount with contact sensing

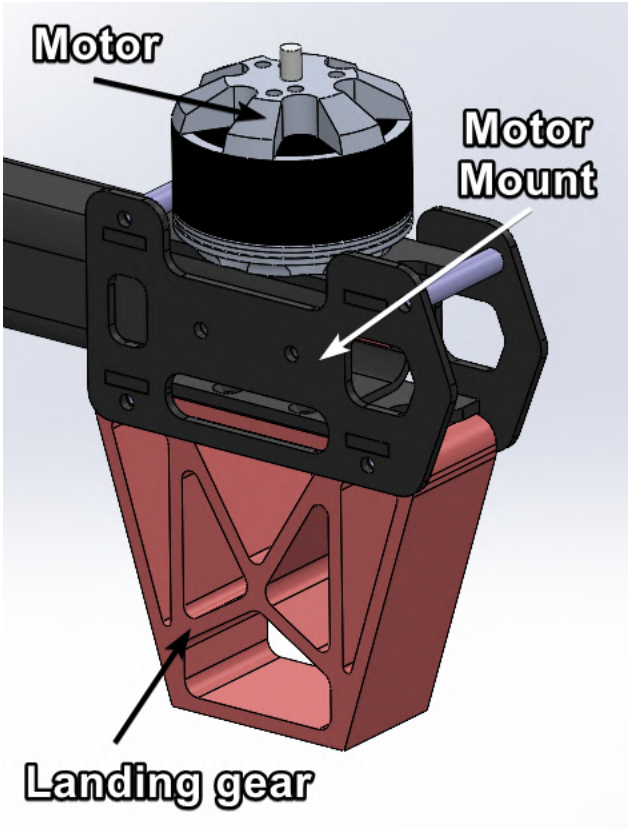

(b) Swarm Drone V3 motor mount with landing gear

Figure 49: Swarm Drone V3 motor mount with collision sensing

Functionally, the design of the contact sensors were specifically-contoured, 3D-printed geometries wrapped with copper tape. Within the airframe, the copper-wrapped contours were separated in two pairs which were wired in parallel to two General-Purpose Input/Output (GPIO) pins on the flight computer. Fig. 50 below outlines this wiring schematic as well as its interface with the Multidrop Bay.

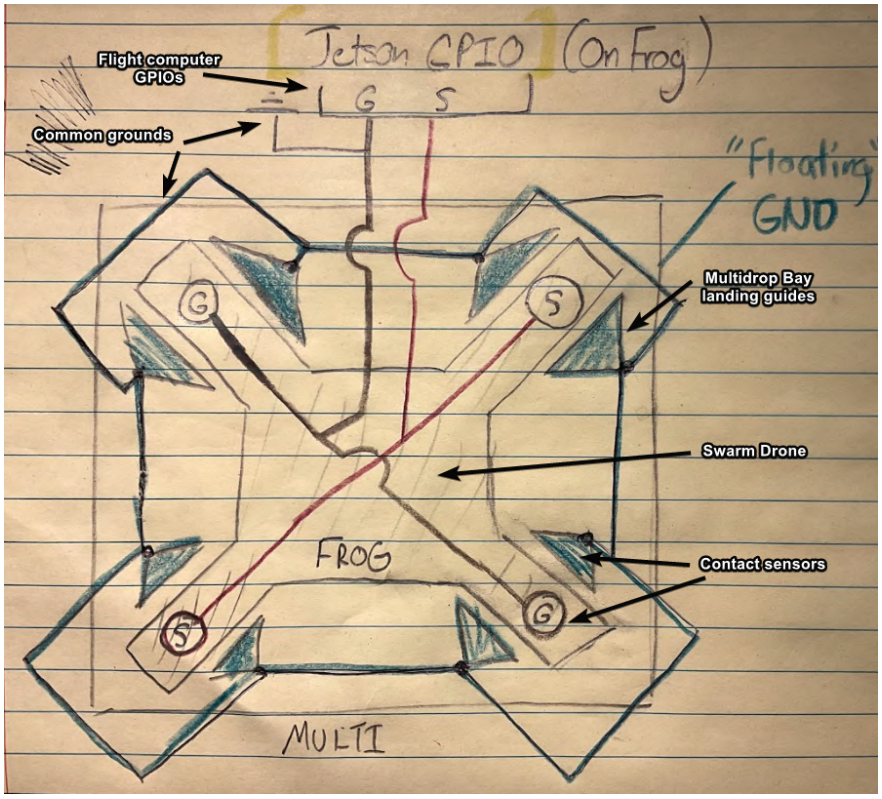

Figure 50: Swarm Drone contact sensing schematic

From Fig. 50, it can be seen that if any of the two adjacent arms of a given Swarm Drone make contact with the landing guides of the Multidrop Bay, at least two of the GPIO pins will be shorted. This allows for the mentioned motor shutoff to be initiated. With this feedback, the Swarm Drones have a hardware failsafe during autonomous landings that increases their reliability and safety.

In addition to new sensing solutions, the new carbon fiber motor mounts replaced dated nylon parts. These prevented fractures of 3D printed components during landings and finalized the Swarm Drone V3 as a robust and versatile test vehicle for Swarm Carrier.

5.9 Simulation

Custom models are being developed for the Swarm Drone and Carrier Drone in the Gazebo simulation environment. To get the vehicles in simulation they are first exported using SolidWorks Universal Robot Description Format (URDF) Exporter [43]. After exporting they are modified to contain common sensors such as GPS and IMU. Motor models are then added for each propeller and the dynamics of each motor are captured using various coefficients. For the Swarm Drone

and Carrier Drone various other additions were necessary to capture the vehicle's systems in their entirety.

The Swarm Drone had an extra sensor for the RealSense added. This was modeled using a multi-camera with Red Green Blue Depth (RGBD) capabilities. Custom software had to be written to extract image information from the simulation and output it to ROS2. An example of the Swarm Drone can be seen in Fig. 51.

The Carrier Drone did not require any additional sensors, however, custom implementations of the motors and their relevant mixers had to be created. Mixers are the foundation to PX4 flight controllers: they define where the propellers are located, how they should spin, and what electronics control them. Initially, a model was added for the Carrier Drone V2. This required a completely new version of a motor mixer as PX4 does not support a decacopter configuration natively. To create the mixer, various files had to be added to the PX4 firmware. Using the propeller locations from Solidworks and rotations derived from other configurations, the motor mixer was created and tested. Figure 52 below shows the Carrier Drone V2 in simulation. Flight capabilities were verified, but never tested on the field due to a design alteration and the switch to a V3 model for the Carrier Drone.

The Carrier Drone V3 used a native configuration supported by PX4, the octocopter. Using their motor mixers a simulation model was created in a similar fashion to the V2. The Carrier Drone V3 can be seen in simulation in Fig. 53.

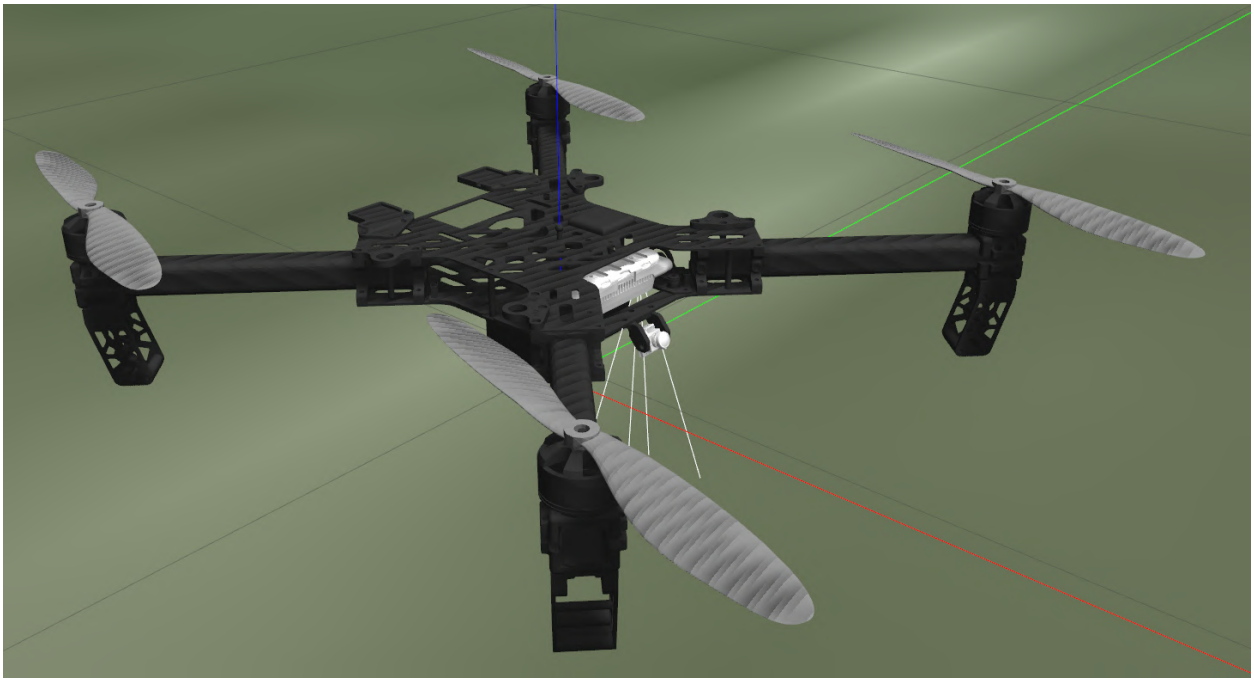

Figure 51: Custom Swarm Drone in simulation

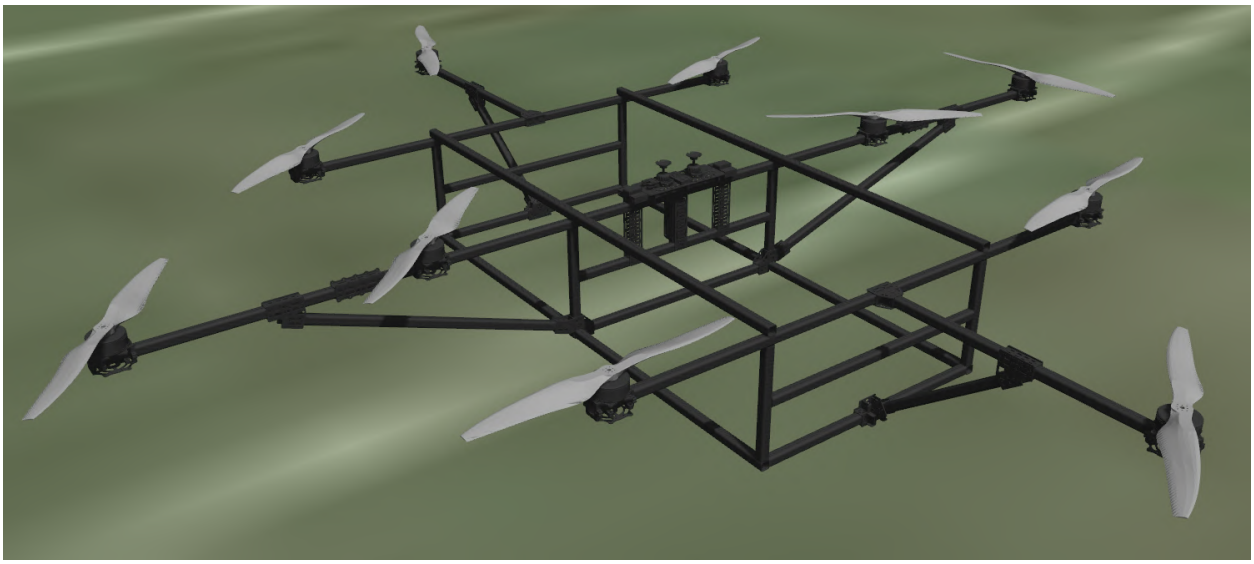

Figure 52: Custom Carrier Drone V2 in simulation

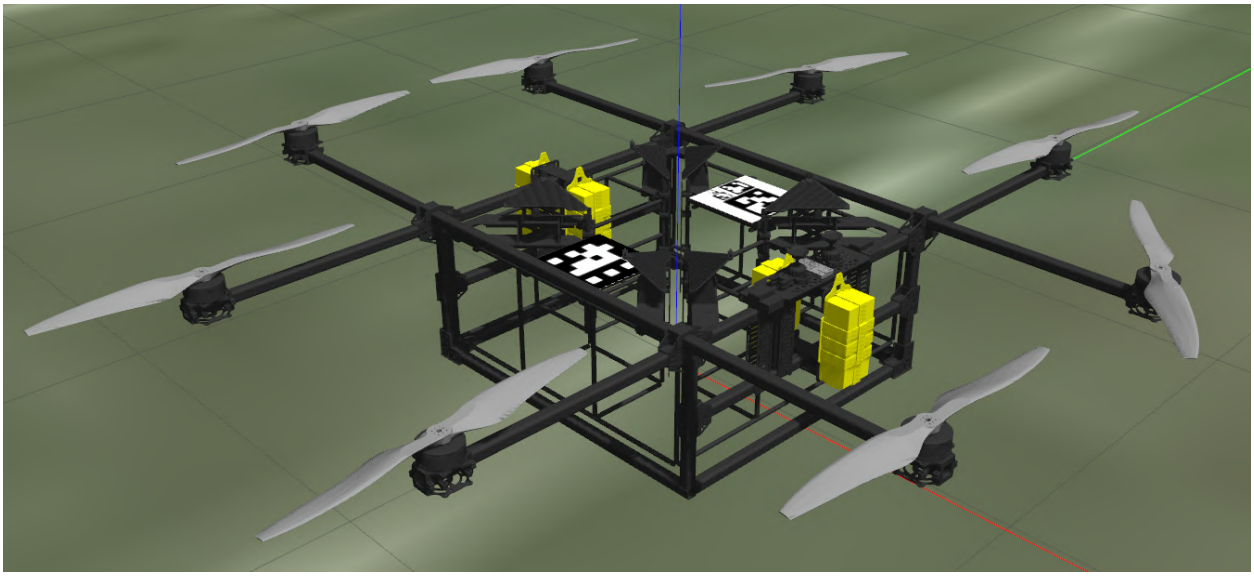

Figure 53: Custom Carrier Drone V3 in simulation

Continuing in the future, more accurate models of the Carrier Drone V3 will be added to simulation. The goal is to model the Multidrop Bay collision model on the top and test precision land with catching in simulation. Other adjustments also need to be done to more accurately fly the Carrier Drone. Currently, it aggressively turns and maneuvers unlike its real life counterpart which must be corrected for realistic comparisons to field tests.

5.10 Visualization

ROSboard is an open source, web based application for visualizing ROS2 topics. An example of this GUI running in the simulation is shown in Fig. 54. This feature allows for the viewing of any sensor (i.e GPS, camera, battery, IMU) or high level flight/mission log. The alternative to this was to simply read data values off of the terminal of the ground station. This was what the team previously used for monitoring the system. ROSboard has been invaluable for field testing and allows for greater insight into what the drones are doing for safety and debugging purposes. One of the main reasons the ROSboard library was chosen was because it is lightweight and extensible. It was simple to extend the base viewer and add support for specific visuals the team wanted. For example, the battery and attitude viewers were both added by request of the team's pilots. Additionally support for the visualization of swarm missions with multiple GPS points was implemented.

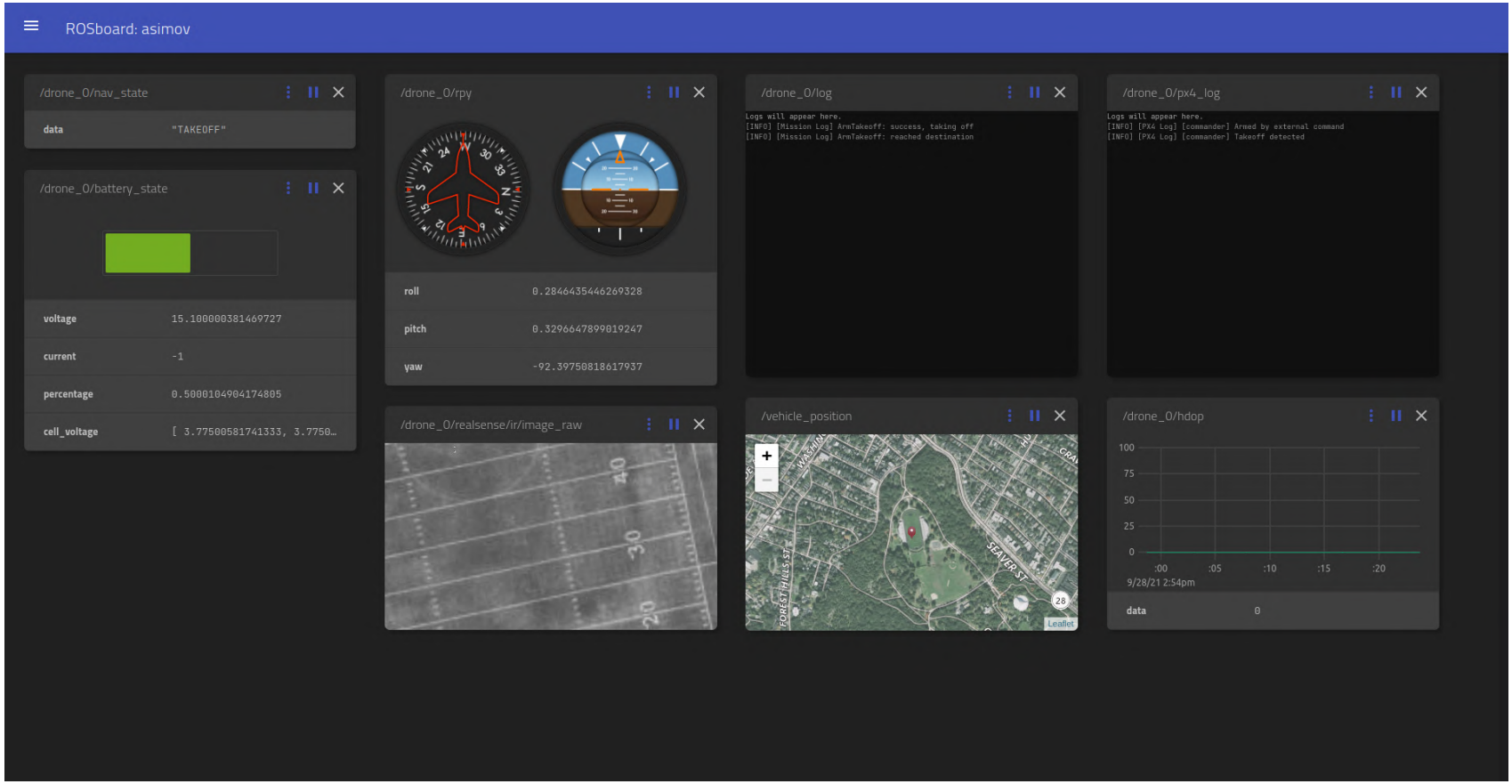

Figure 54: ROSBoard running in simulation

5.11 Integration and Embedded Systems

5.12 Design Validation

An important aspect of the Swarm Carrier project is the design validation of subsystems to ensure safety and reliability. This entailed preparing plans for carefully choreographed tests to evaluate key functions of the system. During July to the end of September of 2021, tests were conducted in accordance with SOPs. These were submitted for static thrust tests, maiden hover of the Carrier Drone, and precision landings using ArUco markers. The following sections outline a history of performed tests alongside tests being planned in the near future.

5.12.1 Thrust Tests

A series of thrust tests was performed in August 2021 on the Carrier Drone's propulsion system. These served to tabulate the operational characteristics for coaxial motors using T-Motor P80III 100kv motors and Foxtech 3010 Carbon Fiber Propellers. Using an RCbenchmark S1780 motor thrust test stand, the motor thrust, voltage, current, torque, and rpm were recorded. First, a control test was recorded where the performance of a single motor was monitored. Then the performance of both the upper and lower motors in a coaxial configuration were measured. An additional test of offsetting the axial distance between the motors was also conducted at 9 inch and 4.5 inch distances. To ensure consistent power calculations, single motor and coaxial tests were performed consecutively to avoid different voltage levels of the LiPo battery. Analysis of this data was done in section 5.3.4. Fig. 55 below shows the S1780 thrust stand with motors and propellers mounted in a coaxial configuration.

Figure 55: RCbenchmark S1780 Motor Thrust Test Stand with Coaxial Configuration

The outcome of the thrust test was a library of data, discussed in Fig. 33, which heavily informed the Carrier Drone's frame design and propulsion systems selection. For example, the Foxtech 3010 propellers were determined to provide inadequate thrust output given the constraints of the system outlined in Sec. 3.3. In addition to the mentioned results from the thrust data, this fact motivated the team to shift to T-Motor GL32X11 32 inch carbon fiber propellers as a replacement.

5.12.2 Precision Land

The precision land test was conducted to view the fidelity and precision of the Swarm Drones to perform a precision landing. Although not tested to full extent of the original Standard Operating Procedure (SOP) submitted, tests occurred with the Swarm Drones trying to land in between two ArUco markers taped to a sheet of foam board. This dry run equivalent to the test demonstrated the ability of the drone to identify the ArUcos and land itself without any pilot intervention.

While performing these tests various problems were faced. It was discovered that the control stack was inconsistent at connecting with the Swarm Drone, precision lands did not land within the desired tolerance, and GPS positioning had high variance. The first problem was analyzed and it was discovered that infinite loops and stalls were occurring at points during Swarm Drone initialization and processing. These problems were the result of invalid access to various objects at runtime and multi-threading issues. To overcome these problems more memory management logic and threading control logic was added. The second problem is still being resolved, however the additional logic for horizontal alignment and vertical descent in precision landing should improve the accuracy of landing. The final issue was resolved by protecting the GPS from Electromagnetic Interference (EMI) interference. After talking to individuals in industry it was decided that copper shielding needed to be added around the GPS and the USB cable from the Realsense camera. Adding a shield significantly diminished the interference affecting the GPS. After fixing the first problem, further tests were done, as seen in Fig. 56, and it was validated that the Swarm Drone can precision land consistently near the ArUcos.

Figure 56: Swarm Drone performing a precision landing during testing

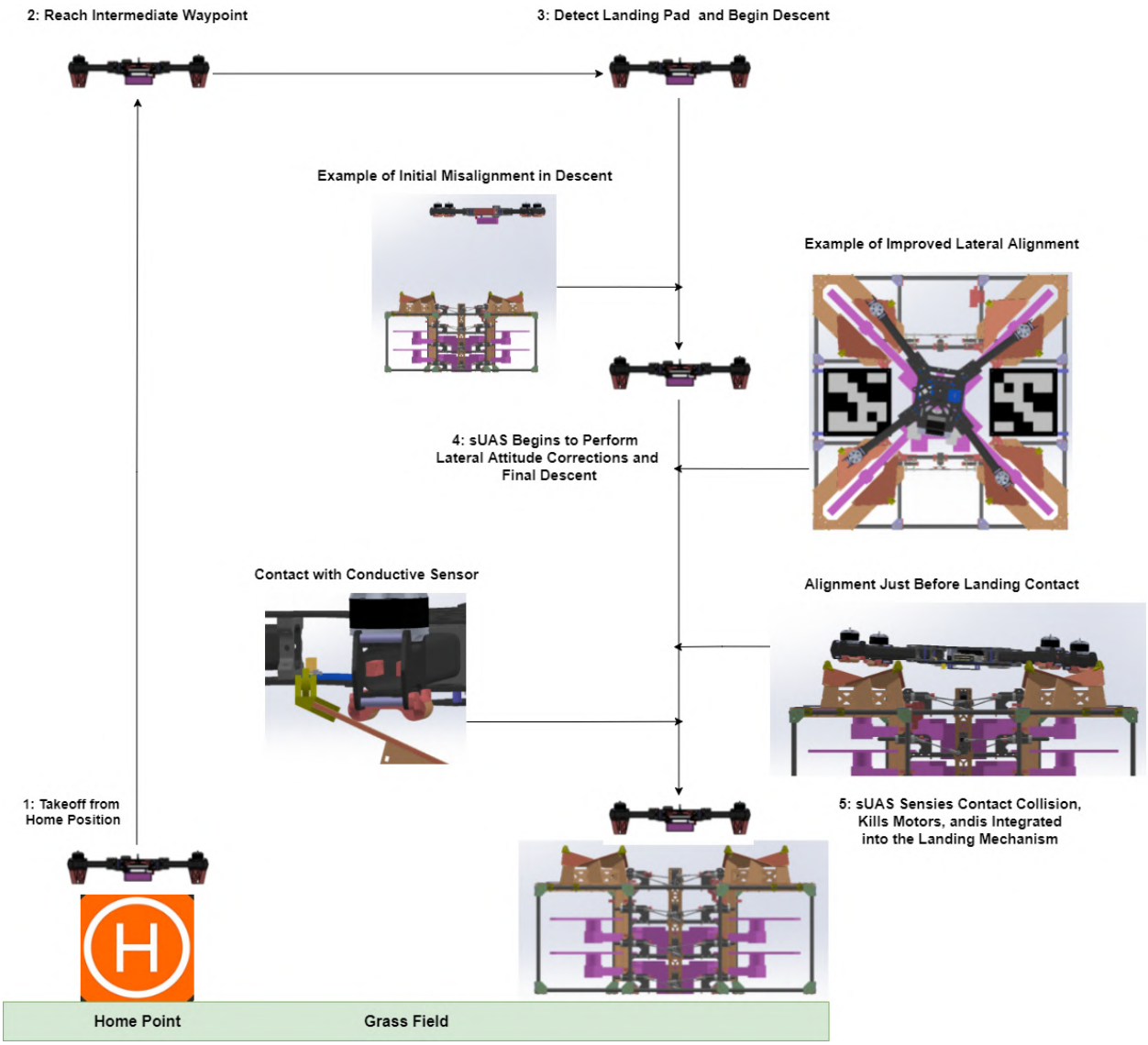

Figure 57: Flowchart: Precision landing test in a Multidrop Bay

5.12.3 Drop Mode Test

The Drop Mode test will evaluate the Drop Mode functionality of the Swarm Drones, which will use this flight mode when deploy out of the Multidrop Bay. The test involves dropping a single Swarm Drone from the bottom of an octoctoper UAS, 30 meters off the ground. If the Swarm Drone fails to activate its Drop Mode in time, a net system on the ground will catch the Swarm Drone. The SOP for this test has already been approved but testing has not been conducted due to time constraints and developmental timeline of the software. Fig. 58 shows the intended test procedure.

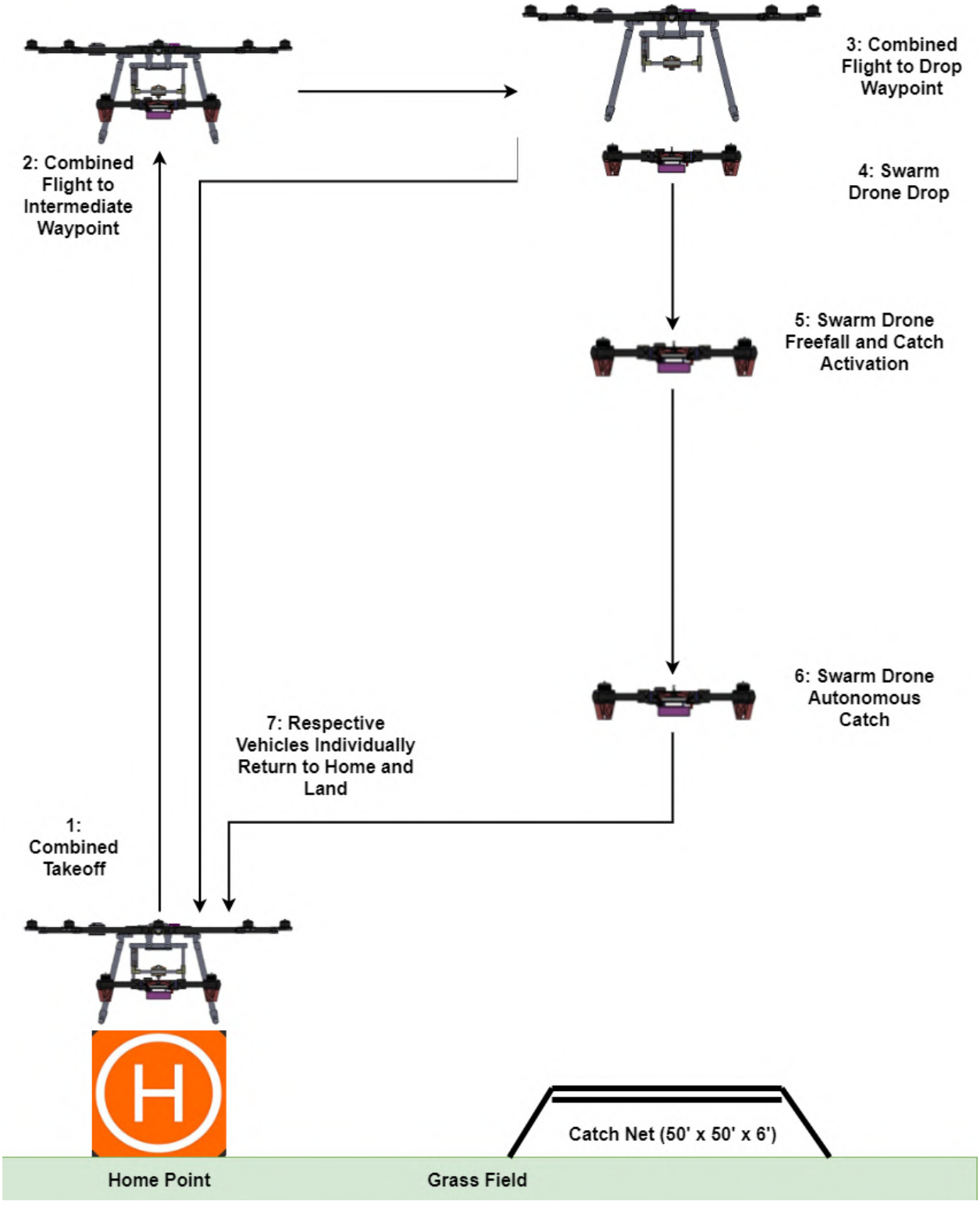

Figure 58: Drop Mode test overview

5.12.4 Carrier Drone V1 Air Frame Test

Given the scale of Carrier Drone designs and their experimental nature, iterative validation of the frame versions was critical. In September 2021, the Carrier Drone V1 was completed and first subject to these evaluations. Tests were a series of ground and air trials of the air frame in a quad-copter configuration. An abbreviated motor configuration, instead of the full 12 motor setup, was employed to remove any potential confounding factors that might influence the team's assessment of the frame only. Tests of the V1 frame specifically involved inspecting the rigidity and tolerance stack-up of the constructed assembly and confirmation of the functionality of power distribution components. In a laboratory environment, the electrical functionality and frame structure was confirmed at the beginning of September 2021.

Subsequent tests of the Carrier Drone V1 involved powered flight trials. The goal of these was to confirm motor configuration, propeller orientation, and the attitude control of the vehicle. In addition to ground confirmations, the main goal of flight tests was to get the vehicle flying reliably enough to tune its on-board controllers [44]. These consist of multi-leveled attitude, rate, velocity, and position PID controllers that must be manually tuned for experimental vehicles. A manual hover test was planned to assess the performance of the vehicle and begin tuning parameters for these controllers to achieve stable flight.

In addition to plans to tune the Carrier Drone's flight controller, multiple cameras and viewing locations were established to inspect the dynamics of the frame in flight. Flexibility, aggressiveness of attitude correction, and the extent of positional drift were critical for performing such assessments. In addition to visual observation, the PX4 flight controller stored data for all of the vehicles sensors after each flight for detailed analysis. This is expanded upon in subsequent paragraphs.

In the middle of September 2021, the Swarm Carrier team conducted a flight test of the Carrier Drone V1 in accordance with the above test criteria. The vehicle passed all pre-flight checks and successfully hovered with no positional drift. Handling was noted to be slightly unresponsive which was indicative of the large size and weight of the vehicle. During the second hover test however, the vehicle experienced a rapid and unexpected throttle increase that lead to an increase in vehicle altitude. This was interpreted as a vehicle runaway by the team members who executed a motor stop of the vehicle after it reached a height 10 ft above its expected hover altitude. This resulted an unpowered freefall from 15 ft and ground impact. The result was medium damage to the frame, light damage to several fixtures, and no damage to electronics or sensors. Fig.59 below shows examples of the frame damage which include buckling failure of the cantilever members holding the motors. Fig.60 below also shows the first successful hover test of Carrier Drone V1. Critically, it shows static frame deformation whose impact on the flight controller is discussed subsequently.

(a) Carrier Drone V1 failure of motor cantilever arm

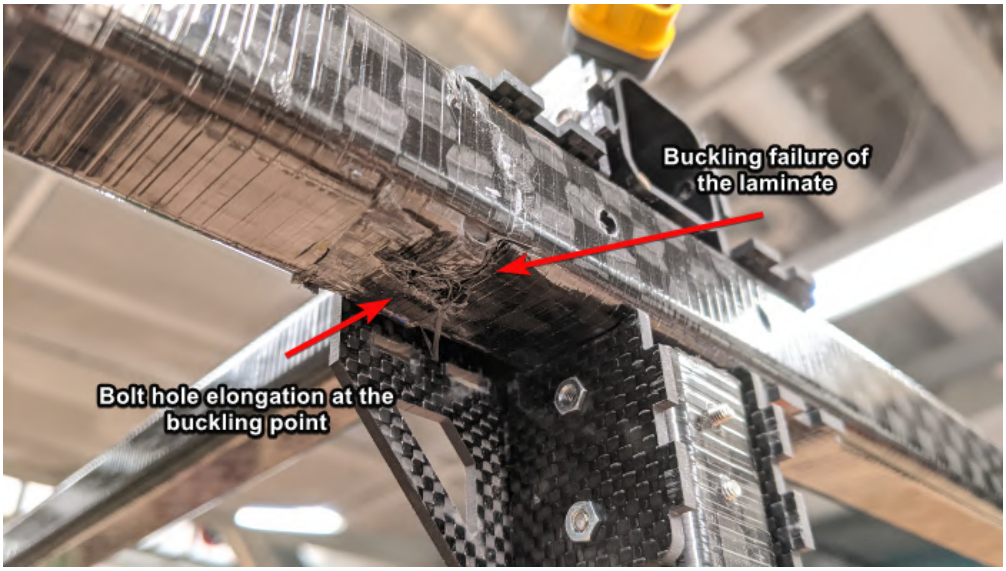

(b) Buckling failure mode of carbon laminate (Carrier Drone frame)

Figure 59: Examples of damage to the Carrier Drone V1 (Post Crash)

Figure 60: Carrier Drone V1 successful hover

The critical takeaway from observation of frame damage was that the motor cantilever arms were the weak point of the Carrier Drone V1 design. During the free fall, the front corners of the frame made impact with the ground first. This resulted in the formation of an instant center of rotation about the front of the frame that accelerated the impact of the rear corners. The resulting impulse caused the momentum of the motors to buckle the cantilever arms they were mounted on. Critical failures occurred at the stress concentrations generated by the bolt holes with the frame's connectors. In addition to subsequent analysis of the flight logs, these visual conclusions motivated the improvements to the Carrier Drone's design outlined in section 5.3.

The crash of the Carrier Drone V1 during the second hover resulted in an investigation of log files in order to understand the reasons and causes behind the uncommanded ascent of the vehicle. To assess flight data, Pixhawk 4 FC logs were analyzed that contained information on every operation, process, and parameter that was set on the vehicle for each flight. This allowed the group to have an extremely in depth look into the control loop, perceived pilot input commands, and parameters set during the final crash.

The analysis determined that during the final seconds of the vehicle's flight before it suddenly ascended, a manual yaw input by the pilot was received by the flight controller. At the 6:05:67 timestamp the pilot gave a slow ramp input to the vehicle, which resulted in the vehicle slowly trying to yaw. The pilot continued to give yaw input but at a higher magnitude now in an effort to get the vehicle to yaw faster, finishing at approximately 30% yaw input at 6:05:852 timestamp. At this point the vehicle control loop started to ramp exponentially in an effort to achieve the desired yaw rate and deflection desired by the pilot. By 6:06:245, the motors tried to ramp to 100% power in order achieve the yaw angular rate setpoint of 145 degrees per second. This had an unintended effect of causing the vehicle to rise in altitude drastically, without pilot input, as the vehicle tried to yaw to the desired setpoint. By 6:06:468, the pilot cut throttle completely, but the vehicle still maintained high individual motor outputs and continued its ascent. The control loop was then commanding an uncontrolled ascent sequence. The pilot then initiated an emergency motor kill to stop the vehicle from ascending. Fig. shows the Pixhawk 4 logs for the timestamps previously mentioned.

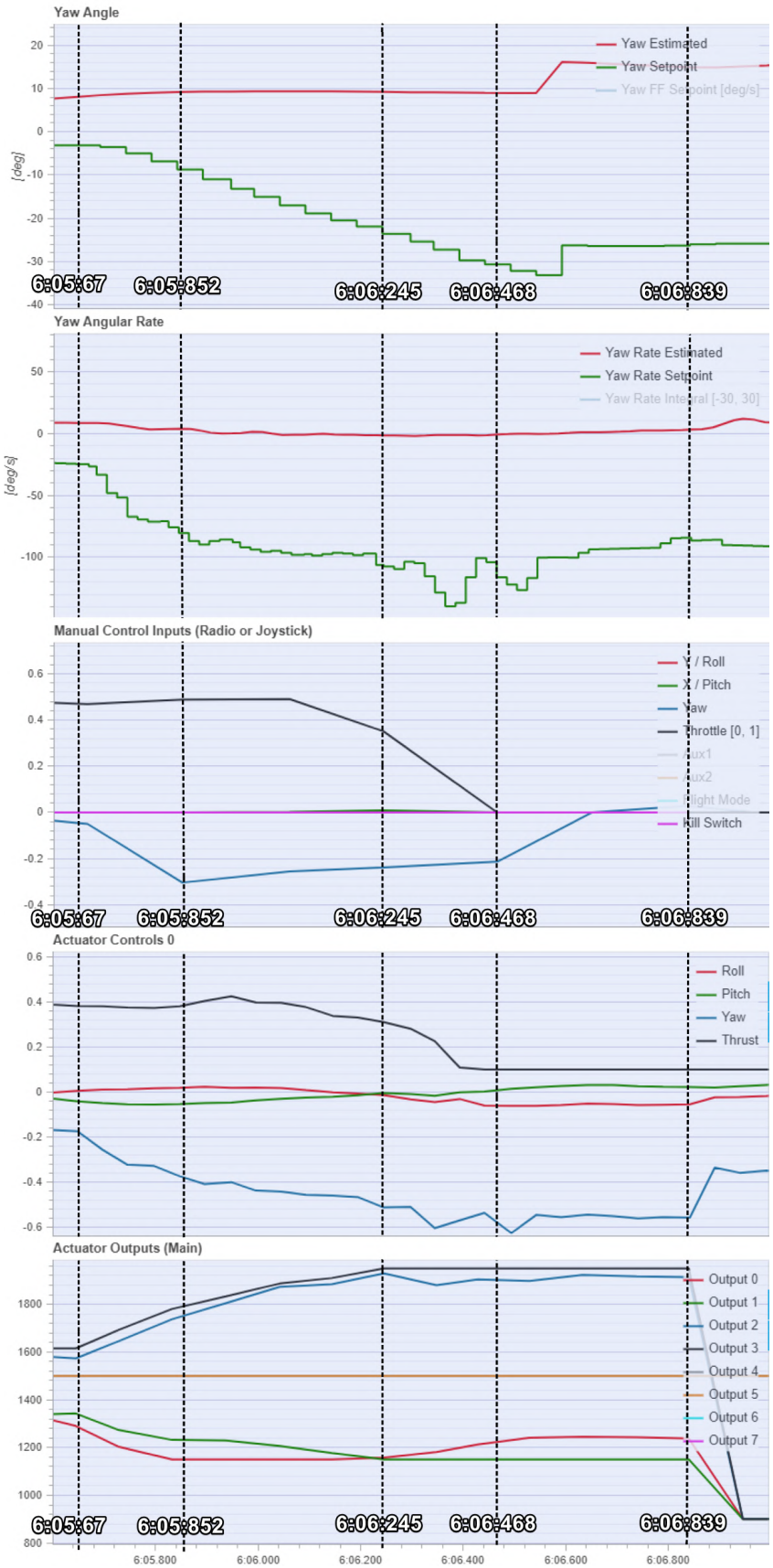

Figure 61: Pixhawk 4 flight logs for Carrier Drone V1 quadcopter hover test

One key factor that caused the ascent was the limits for the yaw rate, pitch rate, and roll rate programmed into the vehicles flight controller. These gains were set for vehicles of much smaller size, meaning that they were incompatible with the scale of the Carrier Drone. This allowed the control loop to try to achieve rates of rotations as high as 220 degrees per second, which would only be possible on smaller vehicles. Another factor was the parameter called Air Mode which exponentially adds rate and magnitude to control loop setpoints to improve vehicle maneuverability. This caused the control loop's yaw response to ramp rapidly which was an unexpected behavior according to the test's procedure.

Moving forward the group will carefully consider flight specific parameters such as rate limits, flight modes, and PID controls. With this new found knowledge on the limited applicability of small sUAS to the larger UAS vehicles, the group will start with a clean slate on tuning the vehicle. In addition further safety measure will be taken for subsequent tests, as chances of such an event are low but not fully erased. The Carrier Drone V3 hover tests will have the vehicle tethered to the ground to create a mechanical hardstop for flight runaways. Safety measures such as tethers will be used until the vehicle has had its flight dynamics fully checked. Despite the failure event, this quadcopter test proved incredible valuable for the team and has defined a faster route to completing the Carrier Drone.

5.13 Design Review: MassDOT

The Swarm Carrier team invited Noel Zamot, as a connection to the MassDOT's UAV review team, to review the system in development. Noel Zamot is a retired Air Force test pilot turned entrepreneur with decades of experience in the aerospace industry and military systems testing. The team originally reached out to Rob Knochenhauer through the FAASTeam Online Directory which provides the public access to drone experts for system evaluation and safety assessment. Alongside Rob K, Andrew Mihaley, Robin Grace, and Terrence McKenna (the other members of the MassDOT), Noel was involved in the establishment of many core FAA regulations for drones in use today. Due to this, the team was highly interested in performing a system review with Noel and his team to evaluate the feasibility, legality, d test plans for the Swarm Carrier System.

The Swarm Carrier team's original plan was to apply for a special exemption (Sec. 44807) for experimental vehicle approval under the FAA. For this process, an FAA representative must physically inspect designs, codebases, and test procedures which was a huge logistics concern for the team. It was this issue that prompted the team to reach out to Noel as an individual with many connections in the drone industry and knowledge of laws.

After getting an understanding of the system, a series of meetings was set up with Noel spanning from the beginning of September to now. Delays between review meetings were required for Noel and his team to reach out to other FAA and industry representatives for information on the testing of the Swarm Carrier. These difficulties were attributed to the legal uniqueness of the Swarm Carrier system in that it violates FAA but is non-commercial and non-DOT sponsored. Therefore, many avenues had to be addressed to find a test plan that suited the Fall semester deadline.

To summarize key legal points, Noel first proposed that the team filed for 44807 to fly at Joint Base Cape Cod which is an officially designated site for experimental vehicle testing under the FAA. However, because the project has no DOD affiliations, the team would have to either go

through the entire 4480 review or find a DOD affiliation through Northeastern to expedite testing. Neither of these outcomes were favorable for the team or MassDOT so other options were pursued.

Next, Noel reached out to FAA representatives regarding advice for student groups testing experimental unmanned aerial systems. The team was then connected to the educational director of the AMA (Academy of Model Aeronautics), Kyle Jaracz, for advice on operating experimental vehicles as an independent student research group. The AMA is a coalition of organized RC hobbyist fliers with FAA approved flying fields all over the US. He recommended that the team test under an amateur flight status, therefore skirting the commercial requirements of the FAA. Noel presented this information to the team and connected members with AMA chapters in the Boston area for final flight approval.

In addition to discussion of regulations, Noel also critiqued the team's test plans and provided valuable feedback to structure the project more efficiently. He provided extensive reviews and feedback on the team's SOP writing strategies, ORM generation for external entities, and system plans. As an external entity, he was able to identify ambiguities that the team could not internally see. Following these reviews, the Swarm Carrier team was able to efficiently draft SOPs and ORMs for external entities, Capstone, Northeastern's Risk Services, and Northeastern's UAV review board (UASRB).

From a test perspective, Noel provided valuable organization of the team's plans to achieve a full system test by the end of the term. Specifically, he promoted compartmentalized tests of subsystems to gain confidence before the final integration of the carrier drone, payload, and swarm drones. This allowed the team to efficiently structure its tests which have been largely successful thus far.

5.14 Regulations

The Swarm Carrier capstone has pivoted away from registering the system as a commercial UAS and instead as a recreational system. This will allow the project to avoid the legal headache of Part 107 regulations and operate a UAS without weight regulations and the 1:1 ratio of pilots to drones [45]. After talking with MassDOT representatives, they highlighted a pathway to operating a UAS under the recreational banner. A stipulation though of the recreational operation of a UAS is that it must be conducted under a community-based organization's approval at a fixed site [46]. To meet this requirement, the MassDOT connected the group with the AMA, a large hobby organization that has fixed flight sites throughout the state of Massachusetts. The AMA informed the capstone group that they must register as AMA members in order to use any AMA field, but seemed very receptive of the idea of using one of their fixed sites for the final system-level demonstration. The group is currently working to reestablish the Northeastern University AMA charter, which the members of the group had previously established during their time in Aerospace NU. As of this point, the project has a clear legal direction that can be used to conduct testing and final demonstration for the end of Capstone II.

6 Project Management

Due to the interdisciplinary nature of Swarm Carrier, substantial project management is required in order to ensure the development of subsystems in context. This is critical to ensure that even the

lowest level tasks are being developed with compatibility at the system-level in mind. To accomplish this, the team is using Trello: a task-tracking software used for organizing goals, meetings, and tests. Alongside communication with industry representatives, professors, and frequent team meetings, Trello will allow the team to continuously communicate and pursue a final prototype rapidly.

6.1 Team Roles and Responsibilities

The swarm carrier team consists of the six members listed as the authors of this report. As an interdisciplinary team, each member plays a specific role in achieving a full-system test. However, there is often overlap between disciplines that must be managed carefully. After extensive meetings, Table 3 below was established as a preliminary layout responsibilities alongside primary disciplines that each member is an expert within.

Table 3: Team member contributions

Team Member	Discipline	Airframes	Payloads	Interface	Autonomy
John Buczek	EE, Power Systems	Thrust validation, electronics debugging, configuration, and developing sensor DAQ for the Carrier Drone	Developing contact sensing electronics for the Multidrop Bay. Integrating sensing solutions for telemetry on all vehicles	Evaluating ROSBoard and developing test methods	Interfacing sensors with current software architectures and supporting tests
Erik Little	ME	Designing fixtures, connectors, mechanisms, and the new deca-motor configuration for the Carrier Drone. Helping with development of Swarm Drone V3s	Completing assembly, tolerance stack-up mitigation, and phase-in changes for the Multidrop bay	Assisting with tests and shaping design requirements around software functionality	Assisting with tests and shaping design requirements around software functionality
Michael Tang	ME, Mechatronics	Designing fixtures, connectors, mechanisms, and the new deca-motor configuration for the Carrier Drone. Developing an FEA workflow for analysing composites using ANSYS ACP	Assisting with assembly of Multidrop Bay, phase in changes, and testing of Swarm Drone to Multidrop interface	Carrying out Pixhawk 4 configuration and parameter debugging	Assisting with tests and shaping design requirements around software functionality
Blake McHale	CE, Vision/ML/Algos	Conducting simulations of all airframes using Gazebo. Modeling real world dynamics to test algorithms	Developing architectures for precision landings around excising hardware capabilities. Interfacing with sensors and actuators with higher level actions	Researching methods of communication between the Pixhawk, computer, and vehicle network. Executing and debugging simulated and real-world tests	Developing precision land, drop-mode, and collaborative searching, queuing, and recovery methods
Josh Field	CE, Vision/ML/Algos	Developing search metrics for swarm autonomy given the operational ranges of airframes	Developing architectures for precision landings around excising hardware capabilities. Interfacing with sensors and actuators with higher level actions	Developing ROSBoard as Swarm Carrier's GUI, aiding in the development of communication between the Pixhawk, computer, and network	Developing precision land, drop-mode, and collaborative searching, queuing, and recovery methods
Noah Ossanna	ME, Mechatronics	Developing motor configurations, connector design, and electronics organization for the Carrier Drone. Releasing the Swarm Drone V3 design with new fixtures, sensors, and electronics	Conducting phase-in changes on the Multidrop Bay and helping with assembly. Testing collision detecting sensing methods and planning test procedures	Assisting with the configuration, calibration, and debugging of Pixhawk flight controllers and sensors	Managing the connection between hardware and software development of high level tasks

Table 3 breaks down the tasks of Swarm Carrier to the high level categories: Airframes, Payloads, Interface, and Autonomy. Airframes constitute the development of flight vehicles like the Swarm and Carrier Drone(s) while Payloads describes the development of sensor modules and the Multidrop Bay. Interface relates to how the system is visualizing data, debugging, and communi-

cating between vehicles. Lastly, Autonomy refers to the development of higher level autonomous actions like precision landing, aerial deployments, and collaborative missions.

6.2 Reality vs Proposed schedule

Currently the work progression is ahead of the proposed timeline. Fig. 62 displays the current Gantt Chart. The current Gantt Chart displays the final Carrier test finishing in November. This is due to the impact of cold weather on the performance of lithium polymer batteries. The entire schedule has been tailored such that all field testing is performed at latest in November.

6.3 Outreach

The Swarm Carrier team has communicated with representatives from T-Motor, Full Throttle Unmanned Aerial Systems, PX4 dev. forums, and Randal Erb (NU COE). These representatives have allowed us to garner a greater understanding of large vehicle dynamics, propulsion systems, and Pixhawk firmware development. In addition to industry outreach, the Swarm Carrier team has extensively communicated with members of the Mass Department of Public transportation (MassDOT) and FAA regarding flight authorization of non-compliant vehicles (section 5.14). With their aid, the approval workflow has transitioned to conversations with the Academy of Model Aeronautics (AMA) who will help the Swarm Carrier team to perform a full system demonstration at a legal field location.

7 Conclusions

The Swarm Carrier System is being substantially developed from previous research with the goal of conducting a full-circle test. Hardware developments have been dedicated to revising the Swarm Drones to their V3 configuration, validating the Carrier Drone's design, and improving the Multidrop Bay. During Capstone II, the group completed assembly of the Carrier Drone V1, and performed an initial hover test. The group has vetted and begun manufacturing for the final version of the Carrier Drone. The team has also continued development of the Multidrop Bay in preparation for a autonomous landing test. A portion of the Swarm Drone fleet has been upgraded to the V3 configuration, with small changes needed to bring all 3 versions to completion. Extensive work has shifted towards testing of precision land, drop mode, and other tests as the systems near completion.

Software development has been focused on building the architecture for controlling the drones. Throughout Capstone II, various improvements have been added to the existing system; consistency in Drop Mode and GPS initialization, as well as updated precision landing logic. With these improvements, simulation tests have moved to field tests for features such as precision landing. There has also been significant work on the GUI for field tests and these systems are being tested actively. In the future, Drop Mode field tests are being prepared for and work on the overall mission algorithms, including path planning, will be completed.

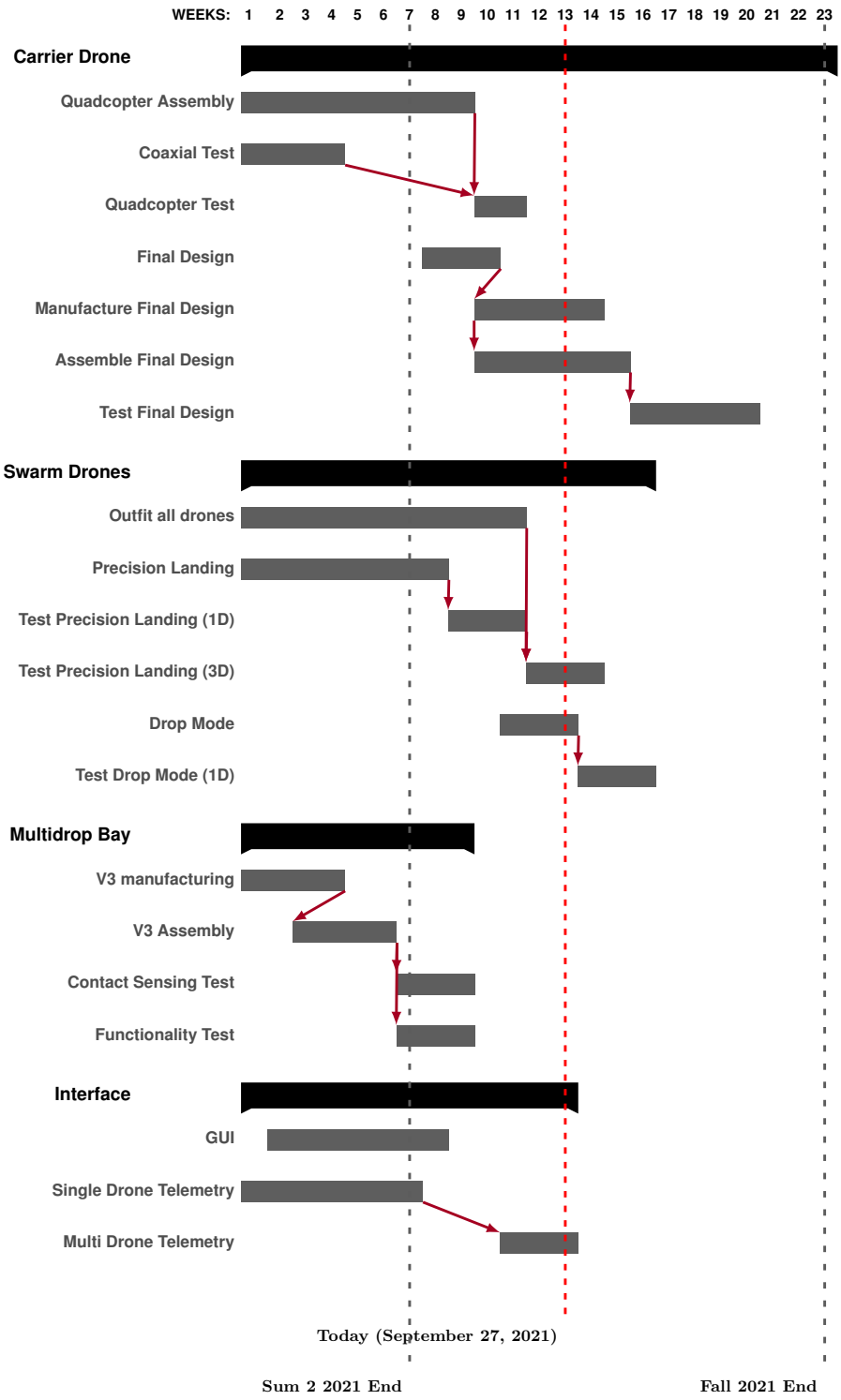

Figure 62: Gantt chart

8 Intellectual Property

8.1 Description of Problem

The problem statement for this capstone project is to design, manufacture, and test a system capable of deploying and recovering a swarm of multirotor UAS.

8.2 Proof of Concept

The capstone has developed extensive systems and tests in order to complete the problem statement. This project is multidisciplinary, as all subsystems of the system heavily use mechanical, electrical, and software intensive concepts. The members of the project have extensive experience in numerous fields of unmanned aerial vehicle (UAV) development and usage, which is extensively used in the development of this capstone

At the subsystem level, the Carrier Drone is responsible for carrying in flight the combined payload of the Multidrop Bay and Swarm Drones. The Carrier Drone is controlled in flight by a Pixhawk 4 (PX4) microcontroller, which is responsible for controlling the motors, internal accelerometers and gyroscopes, global positioning system (GPS), barometer, and telemetry. The PX4 is in communication with an NVidia Jetson Nano Computer, which is responsible for Avionics, interfacing with the Multidrop inter-integrated circuit (i2c) link, and communicating by WiFi with the ground station.

The Multidrop bay is responsible for both holding the Swarm Drones during flight of the Carrier Drone, as well as deployment of Swarm Drones before the mission and recovering the Swarm Drones after the mission. The servos that facilitate the actuation are controlled by a microcontroller. This is then connected to the Carrier Drone and is in constant communication via an i2c link.

The Swarm Drones are the focus of the system, and are responsible for completing the search mission after deployment from the Multidrop Bay, as well as recovery with the Multidrop Bay after completing the search mission. Like the Carrier Drone, the Swarm Drones are outfitted with PX4 microcontrollers which control the motors, internal accelerometers and gyroscopes, GPS, barometer, and telemetry. The PX4 is in communication with an NVidia Jetson Nano Computer, which controls avionics, the external camera used for computer vision during a precision land, and the copper contact sensing between the landing guides of the Multidrop Bay and the copper bottoms of the Swarm Drones.

During the mission, the subsystems of the Carrier Drone, Multidrop Bay, and Swarm Drones are viewable by the ground control. The ground control contains a graphical user interface (GUI) for overall system telemetry display, as well as options for user input. This is then connected by WiFi link to the Carrier Drone and Swarm Drone for constant communication.

The capstone project has many smaller subsystems which combine to form the overall system. To verify the subsystems, individual tests were developed to validate the Swarm Carrier's safety and functionality. These tests focus on smaller subsystems at first, and combine in later tests after validating the base concepts to scale up to a full system test. These tests were carefully developed following approved standard operating procedures (SOPs).

To validate and inform future design decisions on frame design, motor configuration, motor

specification, and propeller type, a thrust test was developed. Using an off the shelf motor thrust stand, the motor thrust, voltage, current, torque, and rpm are recorded. This data is used to measure both single rotor and coaxial propeller configurations to further inform design decisions.

To validate and inform future design decisions on software integration and hardware components of the Multidrop Bay and Swarm Drones, a precision land test was developed. This tests the fidelity and precision of the swarm drones to land in a set location using fully automated computer vision. The test involves one of the Swarm Drones taking flight from the ground, hovering over an ArUco marker, and landing on top of the marker. This validates that the Swarm Drones are capable of automatically landing inside of the Multidrop Bay without manual inputs.

To validate and inform future design decisions on the Swarm Drone and Multidrop Bay, a drop mode test was developed. This tests the ability of the Swarm Drone to arm and stabilize itself after dropping from the Multidrop Bay. This test involves dropping a single Swarm Drone from the bottom of an octocopter UAS and testing whether the drone activates as expected. If the drone does not catch itself as intended, a safety net is in place below to prevent loss of the Swarm Drone. This validates the custom software developed to catch the drone after it is released from the Multidrop Bay, and it can then continue on its mission.

To validate and inform future design decisions on the Carrier Drone, an air frame test was developed. This tests the functionality of the frame as a whole, and sees if there are any vibration issues with the frame. The Carrier Drone takes off without any payloads, and its pitch, roll, and yaw performance are evaluated qualitatively by the pilots. The frame is also analyzed for vibration using the onboard sensors. This test validates design decisions for the current frame, which informs development of the second version of the frame.

8.3 Progress to Date

The Swarm Carrier capstone project has developed a lot of the individual subsystems up to this point. The versions of each individual system are in a variety of different states but are all steadily progressing. The hardware aspect of the project has been working on the Carrier Drone, Swarm Drones, and the Multidrop Bay. The software group of the project has been developing the autonomy for precision landing, drop mode, and GUI.

The Carrier Drone V1 has been designed and manufactured using a custom-built 3 axis tube CNC. The electronics, including electronic speed controllers (ESC), flight controllers (FC), and power distribution boards (PDB) have all been mounted on the vehicle. Many of these electronics mounting plates have been laser-cut out of wood for prototyping purposes. Thrust tests were conducted to tabulate the motor characteristics of planar and coaxial motor configuration to develop the final Carrier Drone motor and propeller configuration. Construction for the Carrier Drone V1 with a quadcopter motor configuration was completed. This quadcopter Carrier was test flown and revealed several issues with the design such as static and dynamic torsion and flight control software. Current work is focused on the design and manufacturing of the Carrier Drone V2.

The Swarm Drones V3 have had two out of three vehicles fitted with the new PX4 FCs and shielding on their cabling to reduce electric and magnetic field (EMF) noise. Testing is still being conducted to validate these new V3 changes to the vehicle. The precision landing feature has been tested alone and has worked proving the aspect of autonomy to land within a small area only using onboard sensors of the Swarm Drone. In these same tests for the Swarm Drone V3s, the GUI has

been proven to be very successful, allowing users in the field to view PX4 parameters. Drop mode for the Swarm Drones has been successful in simulations.

The Multidrop Bay V3 has been manufactured and tested to work with the linkage mechanisms. The V3 has had modifications done to the slots of the linkages to ensure consistent operations. These iterations to the linkage system have produced a system capable of consistently operating with the full weight of a Swarm Drone resting on them. The copper contact sensing on the bay has also been tested. This provides feedback to the swarm drone during landing as to when it has made physical contact with the Multidrop bay.

This summary encapsulates the current progress of the Swarm Carrier capstone project.

8.4 Individual Contributions

Table 4: IP team member contributions

Team Member	Discipline	Airframes	Payloads	Interface	Autonomy
John Buczek	EE, Power Systems	Thrust validation, electronics debugging, configuration, and developing sensor DAQ for the Carrier Drone	Developing contact sensing electronics for the Multidrop Bay. Integrating sensing solutions for telemetry on all vehicles	Evaluating ROSBoard and developing test methods	Interfacing sensors with current software architectures and supporting tests
Erik Little	ME	Designing fixtures, connectors, mechanisms, and the new octo-motor configuration for the Carrier Drone. Helping with development of Swarm Drone V3s	Completing assembly, tolerance stack-up mitigation, and phase-in changes for the Multidrop bay	Assisting with tests and shaping design requirements around software functionality	Assisting with tests and shaping design requirements around software functionality
Michael Tang	ME, Mechatronics	Designing fixtures, connectors, mechanisms, and the new octo-motor configuration for the Carrier Drone. Developing an FEA workflow for analysing composites using ANSYS ACP	Assisting with assembly of Multidrop Bay, phase in changes, and testing of Swarm Drone to Multidrop interface	Carrying out Pixhawk 4 configuration and parameter debugging	Assisting with tests and shaping design requirements around software functionality
Blake McHale	CE, Vision/ML/Algos	Conducting simulations of all airframes using Gazebo. Modeling real world dynamics to test algorithms	Developing architectures for precision landings around excising hardware capabilities. Interfacing with sensors and actuators with higher level actions	Researching methods of communication between the Pixhawk, computer, and vehicle network. Executing and debugging simulated and real-world tests	Developing precision land, drop-mode, and collaborative searching, queuing, and recovery methods
Josh Field	CE, Vision/ML/Algos	Developing search metrics for swarm autonomy given the operational ranges of airframes	Developing architectures for precision landings around excising hardware capabilities. Interfacing with sensors and actuators with higher level actions	Developing ROSBoard as Swarm Carrier's GUI, aiding in the development of communication between the Pixhawk, computer, and network	Developing precision land, drop-mode, and collaborative searching, queuing, and recovery methods
Noah Ossanna	ME, Mechatronics	Developing motor configurations, connector design, and electronics organization for the Carrier Drone. Releasing the Swarm Drone V3 design with new fixtures, sensors, and electronics	Conducting phase-in changes on the Multidrop Bay and helping with assembly. Testing collision detecting sensing methods and planning test procedures	Assisting with the configuration, calibration, and debugging of Pixhawk flight controllers and sensors	Managing the connection between hardware and software development of high level tasks

8.5 Future Work

All future work for the Swarm Carrier system revolves around the three subsystems: Drone Carrier, Swarm Drone, and the Multidrop Bay. Legal work for acquiring an appropriate test site will be

continued with weekly meeting with the Massachusetts Department of Transportation (MassDOT) and other contacts in the Academy of Model Aeronautics (AMA).

For both the Drone Carrier and Swarm Drone, they will use the same autonomy software stack. New additions will include algorithms to perform path planning and communication between multi-vehicles. To support path planning a general storage of the environment must be shared with a discrete map. Drop mode still needs to be implemented in the PX4: further verification of this mode must still occur. Various safety futures will also need to be implemented to handle fault situations.

The Drone Carrier will need to have major revisions to accommodate the V2 octocopter configuration, which means rebuilding the V1 frame and the rewiring the entire power system. This also would require additional tube drilling, and new connector designs to bind together frame components that are longer than the maximum 100 inch length designated by the manufacturer. The group plans on properly simulating the frame in ANSYS Workbench using ANSYS Composite PrepPost (ACP) to get a full understanding on the dynamics of the frame. These upgrades are essential for the Drone Carrier to operate safely and with the complete payload of six Swarm Drones and two Multidrop Bay, as the current coaxial dodecacopter configuration is not sufficient to fly the Carrier Drone for longer than ten minutes.

The Swarm Drones V2 will have to be rebuilt in their V3 configurations with the new PX4 Minis and contact sensing landing gears. The capstone group will be purchasing one more PX4 Mini to retrofit the final Swarm Drone, as they have been determined as the appropriate replacement to the current FC. These updates are vital for ensuring all the systems can achieve the level of autonomy needed for precision landing and integration into the Multidrop Bay.

9 References

[1] A. Gajeski, "The right drone for your department." https://botlink.com/blog/2018/7/9/the-right-drone-for-the-job, Jul 2018.

[2] G. F. Miller, "Persistent Surveillance Unmanned Aerial Vehicle and Launch/Recovery Platform System and method of using with secure communication, sensor systems, targeting systems, locating systems, and precision landing and stabilization systems ," U.S. Patent 10,890,927, Jan. 2021.

[3] H. Chin and K. Carraha, "Airborne Drone Launch and Recovery Apparatus," U.S. Patent 10,179,648, June 2016.

[4] A. Bondyra, S. Gardecki, P. Gąssior, and W. Giernacki, "Performance of Coaxial Propulsion in Design of Multi-rotor UAVs," in *Challenges in Automation, Robotics and Measurement Techniques* (R. Szewczyk, C. Zieliński, and M. Kaliczyńska, eds.), (Cham), pp. 523–531, Springer International Publishing, 2016.

[5] "Introducing alta x." https://freeflysystems.com/alta-x, May 2021.

[6] S. Garrido and S. Nicholson, "Detection of aruco markers." https://docs.opencv.org/3.4.15/d5/dae/tutorial_aruco_detection.html.

[7] M. Colledanchise and P. Ögren, *Behavior Trees in Robotics and AI*. CRC Press, 1st ed., 2018.

[8] L. Meier, "Overview." https://docs.qgroundcontrol.com/master/en/index.html, Aug 2021.

[9] L. Meier, "RTPS/DDS interface: PX4-Fast RTPS(DDS) bridge." https://docs.px4.io/master/en/middleware/micrortps.html, Jun 2021.

[10] P. Doherty and P. Rudol, "A uav search and rescue scenario with human body detection and geolocalization," in *AI 2007: Advances in Artificial Intelligence* (M. A. Orgun and J. Thornton, eds.), (Berlin, Heidelberg), pp. 1–13, Springer Berlin Heidelberg, 2007.

[11] F. Afghah, A. Razi, J. Chakareski, and J. D. Ashdown, "Wildfire monitoring in remote areas using autonomous unmanned aerial vehicles," *CoRR*, vol. abs/1905.00492, 2019.

[12] J. Ornato, A. You, G. McDiarmid, L. Keyser-Marcus, A. Surrey, J. Humble, S. Dukkipati, L. Harkrader, S. Davis, J. Moyer, D. Tidwell, and M. Peberdy, "Feasibility of bystander-administered naloxone delivered by drone to opioid overdose victims," *The American Journal of Emergency Medicine*, vol. 38, 06 2020.

[13] F. Mancini, M. Dubbini, M. Gattelli, F. Stecchi, S. Fabbri, and G. Gabbianelli, "Using unmanned aerial vehicles (uav) for high-resolution reconstruction of topography: The structure from motion approach on coastal environments," *Remote Sensing*, vol. 5, no. 12, pp. 6880–6898, 2013.

[14] J. Buczek, L. Bertizzolo, S. Basagni, and T. Melodia, "What is a wireless uav? a design blueprint for 6g flying wireless nodes," WiNTECH'21, (New Orleans, LA, USA), Association for Computing Machinery, 2021.

[15] P. Pounds, R. Mahony, and P. Corke, "Modelling and control of a quad-rotor robot," 12 2006.

[16] M. S. Bradbury, "Drone Deployment Apparatus for Accommodating Aircraft Fuselages ," U.S. Patent 10,578,398, Mar. 2020.

[17] W. Heinzmann, "Apparatus for Recovery of Unmanned, Reusable Aircraft," U.S. Patent 5,109,788, May 1992.

[18] M. Grubb, "Locking Line Capture Devices for Unmanned Aircraft, and Associated Systems and Methods," U.S. Patent 10,967,987, April 2021.

[19] S. K. McGann and N. McGaha, "Unmanned Aerial Vehicle (UAV) Recovery System," U.S. Patent 10,800,547, Oct. 2020.

[20] C. H. F. Foo and H. L. Hsi, "Apparatus and Method for Aerial Recovery of an Unmanned Aerial Vehicle," U.S. Patent 10,589,859, Mar. 2020.

[21] J. Peverill, A. Woodworth, B. Freudberg, and D. Cottrell, "Capturing Hook for Aerial System ," U.S. Patent 10,308,375, June 2019.

[22] D. Davidson, " Methods and Apparatus to Deploy and Recover a Fixed Wing Unmanned Aerial Vehicle via a Non-Fixed Wing Aircraft ," U.S. Patent 10,133,272, Nov. 2018.

[23] T. S. McKee and S. C. Roden, "UAV Launch and Recovery ," U.S. Patent 9,969,505, May 2018.

[24] M. Yoffe, " Point Take-off and Landing of Unmanned Flying Objects ," U.S. Patent 9,637,245, May 2017.

[25] R. C. Melish, K. J. Neeld, and R. L. Orner, " Unmanned Air Vehicle Recovery System ," U.S. Patent 9,527,604, Dec. 2016.

[26] M. C. Allen, D. D. Hallerberg, and G. P. Timm, "Method for Recovering a UAV," U.S. Patent 9,527,603, Dec. 2016.

[27] J. Goldie, N. Vitale, G. A. Downey, K. Leary, and W. Hafer, "Unmanned Aerial Vehicle(UAV) Recovery System," U.S. Patent 8,464,981, June 2013.

[28] G. H. Lovell, E. C.-K. Hui, and M. K. Umbreit, "Stabilized UAV Recovery System," U.S. Patent 8,172,177, May 2012.

[29] J. Snediker, M. A. Watts, and G. W. Corboy, "UAV Arresting Hook for use with UAV Recovery System ," U.S. Patent 7,143,976, Dec. 2006.

[30] J. W. Lim, K. W. McAlister, and W. Johnson, "Hover performance correlation for full-scale and model-scale coaxial rotors," *Journal of the American Helicopter Society*, vol. 54, no. 3, p. 32005–3200514, 2009.

[31] H. Otsuka and K. Nagatani, "Thrust loss saving design of overlapping rotor arrangement on small multirotor unmanned aerial vehicles," in *2016 IEEE International Conference on Robotics and Automation (ICRA)*, pp. 3242–3248, 2016.

[32] "Matrice 300 rtk –built tough. works smart.." https://www.dji.com/matrice-300?site=developer.

[33] Skydio, "Skydio x2 autonomous drone - skydio inc.." https://www.skydio.com/skydio-x2.

[34] "Corvus one drone." https://www.corvus-robotics.com/corvus-one.

[35] T. M. Cabreira, L. B. Brisolara, and P. R. Ferreira Jr., "Survey on coverage path planning with unmanned aerial vehicles," *Drones*, vol. 3, no. 1, 2019.

[36] J. Malecha, "Drone operations over 55 pounds." https://www.faa.gov/uas/resources/events_calendar/archive/2019_uas_symposium/media/How_To_Drone_Operations_Over_55_lbs.pdf, 2021.

[37] FAA, "Uas certification." https://www.faa.gov/uas/advanced_operations/certification/, Nov 2020.

[38] G. Inc., "Pyrofil mr60h 24k." https://www.rockwestcomposites.com/media/downloads/MR60H-24K_(02-2008).pdf.

[39] "Pyrofil hr50." https://www.rockwestcomposites.com/media/downloads/HR40-14008-Fiber.pdf, author=Grafil Inc.

[40] Stromkalkylator, "Continous current carrying capacity of a trace." http://www.skottanselektronik.com/current_en.html.

[41] B. Prasad, "Busbar size and calculation." https://bralpowerassociate.blogspot.com/2013/10/busbar-size-and-calculation.html, Oct 2013.

[42] D. Faconte, "Behaviortree/behaviortree.cpp: Behavior trees library in c++. batteries included.." https://github.com/BehaviorTree/BehaviorTree.CPP.

[43] "Export a solidworks assembly to urdf." https://wiki.ros.org/sw_urdf_exporter/Tutorials/Export%20an%20Assembly.

[44] "Multicopter pid tuning." https://docs.px4.io/master/en/config_mc/pid_tuning_guide_multicopter.html.

[45] *Federal Aviation Administration, Docket No. FAA-2015-0150.* 2015.

[46] *Federal Aviation Administration, Docket No. FAA-2019-0364*, vol. 84. 2019.